INFLUENCES OF DARK SECTOR ON LOCAL GRAVITATIONAL PHENOMENA

A THESIS SUBMITTED TO THE

UNIVERSITY OF NORTH BENGAL

FOR THE AWARD OF

DOCTOR OF PHILOSOPHY [SCIENCE]

IN

PHYSICS

BY

Samrat Ghosh

SUPERVISOR

Prof. Amitabha Mukhopadhyay

CO-SUPERVISOR

Dr. Arunava Bhadra

High Energy & Cosmic Ray Research Centre

&

Department of Physics

University of North Bengal

Darjeeling-734013

July 2020

DECLARATION

I declare that this ***"INFLUENCES OF DARK SECTOR ON LOCAL GRAVITATIONAL PHENOMENA"*** has been prepared by me under the guidance of **Prof. Amitabha Mukhopadhyay**, Senior Professor of **Department of Physics, University of North Bengal** and **Dr. Arunava Bhadra**, Senior Research Physicist of **High Energy & Cosmic Ray Research Centre, University of North Bengal**. No part of this thesis has formed the basis for the award of any degree or fellowship previously.

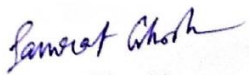

Dated: …6.. July, 2020. (Samrat Ghosh)

High Energy & Cosmic Ray Research Centre
&
Department of Physics
University of North Bengal,
Darjeeling-734013

UNIVERSITY OF NORTH BENGAL

Accredited by NAAC with Grade A

DEPARTMENT OF PHYSICS
P.O. NORTH BENGAL UNIVERSITY
RAJA RAMMOHUNPUR, DIST. DARJEELING,
WEST BENGAL, PIN 734013,
INDIA

ENLIGHTENMENT TO PERFECTION

Railway Station: New Jalpaiguri
Nearest Airport: Bagdogra
Phone: +91-(0) 353-2776338
Fax: +91-(0) 353-2699001
Website:www.nbu.ac.in

Ref. No. .....

Date : .....

CERTIFICATE FROM THE SUPERVISORS

We certify that **Sri Samrat Ghosh** has prepared his thesis entitled **"INFLUENCES OF DARK SECTOR ON LOCAL GRAVITATIONAL PHENOMENA"**, for the award of the Ph.D. degree of the University of North Bengal, under our joint supervision. He has carried out the work at the **High Energy & Cosmic Ray Research Centre** and at the **Department of Physics, University of North Bengal**.

(Dr. Arunava Bhadra)

HECRRC

Co-supervisor

Dated: 06 July, 2020

Senior Research Physicist
High Energy & Cosmic Ray Research Centre
University of North Bengal, Siliguri 734013

Amitabha Mukhopadhyay.

(Prof. Amitabha Mukhopadhyay)

Physics Department

Supervisor

Dated: 06 July, 2020

Professor
Department of Physics
University of North Bengal

Report - Samrat Ghosh.pdf Report - Samrat Ghosh.pdf

URKUND

Urkund Analysis Result

Analysed Document: Samrat Ghosh_Physics.pdf (D76178324)
Submitted: 7/9/2020 11:50:00 AM
Submitted By: nbuplg@nbu.ac.in
Significance: 4 %

Sources included in the report:

https://en.wikipedia.org/wiki/Gravitational_field
https://s3.cern.ch/inspire-prod-files-1/105793720141cd0a249fed89667122cf
https://cyberleninka.org/article/n/303043.pdf
https://www.cosmos.esa.int/documents/1866264/3219248/
BergeJ_WP_Dark_Sector_ONERA.pdf/04d0f4f5-921d-69b4-f0e2-ed5ac4eb0c84?t=1565184621729
https://www.researchgate.net/
publication/222562682_Gravitational_time_delay_of_light_for_various_models_of_modified_gravity
https://www.researchgate.net/
publication/226509122_Gravitational_time_advancement_and_its_possible_detection
https://www.mobt3ath.com/uplode/book/book-46130.pdf
https://arxiv.org/pdf/1710.03518
https://arxiv.org/pdf/1806.09677

Instances where selected sources appear:

26

TO

ALL MY TEACHERS

Acknowledgements

This work was carried out at ***High Energy & Cosmic Ray Research Centre and Department of Physics, University of North Bengal****. I am grateful to all the individuals associated with the* ***High Energy & Cosmic Ray Research Centre, University of North Bengal*** *and* ***Department of Physics, University of North Bengal*** *for supporting me during my Ph.D. work. I would like to express my warmest grateful gratitude to:*
My supervisors of this thesis work– ***Prof. Amitabha Mukhopadhyay*** *and* ***Dr. Arunava Bhadra****, who give me an opportunity to explore a new direction of my life by accepting me as a Ph.D. student. The continuous support and guidance, I am getting, enriched me and inspired me to serve the civilization by serving Science as a physicist and as a human-being too. I have gained confidence and motivation to face and overcome the challenges by their positive outlook and their confident approach to the research work. This learning will always enrich my future path.*
My teachers of our "High Energy & Cosmic Ray Research Centre (HECRRC)"– ***Dr. Samir Kumar Sarkar*** *and* ***Mr. Arindam Mukherjee*** *for teaching me the basics of research methodology and their words of encouragement which boost-up my moral strength always.*
All my seniors of the HECRRC– ***Dr. Prabir Banik, Dr. Biplab Bijay, Dr. Tamal Sarkar, Mr. Sadhan Paul, Dr. Subhranshu Ghosh*** *and all others, for their co-operation and providing an outstanding working environment to me.*

I would like to convey my warmest gratitude to ***Dr. Partha Sarathi Joarder*** *of* ***Bose Institute*** *for helping me to improve my knowledge about "Solar Hydrodynamics".*

I would like to express my thanks from the bottom of my heart to all my colleagues and seniors of my organization ***Idea Cellular Ltd.*** *(presently known as* ***Vodafone Idea Ltd.****), especially* ***Mr. Debabrata Mitra, Mr. Joy Banerjee and Mr. Amit Sharma*** *for supporting me continuously during this period by protecting me from different difficult situations.*

I would like to express my gratitude to my Physics teachers ***Mr. Susanta Dutta*** *and* ***Mrs. Gouri Roy*** *of my school* ***Mal Adarsha Bidya Bhaban****, I started my journey of Physics by holding their hands.*

I would like to convey my special thanks to ***elder Sisters****,* ***my Family Members*** *and* ***my Friends*** *for standing beside me as my supporting system always.*

And few more people dream with me with unaccountable sleepless nights and their unconditional sacrifices always motivate me to achieve my goal,- my father ***Mr. Manik Ghosh****, my mother* ***Mrs. Sumita Ghosh****, my wife* ***Mrs. Bubli Dey Ghosh*** *and my son* ***Ekalabya Ghosh****.*

Abstract

The rotation curve of galaxies and a few other observations suggest that a major part of the matter in disc galaxies is non-luminous or dark. On the other hand the discovery of the accelerating expansion of Universe has led inclusion of a new dominant component into the energy-momentum tensor of the universe having negative pressure, the so called dark energy component. Several other observations which include the cosmic microwave background (CMB) measurements, baryon acoustic oscillations (BAO), lensing in clusters support the existence of dark energy and/or the presence of dark matter halo surrounding the Galactic disc. Consequently on large distance scales, astrophysical and cosmological phenomena are governed mainly by dark matter and dark energy.

There are several proposed candidates for dark matter but despite extensive experimental searches no direct evidence of dark matter has been found so far. There are also proposals for modifications of relativity theory at the fundamental theoretical level which include Modified Newtonian dynamics (MOND), the conformal gravitational theory (based on Weyl symmetry), Grumiller's modified gravity model etc all of which can explain flat rotation curves of galaxies without the need of dark matter. The simplest candidate for dark energy is the cosmological constant (Λ) and the ΛCDM model where CDM refers to cold dark matter, is in accordance with all the existing cosmological observations. But it has a big theoretical problem - the magnitude of Λ ($\sim 10^{-52}\ m^{-2}$) is many orders of magnitude smaller than the expected vacuum energy density in the standard model of particle physics. Hence many other theoretical explanations for the DE have been proposed in the literature in which the parameter w evolves with time or different from -1. A few alternative theories also have been proposed other than the General Theory of Relativity to explain the dark energy consequences, like f(R) gravity model, DGP model which is based on Strings theory etc.

Dark matter/energy is supposed to affect the gravitational phenomena in all distance scales including the local scales. As the evidences of dark sector so far are found only in large distance scale observations, the study of effects of dark energy/matter on local gravitational phenomena may provide important observable

signature of dark sector and may assist to understand the nature of the dark sector. Already some analysis have been performed so far in this direction. In the present thesis work, the influences of dark matter and dark energy on different local gravitational phenomena have been examined theoretically considering different models of dark matter/energy. Emphasis has been given to examine the viability of different models of dark matter and dark energy by comparing the theoretical predictions based on the models with the observations.

In first chapter, the introduction of the thesis work has been given including the basics of dark matter and energy. After outlining the objective of the thesis work, the current status of the local gravitational effects of dark sector has been reviewed.

In second chapter, the effect of dark matter/energy on gravitational time advancement (negative effective time delay) has been studied considering few dark energy/matter models including cosmological constant. It is found that presence of dark energy field gives only (positive) gravitational time delay irrespective of the position of the observer whereas pure Schwarzschild geometry leads to gravitational time advancement when the observer is situated at relatively stronger gravitational field point in the light trajectory. Consequently, there will not be any time advancement effect at radial distances where gravitational field due to dark energy is stronger than the gravitational field due to Schwarzschild geometry.

In third chapter, the expression of gravitational time advancement (negative time delay) for particles with non-zero mass in Schwarzschild space-time geometry has been obtained. The influences of the gravitational field that explains the observed rotation curves of spiral galaxies and that of dark energy (in the form of cosmological constant) on time advancement of particles have also been investigated in this chapter. The present findings suggest that in presence of dark matter gravitational field, the gravitational time advancement may take place irrespective of gravitational field of the observer, unlike the case of pure Schwarzschild geometry where gravitational time advancement takes place only when the observer is situated at stronger gravitational field compare to the gravitational field encountered by the particle during its journey. When applied to the well known case of SN 1987a, it is found that the net time delay of a photon/gravitational wave is much smaller than quoted in this chapter. In the presence of dark matter field, the photon and neutrinos from SN 1987a should have been suffered gravitational time advancement rather than the gravitational time delay.

In fourth chapter, gravitational deflection of light rays due to the space-time metric of global monopole and a Schwarzschild black hole that swallowed a global monopole have been studied considering the asymptotically non-flat behavior of the space-time geometries of the stated configurations. It is found that so obtained gravitational bending angles differ considerably from those obtained from conventional approach, which is essentially applicable to asymptotically flat space time geometries. More importantly the bending angle is obtained negative when the lensing system contains global monopole which is a clear signature of a global monopole system. Implications of the present analysis on the viability of global monopole as an alternative to dark matter hypothesis is discussed.

In fifth chapter, space-time geometry of the halo region in spiral galaxies is derived using the observed galactic flat rotation curve feature and considering the characteristics of cold dark matter in the galaxy. Gravitational lensing due to the derived space time has been studied. The total mass of Abell 370 galaxy clusters estimated from the derived space-time is found to agree well with the gravitational lensing observations.

In sixth chapter, Grumiller's quantum motivated modified gravity model, which modifies the Newtonian potential at large distances and describes the galactic rotation curves of disk galaxies in terms of a Rindler acceleration term, has been tested through the baryonic Tully-Fisher relation. We estimate Rindler acceleration parameter from observed rotation velocity versus baryonic mass data of a sample of sixty galaxies. It has been found that the Rindler parameters describes the observed data reasonably well.

And the last (seventh) chapter, we conclude our findings.

The material/results reported in this thesis have been published/communicated in different journals as shown below:

1. *"Influences of dark energy and dark matter on gravitational time advancement"*, Samrat Ghosh and Arunava Bhadra, The European Physical Journal C volume 75, Article number: 494 (2015).

2. *"Probing dark matter and dark energy through gravitational time advancement"*, Samrat Ghosh, Arunava Bhadra and Amitabha Mukhopadhyay, General Relativity and Gravitation volume 51, Article number: 54 (2019).

3. *"Gravitational lensing by global monopole"*, Kabita Sarkar, Samrat Ghosh and Arunava Bhadra, communicated for publication.

4. *"Space-time geometry of spiral galaxy halo"*, Samrat Ghosh, Arunava Bhadra and Amitabha Mukhopadhyay, communicated for publication.

5. *"Baryonic Tully-Fisher test of Grumiller's modified gravity model"*, Samrat Ghosh, Arunava Bhadra and Amitabha Mukhopadhyay and Kabita Sarkar, communicated for publication.

The conference presentations out of the thesis work are given below

1. *"Influence of dark matter and dark energy on gravitational time advancement"*, Samrat Ghosh, Arunava Bhadra, National Conference on "Exploring the Relativistic Universe", University of North Bengal, West Bengal, December 15-16, (2015).

2. *"Probing Dark Energy through Gravitational Wave Lensing"*, Samrat Ghosh, Arunava Bhadra and Amitabha Mukhopadhyay, National Conference on "Exploring the Cosmos: 2016-17", University of North Bengal, West Bengal, January 16-17, (2017).

3. *"Effect of Dark Energy and Dark Matter on Gravitational Time Advancement for a Relativistic Particle of Non-zero mass"*, Samrat Ghosh, Arunava Bhadra and Amitabha Mukhopadhyay, National Conference on "Exploring the Cosmos: A national Conference on Relativistic Universe", University of North Bengal, West Bengal, February 27-28, (2020).

Preface

A number of astrophysical and cosmological observations univocally suggest that our Universe is composed primarily of new, unfamiliar forms of matter and energy, the so called dark matter and dark energy; the normal matter contributes only $\sim 5\%$ *of the energy density of the universe whereas dark matter and dark energy share approximately* 27% *and* 68% *respectively. However, despite several efforts so far there is no direct evidence of dark matter particles, nor their existence is predicted by any standard theoretical model of particle physics. On the other hand though various models for dark energy are proposed in the literature including modified gravity theories but none of them are free from problems and the origin of dark energy is still a major outstanding issue in physics.*

Both dark matter and dark energy are likely to affect the local gravitational phenomena. In the present thesis work we explore possible signature of various dark matter and dark energy models on some local gravitational observables which may provide independent verification of the existence of dark sectors and distinguish/examine various models of dark sector. Such a study also may throw light on the nature of dark sectors.

Particularly the influence of dark matter/energy on gravitational time advancement is studied and analytical expressions for the time advancement to first order in M *and* Λ *is obtained where* Λ *is the parameter describing the strength of the dark matter/energy. The effect of dark sector on gravitational time advancement for a relativistic particle with non-vanishing mass also is studied in different dark sector models as well as in Schwarzschild space-time. Gravitational lensing due to the space-time metric of Schwarzschild black hole that swallowed a global monopole, which describes well the flat rotation curve of spiral galaxies without the need of any dark matter, is studied to check whether such model can also consistently explain lensing observations. A space-time metric has been proposed in the thesis work taking the dark matter consequences like flat rotation curve of spiral galaxies and considering cold dark matter characteristics of galaxies. Grumiller's modified gravity model, which has been considered as an alternative model to describe dark matter consequences, has been verified by Baryonic Tully-Fisher Relation (BTFR) and the concerned observations involving a sample of sixty galaxies*

Contents

List of Tables

List of Figures

Chapter 1

Introduction and Review

1.1 Introduction

General Relativity (GR) is arguably considered as the most elegant theory in physics. GR pronounces gravitation as the manifestation of space-time geometry. GR has been extremely successful at describing observations and passed all experimental tests conducted so far. GR based cosmology is the cornerstone of the current hot Big Bang description of our Universe. However, some unexpected components turn out to make up most of the Universe's mass-energy budget in the GR description of the observations at large scales.

Recent cosmological observations suggest that the Universe is undergoing a phase of accelerated expansion. The explanation of such accelerated expansion in the purview of general relativity requires the presence of a large amount of some exotic form of energy density with negative pressure, the so-called dark energy. On the other hand, the amount of luminous matter in galaxies is found insufficient to explain the observed galactic rotation curves and thereby the existence of non-luminous or dark matter, that neither interacts with radiation nor with the conventional matter except through the gravitational field or through some feeble interaction, has to be assumed. This dark matter component is also required to be non-relativistic (i.e. cold) in view of structure formation. It appears from a wide variety of astrophysical observations that ordinary baryonic matter constitutes just 4.9% of the energy density in the Universe while dark matter composes about 26.8% and the dark energy contributes most – about 68.3% of the energy density in the Universe [1].

Dark energy models in the framework of general relativity suffer from fine-tuned, unnatural properties as will be elaborated in the subsequent sections. On the other hand, despite extensive efforts, dark matter is still undetected. The nature of dark matter is also not clear. Dark energy and dark matter are two of the major outstanding issues in physics and cosmology today.

1.2 General Relativity:

The journey of exploring the laws of nature had crossed a milestone when Nicolus Copernicus predicted the actual planetary motion and his student Galileo Galilei proved his teacher's prediction by his revolutionary discovery of Telescope. The laws of planetary motion by Johannes Kepler, created a perception about motion inside the solar system which was given a proper and generalized dimension by Isac Newton with his revolutionary Theory of Gravitation [2]. The invention of the telescope and the theory of Gravitation explored the gateway of gathering knowledge about the phenomena not only beyond the Earth but beyond the solar system also. Newton's law of gravitation ($F = \frac{Gm_1m_2}{r^2}$, where F stands for gravitational force, G is the gravitational constant ($= 6.674 \times 10^{-11} Nm^2Kg^{-2}$), m_1 and m_2 are the masses of the particles and r is the distance between these two particles) was highly successful in explaining planetary dynamics. Transforming the Newton's equation into the form of gravitational field using Poisson's equation, one finds:

$$\nabla^2\phi(r,t) = 4\pi G\rho(r,t)$$

where, ∇ is the spatial Laplace operator, $\phi(r,t)$ is the gravitational scalar potential, and $\rho(r,t)$ is the density of the gravitating object. The above expression shows that the gravitational potential varies only with spatial derivatives, not with time derivative, i.e. if the matter distribution varies, the gravitational potential changes instantaneously with the infinite speed which was considered as a prime drawback of Newton's theory of gravitation.

Newton's law of dynamics is based on Galilean transformation, but the constancy of speed ($c = 1/\sqrt{\mu_0\epsilon_0}$) of an electromagnetic wave in Maxwell's theory cannot be explained by the Galilean transformation. If we consider that Galilean

transformation and Maxwell's equation both are correct, an absolute frame of reference (called 'ether') had to be introduced where the electromagnetic waves can be propagated at speed $c = 1/\sqrt{\mu_0\epsilon_0}$. But Michelson-Morley experiment using optical interferometer, invented by Michelson himself, didn't find any evidence of the existence of an absolute reference frame, rather the experiment showed the constancy of speed of light irrespective of the motion of the observer.

In the beginning of the twentieth century, Albert Einstein formulated the Spacial Theory of Relativity (STR) [3] based on two simple postulates: (a) the laws of physics are same in all inertial frames and (b) the speed of light in free space has same value c in all inertial frame. Probably the most revolutionary effect of these two postulates is that space and time are intertwined leading to a single continuum known as space-time. A point to be noted that the special theory of relativity rests on Euclidean geometry and is valid only for inertial observers.

Based on the Principle of Equivalence, Principle of General Covariance and generalizing the Euclidean space-time continuum of special relativity to curved (Riemannian) space-time geometry, Einstein formulated General Theory of Relativity (GR) [4] during the period 1907-15. The curved geometry is essentially described through metric tensor ($g_{\mu\nu}$) which is related to incremental line element as $ds^2 = g_{\mu\nu}dx^\mu dx^\nu$. GR describes gravity not as a force but as a geometric property of space-time. Gravity is a warping of space-time as per GR.

The field equations of GR are given by:

$$G_{\mu\nu} = -\frac{8\pi G T_{\mu\nu}}{c^4}, \tag{1.1}$$

where $G_{\mu\nu} = R_{\mu\nu} - \frac{1}{2}g_{\mu\nu}R$ is the Einstein tensor, $R_{\mu\nu}$ is the Ricci tensor, $g_{\mu\nu}$ is the metric tensor and $T_{\mu\nu}$ is the energy-momentum tensor for matter.

Ricci tensor $R_{\mu\nu}$ can be expressed in terms of metric tensor $g_{\mu\nu}$ via Riemannian connection $\Gamma^\lambda_{\mu\nu}$ as,

$$R_{\mu\nu} = \frac{\delta\Gamma^\lambda_{\lambda\mu}}{\delta x^\nu} - \frac{\delta\Gamma^\lambda_{\mu\nu}}{\delta x^\lambda} + \Gamma^\lambda_{\mu\sigma}\Gamma^\sigma_{\nu\lambda} - \Gamma^\lambda_{\mu\nu}\Gamma^\sigma_{\lambda\sigma} \tag{1.2}$$

where

$$\Gamma^\lambda_{\mu\nu} = \frac{1}{2}g^{\lambda\sigma}\left(\frac{\delta g_{\sigma\mu}}{\delta x^\nu} - \frac{\delta g_{\mu\nu}}{\delta x^\sigma} - \frac{\delta g_{\nu\sigma}}{\delta x^\mu}\right) \tag{1.3}$$

For a given energy-momentum tensor, one would look for solution of the Einstein field equations in terms of metrics that determine the space time geometry for the given source.

A simple but important case when an observer is at a location outside the source. All the components of energy momentum tensor are zero ($T_{\mu\nu} = 0$) outside the source. The Einstein field equations in such a situation turn into

$$R_{\mu\nu} = 0 \tag{1.4}$$

The general static spherically symmetric metric is given by [5];

$$ds^2 = B(r)dt^2 - A(r)dr^2 - r^2(d\theta^2 + sin^2\theta d\phi^2) \tag{1.5}$$

where $B(r)$ and $A(r)$ are two unknown metric coefficients which are the function of r only.

The well known static spherically symmetric vacuum ($T_{\mu\nu} = 0$) solution of the above Einstein's field equation (1.1), is the Schwarzschild solution

$$ds^2 = [1 - \frac{2m}{r}]dt^2 - [1 - \frac{2m}{r}]^{-1}dr^2 - r^2(d\theta^2 + sin^2\theta d\phi^2) \tag{1.6}$$

where $m = \frac{MG}{c^2}$ and M stands for the mass of the gravitating object, G is the gravitational constant and c is the speed of light.

The predictions of GR have been tested by a variety of experiments with increasingly high precision and the theory has passed all such tests conducted till now.

1.3 Dark Energy

Einstein studied the nature of the Universe by using his field equations. On the apparent observational basis, it was thought that the astronomical objects like stars, galaxies are static, i.e. these are not moving at all. He found from his theory that the nature of the Universe is dynamic. The same conclusion was also reached by Friedmann [6] and Lemaitre [7] by studying the nature of the Universe

using Einstein's field equation and employing Robertson-Walker metric. To tally with the contemporary thought of static Universe, Einstein introduced a constant in his field equations, called Einstein's Cosmological constant.

The Friedmann-Lemaitre-Robertson-Walker (FLRW) model of the Universe is outlined below. If one considers that the Universe is homogeneous and isotropic, it can be described by the following generic metric :

$$d\tau^2 = dt^2 - a^2(t)[\frac{dr^2}{1-kr^2} + r^2 d\Omega^2] \tag{1.7}$$

where $a(t)$ is the cosmological scale factor, and k signifies the curvature of the Universe. The above metric is known after Robertson and Walker.

Solving the equation (1.7) using Einstein's field equations the following expressions are found,

$$\frac{\ddot{a}(t)}{a(t)} = -\frac{4}{3}\pi G(\rho + 3p) \tag{1.8}$$

and

$$\frac{\dot{a}^2(t) + k}{a^2(t)} = \frac{8\pi G\rho}{3} \tag{1.9}$$

Where ρ is the effective mass density and p is the pressure.

In 1929, Hubble collected the red-shift versus luminosity distance data of different Galaxies. During the experimental observation of the measurement of the redshift of nearer Galaxies by Hubble and his team,, distance vs redshift relation was found linear when the value of redshift is less than 0.1. The mathematical base of the Hubble experiment is as follows [8]:

The expression of apparent luminosity (l) is given by,

$$l = \frac{L}{4\pi {d_L}^2} \tag{1.10}$$

where L is the absolute luminosity of a source at a distance of d_L.

At large distance, especially in cosmological distances, the expression needs to be modified for the following reasons:

1. If light from a distant luminous object reaches the Earth at time t_0, then the effective area of the sphere drawn around the luminous object and passing through the Earth will be equal to $4\pi r^2 a^2(t_0)$, where r is the coordinate distance between the earth and the luminous light source.

2. The rate of arrival of the photons is lower than the rate at which they are emitted by the redshift factor $a(t_1)/a(t_0) = 1/(1+z)$.

3. the energy $h\nu_0$ of a received photon in the Earth is less than the energy $h\nu_1$ of the emitted photon from the light source by the same redshift factor $1/(z+1)$.

Therefore the effective apparent luminosity on the Earth can be expressed by,

$$l = \frac{L}{4\pi r^2 a^2(t_0)(1+z)^2} \tag{1.11}$$

Comparing with the equation (1.10) and (1.11), one can express,

$$d_L = a(t_0) r (1+z) \tag{1.12}$$

When $z << 1$, the relation between luminosity distance and redshift can be expressed as power series in the form of the redshift $1 + z = a(t_0)/a(t_1)$ and the look-back time $t_0 - t_1$, is given by,

$$z = H_0(t_0 - t_1) + \frac{1}{2}(q_0 + 2){H_0}^2(t_0 - t_1)^2 + ... \tag{1.13}$$

where H_0 is the Hubble constant ($H_0 = \dot{a_0}/a_0$), and q_0 is the deceleration parameter, expressed by,

$$q_0 = \frac{-1}{{H_0}^2 a(t_0)} \frac{d^2 a(t)}{dt^2} \tag{1.14}$$

The expression (1.13) can be inverted to express the Hubble constant (H_0) in the form of redshift,

$$H_0(t_0 - t_1) = z - \frac{1}{2}(q_0 + 2)z^2 + ... \tag{1.15}$$

The coordinate distance r can be expressed from the relation $[\int_{t_1}^{t_0} \frac{dt}{a(t)} = \int_0^r \frac{dx}{\sqrt{1-kx^2}}]$,

$$\frac{t_0 - t_1}{a(t_0)} + \frac{H_0(t_0 - t_1)^2}{2a(t_0)} + ... = r + ... \tag{1.16}$$

dots in the right hand side denotes the third and higher order terms of r. Using the equation (1.15), the solution is found,

$$ra(t_0)H_0 = z - \frac{1}{2}(1 + q_0)z^2 + ... \tag{1.17}$$

Which gives the expression of luminosity distance,

$$d_L = H_0^{-1}[z + \frac{1}{2}(1 - q_0)z^2 + ...] \tag{1.18}$$

For small z, the higher-order terms in z can be neglected and the above equation turns to Hubble's relation. For higher red-shifts, the higher-order terms as well as the deceleration parameter $q_0 = -\ddot{a}(t_0)\frac{at_0}{\dot{a}^2(t_0)}$ will come in consideration. Determination of the value H_0 and q_0 is a big challenge in astronomy because it will help us to know the dynamic nature of the Universe. The expression of luminosity distance is not useful for the redshifts of the order of unity as power series expansion will not be a smart approach in such a scenario. In that case, we have to adopt the measurement technique through the dynamic theory of expansion. To achieve this, the approach of FLRW model has been adopted using Einstein's field equation and Robertson-Walker metric as mentioned earlier through equations (1.7), (1.8) and (1.9):

Critical density plays an important role to define the state of Universe and the critical density (ρ_0) is defined by the density of the Universe which makes the curvature of the Universe flat, i,e. $k = 0$. The Universe is considered as closed if $\rho > \rho_0$ and open if $\rho < \rho_0$.

From equation (1.9), one can get the expression of critical density,

$$\rho_0 = \frac{3H_0}{8\pi G} \tag{1.19}$$

The expressions of proper energy density for different states of Universe is given by the relation $\rho \propto a^{-3-3w}$, where ω is the constant of the equation of state($= p/\rho$):

Considering non-relativistic matter: $p = 0$

$$\rho = \rho_0 (a(t)/a_0)^{-3} \tag{1.20}$$

For relativistic matter: $p = \rho/3$

$$\rho = \rho_0 (a(t)/a_0)^{-4} \tag{1.21}$$

Considering vacuum energy: $p = -\rho$

$$\rho = \rho_0 \tag{1.22}$$

Recent measurements indicate that the Universe is flat, i.e., $k \simeq 0$. Therefore the expression of effective energy density considering the mixture of non-relativistic matter, relativistic matter and vacuum energy, given by,

$$\rho = \frac{3{H_0}^2}{8\pi G}[\Omega_\Lambda + \Omega_M (\frac{a_0}{a})^3 + \Omega_R (\frac{a_0}{a})^4] \tag{1.23}$$

where present epoch energy densities of vacuum (ρ_{Λ_0}), non-relativistic matter (ρ_{M_0}) and relativistic matter (ρ_{R_0}) are given by,

$$\rho_{\Lambda_0} = \frac{3{H_0}^2 \Omega_\Lambda}{8\pi G} \tag{1.24}$$

$$\rho_{M_0} = \frac{3{H_0}^2 \Omega_M}{8\pi G} \tag{1.25}$$

$$\rho_{R_0} = \frac{3{H_0}^2 \Omega_R}{8\pi G} \tag{1.26}$$

The equation (1.9) suggests,

$$\Omega_\Lambda + \Omega_M + \Omega_R = 1 \tag{1.27}$$

Now using equation (1.9) and (1.23), one may write:

$$\begin{aligned} dt &= \frac{dx}{H_0 x\sqrt{\Omega_\Lambda + \Omega_M x^{-3} + \Omega_R x^{-4}}} \\ &= \frac{-dz}{H_0(1+z)\sqrt{\Omega_\Lambda + \Omega_M(1+z)^3 + \Omega_R(1+z)^4}} \end{aligned} \tag{1.28}$$

where $x = a/a_0 = 1/(1+z)$ and z signifies the redshift. From the above equation the expression of the co-ordinate distance ($r(z)$) of the source can be deduced and employing the relation of co-ordinate distance and luminosity distance ($d_L(z) = a_0 r(z)(1+z)$), the expression of luminosity distance can be found,

$$d_L(z) = \frac{1+z}{H_0}\int_{1/(1+z)}^{1} \frac{dx}{x^2\sqrt{\Omega_\Lambda + \Omega_M x^{-3} + \Omega_R x^{-4}}} \tag{1.29}$$

From the above relation, it is quite clear that if the variation of luminosity distance with redshift can be determined experimentally, the value of Ω_{Λ_0}, Ω_{M_0} and Ω_{R_0} can be deduced analytically. In the late 1990s, this job was done by two independent Supernovae search teams led by Riess(1998) and Perlmutter(1999) [9]. They explored the evidence of accelerating Universe by the survey of type Ia Supernovae as shown in figure (1.1). As the peak brightness of Supernovae is quite uniform, the object was selected as a standard candle. Considering higher red-shift Supernovas, each of the observatory teams found that distance vs redshift relation is not linear as demonstrated in the equation, whereas the relation found about to linear for the observed Supernovas of redshift less than 0.1. From the high red-shift Ia-SNa, it was found that the earlier expansion rate was slower than that is today and with the measurement of luminosity distance of low redshift Supernovae observation and statistical data analysis of density parameters showed that the present era is dark energy dominated era with flat curvature. Observations on Cosmic Microwave Background radiation also support the geometrical nature of the Universe. The search for the biggest mystery of physics begins from there, the

source of the energy behind this accelerating Universe is still unrevealed and the energy is known as Dark Energy.

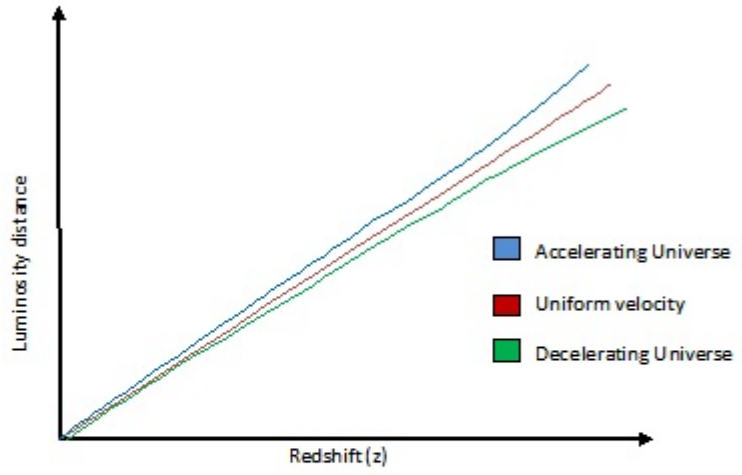

FIGURE 1.1: Luminosity distance vs. cosmological redshift variation curve for type Ia Supernovae

1.4 Dark matter

In 1919, during the observation of Solar Eclipse near the Hyades star cluster, the gravitational deflection angle of the light from the stars indicated the existence of extra mass. Dutch astronomer Jacobus Kapteyn predicted the existence of extra mass by using stellar velocities [10]. In 1930s the concept became stronger when F. Zwicky was calculating the stellar velocities of the Coma cluster by using Virial theorem and he found the evidence of extra unseen mass, addressed as dark matter [11].

After few decades, the strong evidence of Dark Matter was provided by Vera Rubin and Kent Ford [12] with an observation by spectrograph measuring the radius vs velocity curve of the edge of Andromeda Galaxy (a spiral galaxy) and they found that the rotation curve is almost flat.

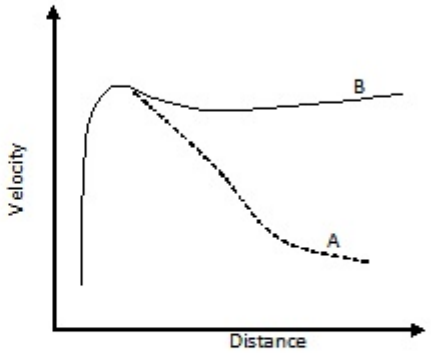

FIGURE 1.2: Flat rotation curve of a spiral galaxy

The dotted line in figure (1.2) was the desired rotation curve without any existence of Dark Matter but Rubin and Ford found the continuous lined flat curve which indicates the presence of extra masses(Dark Matter) in spiral galaxies.

Gravitational lensing of light by massive objects coming from a distance source (like as quasar) is considered as the strong evidence of the presence of Dark Matter. Measuring the distortion geometry due to gravitational lensing, the total mass of the lensing object can be deduced [13]. The Dark Matter distribution has been deduced using the gravitational lensing phenomenon.

Several probable explanations have been provided to theorize the entities, Dark Energy and Dark Matter.

1.5 Candidates to explain Dark Energy:

The FLRW model (equations (1.8) and (1.9)) suggests for expansion of the Universe with time. Any deceleration of the Universe can easily be explained in terms of the deceleration parameter. The effective density of Universe (ρ) and pressure (p) are positive quantities considering that it is composed of normal matters and radiation and the expansion should not be accelerated with time as dictate by equation (1.8). But after the discovery of the accelerating Universe, the perception was changed and it has led inclusion of a new component of the energy-momentum tensor of the Universe having negative pressure, addressed as a dark energy component.

A significant candidate of dark energy component is Cosmological Constant (Λ) which was first-time introduced by Einstein himself to balance the dynamic nature of the Universe. The Einstein's field equations can be expressed as,

$$R_{\mu\nu} - \frac{1}{2} g_{\mu\nu} R^{\lambda}_{\lambda} = -8\pi G T_{\mu\nu} \tag{1.30}$$

With the introduction of Λ the energy-momentum tensor $T_{\mu\nu}$ can be replaced by effective energy momentum tensor $T_{\mu\nu} + \Lambda g_{\mu\nu}$ and consequently equation (1.8) and (1.9) will be re-written as,

$$\frac{\ddot{a}(t)}{a(t)} = -\frac{4}{3}\pi G(\rho + 3p) + \frac{\Lambda}{3} \tag{1.31}$$

and

$$\frac{\dot{a}^2(t) + K}{a^2(t)} = \frac{8\pi G\rho}{3} + \frac{\Lambda}{3} \tag{1.32}$$

Equation (1.31) shows the contribution of Λ is negative to the pressure term and hence it exhibits repulsive nature. The energy which causes the repulsion is greater than the gravitational energy, resulting the cosmological expansion with acceleration.

The energy associated with Λ can be explained by the vacuum energy in particle physics. But the problem is that the value of Cosmological Constant ($10^{-120} m^{-2}$)

in quantum physics is many order smaller than the cosmologically observed value ($10^{-52}m^{-2}$). Considering the perfect fluid equation of state, the value of the constant of the equation of state($\omega = p/\rho$, where p and ρ stand for pressure and energy density respectively) is found -1 for cosmological constant whereas the energy and matter densities vary in different rates throughout the history of Universe. The variable constant of the equation of state can not be explained by the cosmological constant model of dark energy. The problem is known as the coincidence problem.

The coincidence problem of cosmological constant model has been attended by using Scalar-field models of dark energy. Instead of a fix constant of equation of state which arises considering cosmological constant model of dark energy, the periphery can be widen by considering the situation that equation of state can vary with time as mentioned in inflationary cosmology. There are several approaches of scalar-field dark energy models which includes Quintessence [14]; [15]; [16], Phantom [17]; [18], K-essence [19]; [20]; [21]; [22], Chaplygin gas [23]; [24], modified f(r) gravity models [25]; [26] etc.

In Quintessence model of dark energy, the constant of equation of state(ω) is represented as,

$$\omega = \frac{p}{\rho} = \frac{\dot{\phi}^2/2 - V(\phi)}{\dot{\phi}^2/2 + V(\phi)} \tag{1.33}$$

where ϕ represents the scalar-field and $V(\phi)$ stands for the potential energy.

In this model the equation (1.33) shows that the value of ω evolves from 1/3 to -1. For matter dominating era $\omega = 0$, for radiation dominating era $\omega = 1/3$ and for $-1 < \omega \leq -1/3$, the accelerating universe expansion reflects.

On the other hand, for negative kinetic energy, the ω evolves $\omega < -1$ region which is known as the Phantom model of dark energy. In this scenario, the expansion rate will be increased with time and once the expansion rate will exceed the limit of the speed of light, the observable objects of the Universe will unable to interact with each other. This hypothetical condition of the Universe is known as Big Rip.

In the quintessence model of dark energy, the potential energy of the scalar field is used to explain the acceleration of the Universe, whereas it is also possible to arise the condition of accelerating Universe by altering the kinetic energy of the scalar field. This kinetic energy dependent scalar-field explanation of the accelerating

expansion is known K-essence model of dark energy. But all these scalar field theories have their own periphery and limitations. Therefore, some alternative concepts of dark energy models have also been proposed.

DGP (Dvali-Gabadadze-Porrati) theory, based on brane-world model, has given an alternative proposal of acceleration of Universe [27]. In the brane-world model, an extra 5th dimension has been introduced where (3+1) Minkowskian dimension is embedded till a certain distance ($r_* = (r_0^2 r_g)^{1/3}$). The general relativistic effects can be successfully explained within the threshold distance r_* but beyond that distance, the 5th dimension is introduced where large distance phenomena like the cosmological expansion with acceleration can be explained without taking the non-zero vacuum energy in consideration. But the stability of this concept has been questioned by the critics [28].

1.6 Candidates to explain Dark Matter:

Basically two kinds of explanations are there to be represented as the candidates of dark matter. One is matter contributions that are not detected yet and another one is the alternative theories to explain the dark matter phenomena like flat rotation curve of spiral galaxies and gravitational lensing etc without the need of any dark matter.

1.6.1 Matter representation of dark matter:

The cosmic baryonic density can be derived by CMBR (Cosmic Microwave Background Radiation) temperature anisotropies, which suggests $\Omega_{bar} = 0.045$ whereas $\Omega_m = 0.3$. This signifies that most of the matters are non-baryonic dark matter. In fact, the density of luminous matter (Ω_{lum}) less than the Ω_{bar}, i.e., $\Omega_{lum} < \Omega_{bar}$, that means, some baryonic dark matters also exist which is yet to be revealed. This implies that both baryonic and non-baryonic matters contribute to dark matter. Further, the study of structure formation in the Universe demands that dark matter particles should be non-relativistic (cold dark matter).

In baryonic components, like faint stars, cold gas clouds, Rydberg matter etc, have been predicted as dark matter components. The constitutes of non-baryonic dark matter candidates include neutrinos, axions, mirror matters, black hole, etc.

Dark matter in the form of Massive Compact Halo Objects (MACHOs) is proposed in the literature. Low mass stars like brown and red dwarfs may constitute the baryonic dark matter if they located at large distances or at the dark halo of galaxies. Having low mass, Brown dwarfs cannot initiate the thermonuclear reaction, and red dwarfs are massive enough to burn hydrogen in their cores. These can contribute as dark matter but the quantity is too less than the total estimated dark matter. Molecular hydrogen gas, which is treated as cold gas, is also difficult to detect and considered as dark matter candidate. Rydberg matter, a dark matter candidate, is low density condensed phase of matter which is highly transparent of light due to highly excited state and extremely long lifetime. Because of their invisibility, black holes are also proposed as viable MACHOs. Microlensing surveys, however, suggest that the mass density of MACHOs is not sufficient to explain the required amount of dark matter.

Weak interacting particles are considered for dark matter particles as they cannot be detectable by telescopes. Neutrinos are only known dark matters which contribute significantly to cosmic energy density and are detected in nature. However, the mass density of neutrinos is not large enough to explain the dark matter fraction of the cosmic average density. Axions, which are introduced to solve the problem of CP violation in particle physics and are interact weakly, are also proposed as a candidate for dark matter.

Among the weakly interacting particles WIMP or Weakly Interacting Massive Particles are the most favored candidate for dark matter. Beyond the Standard Models, several theories predict the existence of WIMP. For instance, the lightest supersymmetric particle in supersymmetric theories may act as WIMP. Other possible WIMPs include the lightest particle in Little Higgs models, lightest Kaluza-Klein particle, etc.

1.6.2 Alternative models to explain dark matter effects

Among the alternative approaches to explain the dark matter consequences include MOND (Modified Newtonian Dynamics) [29], Conformal theory based on Weyl gravity [30], modified f(r) gravity [31] etc. These models explain dark matter effects without invoking any dark matter.

MOND is a modification of Newtonian dynamics to explains the flat rotation curve which is considered as a dark matter effect as earlier discussed. This concept was proposed by M. Milgrom in 1983. The base of this modification is to segregate into two sections based on of high and low acceleration. As per this proposal, The dynamics of an object under a gravitating object follow the Newtonian behavior at high acceleration, whereas it shows deep-MOND behavior at low acceleration. The MOND equation of force is given by,

$$F = m\mu(x)(\frac{a}{a_0})a \tag{1.34}$$

where F is the Newtonian force, m is the mass of the object, a is the acceleration, $\mu(x)$ is known as interpolating function, a_0 is the constant which denotes the transition between Newtonian and MOND domain. To synch with Newtonian mechanics, the condition will be as followed,

$$\mu(x) \to 1 \qquad \text{for} \qquad x \gg 1$$

whereas, the following condition will be obeyed to be consistent with the dark matter observation,

$$\mu(x) \to x \qquad \text{for} \qquad x \ll 1$$

If an object of mass m moving around a gravitating object of mass M in a circular orbit with linear velocity v, then we get,

$$\frac{GMm}{r^2} = \frac{m(\frac{v^2}{r})^2}{a_0}$$

$$\Rightarrow v^4 = GMa_0$$

The above expression from MOND describes the flat rotation curve of dark matter effect but it can not construct a satisfactory cosmological model and other observed property of galaxy clusters.

Mannheim and Kazanas [30] proposed an alternative model of dark matter effect based on conformal invariant Weyl gravity. They have found the following metric which explain the flat rotation curve of spiral galaxies:

$$ds^2 = -B(r)dt^2 + \frac{dr^2}{B(r)} + r^2(d\theta^2 + sin^2\theta d\phi^2) \tag{1.35}$$

where,

$$B(r) = 1 - \frac{\beta(2 - 3\beta\gamma)}{r} - 3\beta\gamma + \gamma r - \kappa r^2 \tag{1.36}$$

β, γ, and k stand for the integration constants. Putting the value of $k = \gamma = 0$, the metric provides the Schwarzschild metric, and when $\gamma = 0$, it will give SDS metric. γ is the parameter in the above metric which represents the dark matter effects, and the value of γ was found $10^{-26}m^{-1}$ based on the observational data of several galaxies.

Grumiller also proposed a model for gravity at large distances based on modified general relativity and proposed a metric to define large distance phenomena like dark energy and dark matter [31].

Another proposal to explain dark matter is based on f(r) gravity, which was proposed by H. A. Buchdahl in 1970 [32]. This is basically modified general relativity, which is a family of theories based on several circumstances. An arbitrary function has been introduced which gives the freedom to explain the dark sector effects.

1.7 Objectives of the present work

Does dark sector really exist or the observations pertaining to dark sector simply hint a problem with general relativity? What are the nature of dark sector ? The dark sector is still dark despite a long effort. If exists, dark energy/matter is likely to affect the gravitational phenomena in all distance scales including the local scales. As the evidences of dark sector so far are found only in large distance scale observations, the study of effects of dark energy/matter on local gravitational phenomena are important not only to confirm their presence but it may also help to understand the nature of the dark sector. Already several analysis have been performed so far in this direction, as will be reviewed in the next section, but certain aspects have not been addressed adequately.

In this thesis work we have examined the influences of dark energy and dark matter on different local gravitational phenomena critically considering different models of dark energy and dark matter. Emphasis will be given to discriminate the models of dark energy and dark matter by comparing theoretical predictions with the observations. We shall particularly investigate the influence of dark sector on several gravitational phenomena like gravitational time delay, gravitational time advancement, gravitational lensing etc. We shall construct static spherically symmetric metric for galactic halos based on flat rotation curve and cold dark matter approximation and shall examine whether such model is consistent with gravitational lensing observations. We shall also check whether some alternative dark matter models are consistent with Tully-Fisher relation or not.

1.8 Current status of studies on local gravitational influences of dark sector

The observation of gravitational influences on a few observables, namely perihelion shift of planets, bending of light by gravitating object, the time delay due to gravitating object and red-shift of photons, in the Solar System neighborhood provide the classical evidences in favor of the theory of GR. The influences of dark sector have been studied so far on all such classical gravitational observables which impose some constraints on dark sector parameters. However, solar system experiments put only upper bound on the dark sector parameters compared to the value obtained in cosmological observations.

The parametrized post-Newtonian (PPN) formalism is usually employed to describe the gravitational theories in a weak gravitational field equation (1.6) [5]. The PPN description provides the advantage of comparing predictions of GR with those from several alternative metric theory of gravity. However, the PPN formalism cannot, in general, accommodate the effect of the dark sector.

The geodesic equations for general static spherically symmetric metric as given in equation (1.5) give

$$A(r)(\frac{dr}{dp})^2 + \frac{J^2}{r^2} - \frac{1}{B(r)} = -E \tag{1.37}$$

where p is a parameter describing the trajectory and proportional to the proper time(τ),

$$J = r^2 \frac{d\phi}{dp}$$

and E is a constant which is equal to zero for photons and greater than zero for the material particles. Replacing the dp by the expression $d\phi$, we get,

$$\frac{A(r)}{r^4}(\frac{dr}{d\phi})^2 + \frac{1}{r^2} - \frac{1}{J^2 B(r)} = -\frac{E}{J^2} \tag{1.38}$$

If the external space time geometry due to the gravitating object is described by Schwarzschild metric equation (1.6), the above equation can be expressed as,

$$\frac{1}{r^4}(\frac{dr}{d\phi})^2 + \frac{B(r)}{r^2} - \frac{1}{b^2} = 0 \tag{1.39}$$

where, $E = 0$ for light trajectory and $b = r^2 \frac{d\phi}{dp}$, addressed as impact parameter.

Expressing $u = 1/r$ and differentiating equation (1.39) with respect to ϕ, we get the second order differential equation,

$$\frac{d^2u}{d\phi^2} + u = 3mu^2 \tag{1.40}$$

The general solution of the above equation is given by,

$$u = \frac{sin\phi}{R} + \frac{3m}{2R^2}(1 + \frac{1}{3}cos2\phi) \tag{1.41}$$

where, R is related with the closest distance(r_0) of light trajectory from the centre of the gravitating object by the expression,

$$\frac{1}{r_0} = \frac{1}{R} + \frac{m}{R^2} \tag{1.42}$$

The above equations are crucial to examine the influences of Schwarzschild geometry on different gravitational phenomena.

In the presence of cosmological constant (Λ), the exterior space-time due to a static spherically symmetric mass distribution is Schwarzschild-de Sitter (SDS) metric which is described by equation (1.5) with

$$B_\Lambda(r) = 1 - \frac{2m}{r} - \frac{1}{3}\Lambda r^2 \tag{1.43}$$

and

$$A_\Lambda(r) = [1 - \frac{2m}{r} - \frac{1}{3}\Lambda r^2]^{-1} \tag{1.44}$$

B(r) and A(r) are replaced by $B_\Lambda(r)$ and $A_\Lambda(r)$ respectively in equation (1.5).

For SDS geometry, ignoring higher order terms in Λ, the orbit equation reads,

$$\frac{d^2u}{d\phi^2} = \frac{m}{L^2} - u + 3mu^2 - \frac{\Lambda}{3L^2u^2} \tag{1.45}$$

The above equation is employed to determine the effect of Λ on various gravitational phenomena.

1.8.1 Influences of Dark sectors on perihelion shift of planets

The ability to explain perihelion shift of planets is a prominent success of general theory of relativity. At perihelia(r_-) and aphelia (r_+) of the orbit, r reaches at minimum and maximum with respect to the angular displacement and thus the $dr/d\phi$ vanishes at these two points. Applying this condition in equation (1.38) [5], we get,

$$\frac{1}{r_\pm} - \frac{1}{J^2B(r_\pm)} = -\frac{E}{J^2} \tag{1.46}$$

For the Schwarzschild metric in equation (1.6), the expression of precession of perihelia shift of planets becomes [33],

$$\Delta\phi_{Sch} = \pi\frac{6m}{L} \tag{1.47}$$

where $L(= l(1-e^2))$ is the semi-latus rectum of the elliptical orbit, e and l stand for the eccentricity and length of the semi-major axis of the orbit respectively.

The PPN metric is essentially an expansion about the Minkowski metric (g_{ij}) in terms of some dimensionless small gravitational (Newtonian) potential (U, ψ, φ) so that in isotropic coordinates

$$g_{00} = -1 + 2U - 2\beta U^2 + ... \tag{1.48}$$

$$g_{ij} = \delta_{ij}(1 + 2\gamma U + ...) \tag{1.49}$$

Where,

$$U(x,t) = \int \frac{\rho(x^{'},t)}{|x-x'|}d^3x' \tag{1.50}$$

where γ and β are first PPN parameters.

For the PPN metric, the expression of perihelion shift is given by [34],

$$\delta\phi = \frac{6m\pi}{L}(\frac{1}{3}(2+2\gamma-\beta) + \frac{1}{6}(2\alpha_1 - \alpha_2 + \alpha_3 + 2\kappa)\eta + \frac{JR^2}{2mL}) \tag{1.51}$$

where m is the mass of two-body system, i.e., m_1 and m_2 are the masses of two objects then $m \equiv m_1 + m_2$ and $\eta = m_1 m_2/m^2$, R and J are the mean radius of the oblate body and dimensionless measure of its quadrupole moment respectively, γ and β are the PPN parameters and α_1, α_2, α_3 and κ parameters are dependent on the ratio of masses of two-body system. The parameters α_1, α_2, α_3 and κ will be negligible for the mass of Mercury.

The contribution of Λ leads an additional shift over the Schwarzschild expression [35], [36], [37], [38], [39], [40].

$$\Delta\phi_\Lambda = \Delta\phi_{Sch} + \frac{\pi c^2 \Lambda l^3}{m}(1-e^2)^3 \tag{1.52}$$

Where $\Delta\phi_{Sch}$ is the perihelion shift due to Schwarzschild geometry as given in equation (1.47).

Several elaborated works on the effect of the cosmological constant on perihelion shift are discussed in the literature. Kerr et. al. found the general expression for effect of Λ on pericentre precession considering the arbitrary orbital eccentricity [41]. Iorio investigated the effect of the cosmological constant on perihelion precession for several solar planets in the frame-work of SDS space-time. Miraghaei and Nouri-Zonoz studied the perihelion shift of Mercury on the Newtonian limit of SDS metric and found the effect of Λ on perihelion shift [40].

Arakida studied the effect of the cosmological constant on the perihelion shift of planets and found a general expression for all orbital eccentricity [42].

The perihelion shift of planets due to alternative dark matter and dark energy models have been addressed by several authors.

One of the significant alternatives of Einstein's theory of general relativity is provided by Weyl gravity where conformal invariance of space-time has been used. The static spherically symmetric metric solution of Weyl gravity was obtained by Mannhein and Kazanas [30] which is found consistent with the experimental tests of gravitation in a weak gravitational field. As mentioned in equation (1.35) and (1.36), the static spherically symmetric vacuum solution of conformal gravity is given by:

$$ds^2 = -B(r)dt^2 + \frac{dr^2}{B(r)} + r^2(d\theta^2 + sin^2\theta d\phi^2) \tag{1.53}$$

where,

$$B(r) = 1 - \frac{\beta(2 - 3\beta\gamma)}{r} - 3\beta\gamma + \gamma r - \kappa r^2 \tag{1.54}$$

β, γ, and k stand for the integration constants. Putting the value of $k = \gamma = 0$, the metric provides the Schwarzschild metric and when $\gamma = 0$, it will give SDS metric. An explanation of the flat rotation curve of spiral galaxies has been provided by this metric solution of Weyl Conformal gravity which can be presented as an alternate solution of Dark matter problem.

The Precession of perihelion shift of planets was investigated using the above metric [43] and the expression of perihelion shift found for Weyl gravity is:

$$\delta\phi \approx \frac{6\pi\beta}{l(1-e^2)} + \frac{3\pi}{\beta}\kappa l^3(1-e^2)^3 - \frac{\pi}{\beta}\gamma l^2(1-e^2)^2 \tag{1.55}$$

where, β stands for $MG/c^2(\equiv m)$ and κ is equivalent to the cosmological constant $(\Lambda/3)$. If the equation (1.55) can be investigated minutely, it can be observed that the first term of right-hand side denotes the Schwarzschild term of perihelion precession of planets whereas the second term is the contribution for the cosmological constant and third term has been appeared due to the effect of γr term in the equation (1.54).

The perihelion shift has also been studied for quintessence model [44], MOND [45]; [46], f(r) gravity models [47]; [48].

Using the solar quadruple moment $J = (2.2 \pm 0.1) \times 10^{-7}$ [49] and substituting the orbital elements and constants for Mercury in solar orbit, the expression of perihelion shift is found,

$$\delta\phi = 42.\text{"}98(\frac{1}{3}(2 + 2\gamma - \beta) + 3 \times 10^{-4}\frac{J}{10^{-7}}) \tag{1.56}$$

Messenger spacecraft provided a significantly improved knowledge about orbital motion. Adopting the Cassini boundary limit of γ, the bound of β is given by $\beta - 1 = (-4.1 \pm 7.8) \times 10^{-5}$.

To detect the influence of Cosmological constant comparing with the Schwarzschild term, the perihelion shift of Mercury of 43" per century, is in full agreement of Einstein's theory of General Relativity with the accuracy of $430\mu as$ and the cosmological constant was constrained up to 10^{-41} order approximately [50]; [37] and achieved up to 10^{-42} order with -0.0036 ± 0.005 arc-secs accuracy level [51]. Including Sun's angular momentum and uncertainty of solar quadrupole moment, the Λ was constrained up to 10^{-43} order [52], i.e., 10^{-9} more precession level need to achieve to get the effect of dark energy. And to detect the dark matter effect, the ratio between Schwarzschild term and dark matter contribution (i.e. γ contribution) is very important and it is approximately in the order of 10^{-11} [43].

1.8.2 Influences of dark sectors on gravitational deflection of light:

Gravitational deflection of electromagnetic wave provides a prime evidence in favor of general relativity. The expression for deflection angle of electromagnetic wave due to a gravitating object (lens), coming from a source to an observer situated at r distance from the centre of the gravitating object, can be deduced from the geodesic equations (from the general equation of motion as mentioned in equation (1.38), considering $E = 0$ for electro-magnetic wave) which is given by,

$$\phi(r) - \phi_\infty = \int_r^\infty A^{1/2}(r)[(\frac{r}{r_0})^2(\frac{B(r_0)}{B(r)}) - 1]^{-1/2}\frac{dr}{r} \tag{1.57}$$

Implementing several metric solutions on the above expression, the gravitational deflection angle for the different gravitational models can be obtained.

For Schwarzschild metric the above expression of gravitational deflection becomes:

$$\Delta\phi_{sch} = \frac{4m}{r_0} \tag{1.58}$$

where the closest approach of the e.m. wave trajectory is denoted as r_0.

1.8.2.1 Approaches to deduce gravitational deflection angle on several dark sector models:

The early studies concluded that there should not be any effect of Λ on gravitational bending of light [35], [53], [37]. The motion of electromagnetic wave in SDS space-time can be described through the Lagrangian $\mathcal{L}$ of the space-time:

$$2\mathcal{L} = B_\Lambda(r)\dot{t}^2 - B_\Lambda^{-1}(r)\dot{r}^2 - r^2\dot{\phi}^2 \tag{1.59}$$

where $B_\Lambda(r) = 1 - \frac{2m}{r} - \frac{1}{3}\Lambda r^2$ and dot stands for the differentiation with respect to the affine parameter (λ). The motion is restricted to the $\theta = \pi/2$ plane. The conserved quantities, E (energy) and angular momentum (l'), can thus be expressed as

$$E \equiv B_\Lambda(r)\frac{dt}{d\lambda} \tag{1.60}$$

$$l' \equiv r^2\frac{d\phi}{d\lambda} \tag{1.61}$$

The null geodesic equation for the space time is given by,

$$\frac{d\phi}{dr} = \pm\frac{1}{r^2}[\frac{1}{b^2} - \frac{B_\Lambda(r)}{r^2}]^{-1/2} \tag{1.62}$$

where, $b \equiv l'/E$ which denotes impact factor in Schwarzschild space-time expression (1.39) as $\frac{dt}{dp} = -\frac{1}{B(r)}$ can be deduced from the Lagrangian. The second order differentiation leads,

$$\frac{d^2u}{d\phi^2} + u = 3mu^2 \tag{1.63}$$

That is exactly the same as the path equation in Schwarzschild geometry as equation (1.40). Note that the path equation does not involve Λ. Consequently the orbit equation will be same to the orbit equation for Schwarzschild metric in equation (1.41),

$$u = \frac{sin\phi}{R} + \frac{3m}{2R^2}(1 + \frac{1}{3}cos2\phi) \tag{1.64}$$

Absence of Λ in the above expression apparently suggests that there should not be any effect of the cosmological constant on the deflection of light. The bending angle in Schwarzschild space-time is estimated considering the limit $r \to \infty$ in the light orbital equation, and the angle between the two asymptotic directions gives the total deflection angle. For SDS space-time, however, $r \to \infty$ makes no sense. The de-Sitter horizon is $r_\Lambda = \sqrt{3/\Lambda}$ as may be obtained from the SDS metric. Rindler and Ishak thus proposed an alternative solution in which the angle is evaluated through the tangent on the light trajectory with the co-ordinate direction at a given arbitrary point. Subsequently, they obtained the expression for deflection angle in de-Sitter geometry as follows:

$$\Delta\phi_{\Lambda\,Rindler} = 2[\frac{2m}{R} - \frac{4m^3}{R^3} - \frac{\Lambda R^3}{12m}] \tag{1.65}$$

In SDS geometry expressed in equation (1.43) and (1.44), the tangent of the angle (ψ) of the light trajectory made with the coordinate point at a given point, is given by [54], [55],

$$tan\psi = rB_\Lambda(r)^{1/2}|\frac{d\phi}{dr}| \tag{1.66}$$

The above equation can be written for the null geodesics [56],

$$tan\psi = [\frac{B_\Lambda(r_0)}{B_\Lambda(r)}\frac{r^2}{r_0^2} - 1]^{-1/2} \tag{1.67}$$

Avoiding the higher order of m and Λ,

$$tan\psi = \frac{r_0}{r} + \frac{m}{r} - \frac{mr_0}{r^2} - \frac{\Lambda r_0 r}{6} + \frac{\Lambda r_0^3}{6r} \tag{1.68}$$

When $r >> r_0$ and the angles ψ and ϕ are very small and avoiding the higher order terms of m, Λ and r_0/r, the expression of deflection angle will be,

$$\Delta\phi_\Lambda = 2[\frac{2m}{r_0} - \frac{mr_0}{r^2} - \frac{\Lambda r_0 r}{6} + \frac{\Lambda r_0^3}{6r}] \tag{1.69}$$

Generalizing the results of Rindler and Ishak [54], Bhadra et. al. [55] calculated the angle between the lensed light trajectory at the source and the observer location as follows,

$$\Delta\phi_\Lambda = \frac{4m}{r_0} - mr_0(\frac{1}{d_{LS}^2} + \frac{1}{d_{LO}^2}) - \frac{\Lambda r_0}{6}(d_{LO} + d_{LS}) + \frac{\Lambda r_0^3}{6}(\frac{1}{d_{LO}} + \frac{1}{d_{LS}}) \tag{1.70}$$

where, d_{LO} and d_{LS} is the coordinate distances of gravitating object from observer and source respectively. For a small angle, R can be replaced as r_0.

Additionally, Bhadra et. al. [55] have given importance to a reference object to study the bending of a light trajectory by a gravitating object. Considering the

reference object, it has been found that the contribution of cosmological constant (Λ) is dependent on the distance between the source and the reference object.

Sereno [57], [58] has also supported the local coupling between the mass of the lens and the Λ in the expression of deflection angle in SDS metric. As per Sereno the gravitational deflection angle is expressed by as follows:

$$\begin{aligned}\Delta\phi_{Sereno}\approx\pi - \tfrac{4m}{b} + b(\tfrac{1}{r_{LS}} + \tfrac{1}{r_{LO}}) - \tfrac{15m^2\pi}{4b^2} - \tfrac{128m^3}{3b^3} + \tfrac{b^3}{6}(\tfrac{1}{{r_{LS}}^3} + \tfrac{1}{{r_{LO}}^3}) \\ - \tfrac{3465m^4\pi}{64b^4} - \tfrac{3584m^5}{5b^5} - \tfrac{2mb}{{r_\Lambda}^2} - \tfrac{mb^3}{4}(\tfrac{1}{{r_{LS}}^4} + \tfrac{1}{{r_{LO}}^4}) \\ + \tfrac{3b^5}{40}(\tfrac{1}{{r_{LS}}^5} + \tfrac{1}{{r_{LO}}^5}) - \tfrac{b^3}{2r_\Lambda}(\tfrac{1}{r_{LS}} + \tfrac{1}{r_{LO}})\end{aligned} \tag{1.71}$$

b stands for impact parameter and can be replaced by r_0 for a small deflection angle.

Schucker supported the approach of Rindler and Ishak and found the effect of cosmological constant due to isolated spherical mass without using lens equation [59]. Lake also supported the work and showed the effect of the cosmological constant using two opposite sources [60]. Bhattacharya et. al. used the Rindler-Ishak procedure to analyze the gravitational deflection of light using the Einstein-Strauss vacuole model with cosmological constant [61].

In the contrary, some authors questioned the contribution of Λ on the gravitational deflection of light. Khriplovich and Pomeransky demonstrated that it doesn't affect practically on gravitational lensing using Friedmann-Robertson-Walker coordinates [62]. Park also concluded that no correction was needed involving cosmological constant by solving null geodesic equations [63].

Ishak derived the contribution of the cosmological constant on gravitational deflection from the gravitational potential and Fermat's principle [64]. He further found the Λ contribution on geometrical time delay term for the bending of light.

Miraghaei and Nouri-Zonoz studied the gravitational deflection on the Newtonian limit of SDS metric and found the effect of Λ on general relativistic approach [40].

Arakida and Kasai re-examined the effect of the cosmological constant on gravitational deflection of light and showed that the Λ appears in the orbital equation

of light [65]. Aghili et. al. studied the effect of cosmological constant for time varying cosmological expansion, i.e. when Hubble constant varies with time[66].

Biressa et. al. studied the effect of cosmological constant on gravitational lensing to calculate projected mass of lens including cosmological constant [67].

Butcher argued accepting the cosmological constant correction on gravitational lensing of light that the effect is negligible in the practical way as it is smaller than the uncertainty from unlensed distances [68].

Guenouche and Zouzou investigated the gravitational lensing in the framework of the Einstein-Straus solution with positive cosmological constant considering closed Universe [69].

The local influence of gravitational deflection has been studied in scaler field model of dark energy [70], where a spherically symmetric static metric was developed in quintessence model of dark energy and studied the effect on gravitational deflection. The metric they have developed is as follows:

$$ds^2 = (1 - \frac{2m}{r} - \frac{\alpha}{r^{3w+1}})dt^2 - (1 - \frac{2m}{r} - \frac{\alpha}{r^{3w+1}})^{-1}dr^2 - r^2(d\theta^2 + sin^2\theta\phi^2) \quad (1.72)$$

where α is a constant of integration and w is the constant of the equation of state which varies $-1 \leq w < 0$ where$-1 \leq w < -1/3$ shows the nature of dark energy dominating accelerating universe and $w = 0$ signifies matter-domination and $w = 1/3$ radiation domination.

Using the quintessence based metric, the second order equation of motion is given by:

$$\frac{d^2u}{d\phi^2} + u = 3mu^2 + \frac{3\alpha(w+1)u^{2w+2}}{2} \quad (1.73)$$

Solving the equation analytically, they have found the solution of the above second order equation for different values of the constant of equation of state w, for example, for $w = -1/3$,

$$\Delta\phi_{quintessence} = \frac{4m}{r_0} + \frac{4m}{r_0(1-\alpha)^{3/2}} \quad (1.74)$$

and for $w = -1$, which is equivalent to the cosmological constant model, no influence of cosmological constant is noticed, i.e. at $w = -1$, the gravitational deflection angle term turns into a pre-Rindler-Ishak expression of gravitational deflection in SDS space-time.

$$\Delta\phi_{quintessence} = \Delta\phi_{\Lambda} = \frac{4m}{r_0} \tag{1.75}$$

Rectifying the evaluation process by applying Rindler-Ishak [54] approach, the influence of dark energy in the quintessence metric has been deduced [71].

On the other hand, the gravitational deflection is the prime evidence of dark matter. This phenomenon has been used as a tool to verify different approaches of dark matter effect associated models. As mentioned earlier Modified Newtonian Dynamics(MOND) is a significant model to represent dark matter effects. Gravitational bending in MOND, has been studied by several physicists [72], [73], [74].

The gravitational deflection angle in MOND, is given by:

For $r_0 > r_c$,

$$\Delta\phi_{MOND} = \pi\frac{\sqrt{Ga_0M}}{c^2} \tag{1.76}$$

For $r_0 \leq r_c$,

$$\Delta\phi_{MOND} = \frac{2GM}{c^2r_0}\sqrt{\frac{r_c - r_0}{r_c + r_0}} + \frac{2GM}{c^2r_c}\sqrt{\frac{r_c - r_0}{r_c + r_0}} + \frac{2\sqrt{Ga_0M}}{c^2}sin^{-1}\frac{r_0}{r_c} \tag{1.77}$$

For $r_c \to \infty$, the above expression turns into Newtonian expression of gravitational deflection angle,

$$\Delta\phi_{Newtonian} = \frac{2GM}{c^2r_0} \tag{1.78}$$

where r_0 is the impact parameter of light trajectory and r_c is the critical radius of Newtonian mechanic and MOND in flat rotation curve, expressed by $r_c = \sqrt{GM(r_c)/a_0}$, a_0 is a constant called critical accelerating parameter, (M is the effective mass of gravitating object) [75].

It should be mentioned that the general relativistic correction of factor '2' has also been adopted in MOND expression for the expression of the deflection angle.

Now considering the conformal Weyl gravity metric as mentioned in equations (1.35) and (1.36) [30], the expression of gravitational deflection angle was studied [76] and then further reexamined by Sultana and Kazanas [77], based on the approach by Rindler and Ishak [54].

$$\Delta\phi_{Weyl} = \frac{4m}{b} - \frac{2m^2\gamma}{b} - \frac{\kappa b^3}{2m} \tag{1.79}$$

where b stands for the impact parameter and can be replaced by closest approach(r_0) of light trajectory from the centre of the gravitating object and γ represents the dark matter effect and κ is equivalent to cosmological constant ($\Lambda/3$). But objection raised by Cattani et. al. [78] due to negative contribution of dark matter effect which is represented by γ, where the contribution should be enhancement effect on Schwarzschild term of lensing angle. They analyzed the issue and explained that the actual conformal metric as mentioned in equation (1.36) is given as follows:

$$B(r) = \alpha - \frac{2m}{r} + \gamma r - \kappa r^2 \tag{1.80}$$

where $\alpha = (1 - 6m\gamma)^{1/2}$ and $\alpha = 1$ approximated for the distances neither too large nor too small. But no such approximation is made in this work. As per this work, negative contribution of γ was appeared due to avoiding the first order terms associated with $\alpha \neq 1$ and the expression of gravitational deflection for Weyl gravity considering all the first order terms of γ, is given by,

$$\Delta\phi_{weyl} = \frac{4m}{r_0} - \frac{\kappa r_0^2}{2m} + \frac{15m^2\gamma}{r_0} \tag{1.81}$$

The above expression of the deflection angle shows the positive contribution of γ term which holds the practical dark matter influence.

Sultana reexamined the gravitational deflection of light on conformal Weyl gravity to get the 2nd order contribution of γr and found that the contribution is insignificant [79].

Lim and Wang derived an exact solution for gravitational lensing using static spherically symmetric metric for SDS and Mannhein-Kazanas metric of Weyl gravity both [80].

The gravitational lensing effect was also studied in f(r) gravity model [81], [47], [48].

Starting from Eddington and his co-workers, several attempts have been made to measure gravitational deflection angle. For the PPN metric, the of gravitational deflection is given by [34],

$$\delta\phi = \frac{1}{2}(1+\gamma)\frac{4m}{r_0}(\frac{1+cos\psi}{2}) \tag{1.82}$$

where m is the mass of the gravitating object, ψ is the angle between observer to lens line and incoming direction of photon to the observer and γ is the first PPN parameter that varies from theory to theory. For example, for Schwarzschild metric $\gamma = 1$.

Eddington and his co-workers first time attempted the experimental observation [82] and they found the deflection angle with 30 percent accuracy and the result was scattered between one half and twice the Einstein value of lensing angle. However, the scenario has been changed after the development of radio interferometry measurements. The very long baseline radio interferometer (VLBI) provided improved precession level of the deflection angle. The modern techniques have the capability to produce the accuracy more than 100 micro-second.

The solar system gravitational bending observations do not put stringent constraint on Λ; to detect the influence of cosmological constant the precession level of measuring bending angle needs to be approximately 10^{-18} times higher than the precision level of detecting contribution of Schwarzschild term (from equation (1.70)) if the source is situated at kpc distance [55]. However, the contribution of Λ to the deflection angle can be larger than the second-order term in the deflection angle lensed by pure Schwarzschild geometry for several cluster lens systems [64]. The effect of Weyl model of dark matter (equation (1.81)), is negligibly small [77].

1.8.3 The influences of dark sector on gravitational time delay:

The gravitational time delay is a phenomenon where the object under gravity suffers time delay when it moves under the influence of gravitating object, if we compare the total traveling time of the object, required in absence of the gravitating object. Shapiro first proposed the phenomenon of gravitational time delay and carried out a measurement with Lincoln Laboratory collaboration using a radar signal that traveled to a planet and reflected back to earth [83]. To derive the theoretical expression of gravitational time delay, again the general equation of motion, equation (1.37), is used. Replacing dp by dt using the relation $\frac{dt}{dp} = \frac{1}{B(r)}$, one obtains

$$\frac{A(r)}{B^2(r)}(\frac{dr}{dt})^2 + \frac{J^2}{r^2} - \frac{1}{B(r)} = -E \tag{1.83}$$

For light trajectory, $E = 0$ and $\frac{dr}{dt}$ must be vanished at the closest approach of light trajectory (at $r = r_0$), so equation (1.83) gives,

$$J^2 = \frac{r_0^2}{B(r_0)} \tag{1.84}$$

Therefore, the equation of motion for light trajectory, is given by,

$$\frac{A(r)}{B^2(r)}(\frac{dr}{dt})^2 + (\frac{r_0}{r})^2\frac{1}{B(r_0} - \frac{1}{B(r)} = 0 \tag{1.85}$$

From the above equation, the time required to travel for a light beam from r_0 to r or vice-versa is given by,

$$t(r, r_0) = \int_{r_0}^{r} (\frac{A(r)/B(r)}{1 - \frac{B(r)}{B(r_0)}(\frac{r_0}{r})^2})^{1/2} dr \tag{1.86}$$

For Schwarzschild metric, we get

$$t_{Sch}(r, r_0) \simeq \sqrt{r^2 - r_0^2} + 2mln(\frac{r + \sqrt{r^2 - r_0^2}}{r_0}) + m(\frac{r - r_0}{r + r_0})^{1/2} \tag{1.87}$$

The first term in the above expression denotes the time required for light to travel in a straight line with unit velocity of light. Second and third terms reflect the gravitational contribution of traveled time, and positive term expresses the time delay effect.

1.8.3.1 Approaches to deduce gravitational time delay on several dark sector models:

The influences of dark energy and dark matter have been studied in several works. Kagramanova et al [37] studied the influence of dark energy in SDS metric as mentioned in equation (1.43) and (1.44). As per the study, the expression of gravitational time delay is

$$t_\Lambda(r, r_0) \simeq \sqrt{r^2 - r_0^2} + 2mln(\frac{r + \sqrt{r^2 - r_0^2}}{r_0}) + m(\frac{r - r_0}{r + r_0})^{1/2}$$
$$+\frac{\Lambda}{18}[(\sqrt{r^2 - r_0^2})(2r^2 + r_0^2) + 3m(4r\sqrt{r^2 - r_0^2} + r_0^2(2 + \frac{\sqrt{r^2 - r_0^2}}{r + r_0}))] \quad (1.88)$$

where Cosmological constant(Λ) associated term reflects the dark energy contribution on gravitational time delay in SDS space-time.

On the other hand, Asada examined the gravitational time delay of light in several modified gravity models [84]. He introduced a general static spherically symmetric metric, represented as,

$$A(r) \approx 1 - \frac{2m}{r} + A_m r^m \quad (1.89)$$

and

$$B(r) \approx 1 + \frac{2m}{r} + B_n r^n \quad (1.90)$$

where $m = GM/c^2$, M is the mass of gravitating object and A_m, B_n, m and n are varies with dark energy model to model. For example, when $n = 2$, $A_n = -B_m = -\Lambda/3$, the metric represents Schwarzschild-De-Sitter(SDS) metric and for $n = 1/2, A_n = -2B_n = \pm 2\sqrt{m/r_c^2}$, it shows the DGP model of dark energy.

Asada deduced the expression of gravitational time by considering the radio signal transmitted from earth (situated at r_E co-ordinate distance), reflected back from a reflector, situated at r_R co-ordinate distance and r_o is the closest approach of the signal's trajectory from the centre of the gravitating object and the expression is given by:

$$\delta t = 2(\sqrt{r_E^2 - r_o^2} + \sqrt{r_R^2 - r_0^2}) + 2m(2ln\frac{r_E + \sqrt{r_E^2 - r_0^2}}{r_0} + 2ln\frac{r_R + \sqrt{r_R^2 - r_0^2}}{r_0} + \sqrt{\frac{r_E - r_0}{r_E + r_0}} + \sqrt{\frac{r_R - r_0}{r_R + r_0}}) + \delta t_{DE} \quad (1.91)$$

where δt_{DE} denotes dark energy effect contribution in time delay expression, expressed as (for $n = m > 0$),

$$\delta t_{DE} = r_0^{n+1}(\int_1^{R_E} + \int_1^{R_R})dR \times (-A_n\frac{R^{n+3} - 2R^{n+1} + R}{(R^2-1)^{3/2}} + B_n\frac{R^{n+1}}{\sqrt{R^2-1}}) \quad (1.92)$$

where $R \equiv r/r_0$, $R \equiv r_E/r_0$ and $R_R \equiv r_R/r_0$. And taking $r_R >> r_0$ and $n \neq 0$, the following expression was obtained by Asada,

$$\delta t_{DE} = \frac{B_n - A_n}{n+1}(r_E^{n+1} + r_R^{n+1}) + \frac{B_n + A_n}{2(n-1)}(r_E^{n-1} + r_R^{n-1} - 2r_0^{n-1})r_0^2 + O(r_0^4) \quad (1.93)$$

The above equation is a generalized expression of dark energy effect in gravitational time delay for different models with different values of A_n, m and n as mentioned earlier.

Schucker and Zaimen studied the effect of cosmological constant on gravitational time delay for an isolated spherical mass [85].

Ishak derived the contribution of the cosmological constant on gravitational time delay from the gravitational potential and Fermat's principle [64]. He also found the Λ contribution on geometrical time delay term.

Guenouche and Zouzou investigated the gravitational time delay in the framework of the Einstein-Straus solution with positive cosmological constant considering closed Universe [69].

Effect of dark energy on Gravitational time delay was also studied in quintessence model of dark energy [86]. Considering the quintessence metric as mentioned in equation (1.72), the quintessence model based expression of gravitational time delay is given by,

$$t_{Quintessence}(r, r_0) = t_{Sch} + \int_{r_0}^{r} (1 - \frac{r_0^2}{r^2})^{-1/2} [\frac{r^{3\omega+1} - r_0^{3\omega+1}}{r_0^{3\omega-1} r^{3\omega+1} (r^2 - r_0^2)} + \frac{2}{r^{3\omega+1}}] \frac{\alpha}{2} \quad (1.94)$$

The quintessence term in the above equation was solved for different values of ω. For example, if $\omega = -1/3$, the quintessence associated term will be $\alpha r \sqrt{1 - \frac{r_0^2}{r^2}}$ and for $w = -1$, which is actually signifies the cosmological constant model, that will be $\frac{\alpha r}{6}(2r^2 + r_0^2)\sqrt{1 - \frac{r_0^2}{r^2}}$ which supports the cosmological constant associated expression of gravitational time delay when $\alpha \equiv \Lambda/3$ and avoiding higher-order and multiplication terms of Λ and m.

The gravitational time delay was also studied under the influence of dark matter environment which is provided in Weyl gravity by Mannhein and Kazanas [30] and the metric represented by the equation (1.35) and (1.36). The effect of dark matter on gravitational time delay was studied using the conformal metric by Ederly and Paranjape [76] and found the expression of time delay, to travel for a radar signal from r_0 to r distance considering the centre of the gravitating object(of mass M) as co-ordinate centre, as follows,

$$\begin{aligned} t_{weyl}(r, r_0) \simeq \sqrt{r^2 - r_0^2} + 2\beta ln \frac{r + \sqrt{r^2 - r_0^2}}{r_0} + \beta \sqrt{\frac{r - r_0}{r + r_0}} \\ -\frac{\gamma}{2}(\frac{r^3 - r_0^3}{\sqrt{r^2 - r_0^2}}) + \frac{\kappa}{6}(2r^2 - r_0^2)\sqrt{r^2 - r_0^2} \end{aligned} \quad (1.95)$$

As mentioned earlier, β in above equation (1.95) stands for $GM/c^2 (\equiv m)$, γ represents the dark matter effect and κ is equivalent to cosmological constant($\Lambda/3$). The above equation (1.95) reflects the dark matter effect associated term as well

as the Schwarzschild metric related term as mentioned in equation (1.87) and dark energy associated Λ term as shown earlier in equation (1.88).

Farrugia et. al. studied the gravitational time delay in f(r) gravity model [48].

If a radar signal is sent to a planet or satellite from Earth and passes through the vicinity of the Sun, the expression of gravitational time delay under PPN metric is given by [34],

$$t(r, r_0) = \frac{1}{2}(1+\gamma)[240 - 20ln(\frac{r_0^2}{r})]\mu s, \tag{1.96}$$

Several high precession measurements were made using radar signal passing near the conjunction of a gravitating object after the discovery of the significant consequence of general relativity by Irwin Shapiro in 1964. A round trip travel time, through the vicinity of the gravitating object, is to be measured to get the gravitational time delay value and fit the value of γ can be found based on least square fit method, which depends on which space-time metric has been adopted, by using equation (1.96). To measure the gravitational time delay by Sun as a gravitating object for a radar signal, few artificial satellites like Voyager-2, Mariners 6 and 7, Viking Mars landers and orbiters, Cassini spacecraft, were used as re-transmitters of the radar signal and Mercury, Venus or Saturn was used as reflectors.

The gravitational time delay measurements restrict up to $(\gamma - 1 = (2.1 \pm 2.3) \times 10^{-5})$ γ by Cassini spacecraft taking Saturn as a re-transmitter and reflector [87].

The gravitational time delay relates with frequency shift. The relative change of frequency,

$$y = \frac{\nu(t) - \nu_0}{\nu_0}$$

where ν_0 is the emitted frequency of the wave and $\nu(t)$ is the received frequency at the Earth. The Schwarzschild contribution to the change of frequency (y) is in the order of 10^{-10} order and the Cassini spacecraft measured in the order of 10^{-13}.

The time delay measurements though provide most stringent constraint on the PPN parameter γ but restrict Λ loosely; the Cassini observations suggest $\Lambda \leq 10^{-24}\ m^{-2}$ [37]. The dark matter parameter in equation (1.89) is constrained upto

$10^{-23}cm^{-1}$ order using the Shapiro time delay [76] where the value of γ is in the order of $10^{-28}cm^{-1}$.

1.8.4 The influences of dark sector on gravitational frequency-shift:

The concept of gravitational frequency-shift arises theoretically from the concept of proper time($d\tau$) which is defined by the time interval measured by the clock of an observer in rest, i.e. spatial co-ordinate interval $dx^i = 0$. The expression of proper time is given by,

$$d\tau = \sqrt{g_{00}}dx^0 \tag{1.97}$$

$\sqrt{g_{00}} = B(r)$ in equation (1.5).

If we compare the proper time interval at two distinct point of space but both correspond to the same interval of co-ordinate time, then the ratio of proper time interval is given by,

$$\frac{d\tau_1}{d\tau_2} = \sqrt{\frac{g_{00}(x_1)}{g_{00}(x_2)}} \tag{1.98}$$

where the $d\tau_1$ and $d\tau_2$ are the proper time interval at x_1 and x_2 position respectively. And considering ν_1 and ν_2 are the frequencies of a photon at x_1 and x_2 points respectively, then the above equation can be expressed as,

$$\nu_2\sqrt{g_{00}(x_2)} = \nu_1\sqrt{g_{00}(x_1)} \tag{1.99}$$

The above equation expresses the frequency shift under the gravitational influence. Using Schwarzschild metric ($g_{00} = B(r) = 1 - \frac{2m}{r}$) as mentioned equation-(1.6), the expression of gravitational frequency shift will be as follows:

$$\frac{\nu_2}{\nu_1} \simeq 1 - \frac{m}{r_2} + \frac{m}{r_1} \tag{1.100}$$

The higher order terms of m/r_1 and m/r_2 are avoided, where $m = GM/c^2$ and ν_1 and ν_2 are the frequencies of same photon traveling from r_1 and r_2 co-ordinate distance respectively.

1.8.4.1 Approaches to deduce gravitational frequency-shift on several dark sector models:

The gravitational frequency shift has been also studied in several models of dark sectors. Kagramanova.et.al. [37] and Sereno. et.al. [38] have studied the gravitational frequency shift in Cosmological constant model of dark energy by using SDS metric as shown in equation (1.43) and (1.44).

The expression of gravitational shift in SDS metric is given by,

$$\frac{\nu_2}{\nu_1} \simeq 1 - \frac{m}{r_2} + \frac{m}{r_1} - \frac{\Lambda}{6}(r_2^2 - r_1^2) \tag{1.101}$$

The higher order terms of m/r_1 and m/r_2 are avoided,, where $m = GM/c^2$ and ν_1 and ν_2 are the frequencies of same photon traveling from r_1 and r_2 co-ordinate distance respectively and Λ stands for the cosmological constant.

The gravitational frequency shift was also studied in Quintessence model dark energy using the metric as mentioned earlier in equation (1.72) and expression of gravitational frequency shift was found by [70], [88],

$$\frac{\nu_2}{\nu_1} \simeq 1 - \frac{m}{r_2} + \frac{m}{r_1} + \Delta\nu_{quintessence} \tag{1.102}$$

where,

$$\Delta\nu_{quintessence} = \frac{\alpha}{2}\left(\frac{1}{r_2^{3\omega+1}} - \frac{1}{r_1^{3\omega+1}}\right) \tag{1.103}$$

The significance of ω, α are mentioned earlier in equation (70).

Farrugia et. al. investigated the gravitational frequency shift in f(r) gravity model [48].

The gravitational frequency shift under the PPN metric is expressed by,

$$\Delta\nu = (1+\beta)\frac{\Delta U}{c^2} \tag{1.104}$$

where β is the PPN parameter. The first time the gravitational frequency shift was successfully measured in Pound-Rebka-Snider experiment of 1960-1965 using gamma-ray photon at Harvard University.

In recent times, an advanced hydrogen maser clock, placed on International Space Station and an atomic clock based on Cesium called PHARAO (Project D'Horloge Atomique par Refroidissement d'Atomes en Orbit) are used to measure the gravitational frequency shift under the Atomic Clock Ensemble in Space(ACES) project.

The precession level has been achieved so far up to 10^{-15} order using clock comparison and 10^{-15} H-maser in GP-A redshift measurement [89]. But to sense the effect of dark energy, the accuracy must be reached at least 10^{-38} order [37].

1.8.5 Gravitational wave and a wider aspect to detect the influences of dark sector:

The theory of general relativity suggests that the ripple of space-time perturbation will travel in the form of a wave in the transverse direction of propagation, which can be expressed as follows:

$$(-\frac{\delta^2}{\delta t^2} + c^2\Delta^2)h_{\mu\nu} = 0 \tag{1.105}$$

where, $h_{\mu\nu}$ is a very weak perturbation of space-time metric, nearly Minkowsky metric in Spacial Relativity, c stands for speed of light, $\Delta = (\frac{\delta^2}{\delta x^2} + \frac{\delta^2}{\delta y^2} + \frac{\delta^2}{\delta z^2})$, the spatial second order differential operator. No component of the metric perturbation ($h_{\mu\nu}$) is found in direction of wave propagation.

Gravitational effects have been tested so far in different distance scales and gravity strength areas (like weak and strong gravity regions). Gravitational wave astronomy has been explored the possibilities to test the gravitation in large scale and strong field regime as it can travel a large distance without any interruption, unlike electromagnetic wave. The recent detection of gravitational wave by LIGO, has opened up the window to explore the reality of dark sector and many other

unresolved astronomical problems. Total five binary black-hole [90], [91], [92], [93], [94], [95] and a binary neutron star [96] sourcing GW have been detected so far.

A recent observation by advanced LIGO and Virgo detectors, a strong signal of gravitational wave event GW170817 has been detected from a merger of binary neutron stars [97] and a gamma-ray(GRB170817A) was also detected from the same region of gravitational wave source by the same LIGO-Virgo detectors. The detection of GW170817 was the first multi-messenger astronomical observation from where both gravitational wave and electromagnetic wave have been detected. These observations enable to be used as the sources of standard siren which able to measure the astronomical distances of the sources using gravitational waves. Measuring distances of the source by siren and red-shift of the electromagnetic wave, the Hubble constant can be measured and using this way, the dynamic nature of the Universe can be analyzed with high precision and existence and effect of dark energy will be re-verified. On the other hand, dark matter, in the form of axions or ultra-light bosons, form clouds around a black-hole, which is observable with gravitational waves [97].

Chapter 2

Influences of dark energy and dark matter on gravitational time advancement

2.1 Introduction

As mentioned in last chapter, the discovery of the acceleration of the universe's expansion [9, 98–100] has led inclusion of a new component into the energy-momentum tensor of the universe having negative pressure, the so called dark energy component. On the other hand data from rotation curve surveys [101] and few other observations [102, 103] demand that there is a dominating component of matter in galaxies which is non-luminous or dark. Several other observations which include the cosmic microwave background (CMB) measurements [104, 105, 107, 107], baryon acoustic oscillations (BAO) [108–110], lensing in clusters [111, 112] support the existence of dark energy as well as the presence of dark matter halo surrounding the Galactic disc. Consequently on large distance scales, astrophysical and cosmological phenomena are governed mainly by dark matter and dark energy.

The simplest candidate for dark energy is the cosmological constant (Λ): a constant energy density with equation-of-state parameter w=-1 and the ΛCDM model where CDM refers to cold dark matter, is in accordance with all the existing cosmological observations [113, 114] such as the cosmic microwave background (CMB)

anisotropies, the large scale structure, the scale of the baryonic acoustic oscillation in the matter power spectrum and the luminosity distance of the supernovae type Ia but it has a big theoretical problem - it's size ($\sim 10^{-52}\ m^{-2}$) is many orders of magnitudes below the expected vacuum energy density in the standard model of particle physics [115]. Hence many other theoretical explanations for the DE have been proposed in the last chapter in which the parameter w evolves with time or different from -1 such as the quintessence [14–16], k-essence [19–22], phantom field [17, 18]], Chaplygin gas [23, 24] models. There are also proposals for modification of general relativity which include Scalar tensor theories [116] or f(R) gravity models [25], conformal gravity model [30, 117], massive gravity theories [118] including Dvali-Gabadadze-Porrati (DGP) braneworld gravity [27, 119] models etc., which lead to late-time accelerated expansion without invoking any dark energy.

Like dark energy, there are also several candidates for dark matter [120] such as WIMPs, Axions, Sterile neutrinos etc. There are proposals for modifications at the fundamental theoretical level as well which include MOND [29, 121–123] that suggests modifications in Newtonian dynamics. The evidence of presence of non-baryonic dark matter from the CMB data, however, questions the MOND like schemes. The conformal gravitational theory [30, 117], which is based on Weyl symmetry, also can explain flat rotation curves of galaxies without the need of dark matter.

Dark energy/matter is likely to affect the gravitational phenomena in all distance scales including the local scales. Several investigations have so far been made to estimate the influence of dark energy (mainly through cosmological constant) on different local gravitational phenomena which include the three classical observables - the perihelion shift of planets [35, 37], gravitational bending of light [37, 54, 55, 57, 58] and gravitational time delay (or Shapiro time delay) [37, 84, 124] which are already elaborated in last chapter. Due to the tiny value of Λ, the influence of dark energy has been found very small, not detectable by the ongoing experiments. Out of the local gravitational phenomena the effect of Λ is found maximum in the case of perihelion precession of planets and the observations on perihelion precession of mercury put an upper bound of $\Lambda \leq 10^{-42}\ m^{-2}$ [52]. On the other hand analysis of the perihelion precession of Mercury, Earth, and Mars also lead to a upper bound $3 \times 10^{-19}\ g/cm^3$ for dark matter density (ρ_{dm}) [125]

whereas the rotation curve data implies that ρ_{dm} in the Milky Way at the location of solar system is $\rho_{dm} = 0.5 \times 10^{-24}\ g/cm^3$ [126].

In this chapter, we would like to examine the influence of dark energy and dark matter on gravitational time advancement. Gravitational time advancement effect takes place when the observer is situated at stronger gravitational field in respect to the gravitational field encountered by the photon while traversing to a certain path [127]. We found that dark energy and dark matter do affect the gravitational time advancement and though the magnitude of the effect is small, it induces an interesting observational consequence, at least in principle.

The organization of the chapter is the following. In the next section(2.2) we discuss briefly the gravitational time advancement effect. The influence of Dark energy and dark matter on Gravitational Time Advancement are evaluated in Section 2.3. The results are discussed in section 2.3.1 and 2.3.2 and finally we conclude in section 2.4.

2.2 Gravitational Time Advancement

The gravitational time delay is one of the classical solar system tests of General relativity. The general perception about gravitational time delay is that due to influence of gravitating object the average global speed of light is reduced from its spacial relativistic value c_0 and hence the signal always suffers an additional time delay. But depending upon the position of the observer, the delay can as well be negative which was mentioned as gravitational time advancement [127]. To exemplify the effect let us consider light is propagating in a gravitational field between two points A and B. Assuming standard Schwarzschild geometry, i.e.

$$ds^2 = -(1 - 2\mu/r)dt^2 + (1 - 2\mu/r)dr^2 + r^2/d\Omega^2\ , \tag{2.1}$$

total coordinate time required for the round trip journey between the points A and B (or between the points B to A and back) to the first order in $\mu = GM/c_0^2$, is given by [125]

$$
\begin{aligned}
c_0\Delta t_{AB} &= 2\left(\sqrt{r_A^2-r_o^2}+\sqrt{r_B^2-r_o^2}\right)+ \\
&\quad +4\mu\left(ln\frac{r_A+\sqrt{r_A^2-r_o^2}}{r_o}+ln\frac{r_B+\sqrt{r_B^2-r_o^2}}{r_o}\right)+ \\
&\quad 2\mu\left[\left(\frac{r_A-r_o}{r_A+r_o}\right)^{1/2}+\left(\frac{r_B-r_o}{r_B+r_o}\right)^{1/2}\right] \qquad (2.2)
\end{aligned}
$$

where r_A and r_B are the radial coordinates of the point A and B respectively and r_o is the closest distance to the gravitating object in the photon path.

Suppose the point A is located at relatively much weaker gravitational field due to mass M than the point B i.e. $r_A >> r_B$ where r_A and r_B are the values of coordinate r evaluated at the position A and B respectively. Hence the proper time, between transmission and the reception of the signal to be measured by the observer at the point A, is

$$
\begin{aligned}
c_0\Delta\tau_{AB} &\simeq (1-\frac{\mu}{r_A})\Delta t_{AB}\simeq 2\left(\sqrt{r_A^2-r_o^2}+\sqrt{r_B^2-r_o^2}\right) \\
&\quad +4\mu\left(ln\frac{r_A+\sqrt{r_A^2-r_o^2}}{r_o}+ln\frac{r_B+\sqrt{r_B^2-r_o^2}}{r_o}\right)+ \\
&\quad 2\mu\left[\left(\frac{r_A-r_o}{r_A+r_o}\right)^{1/2}+\left(\frac{r_B-r_o}{r_B+r_o}\right)^{1/2}\right]. \qquad (2.3)
\end{aligned}
$$

In the above expression the first term on the right hand side is the usual the special-relativistic time of travel. The rest two terms are general relativistic corrections. As a result, the observed time will be higher than the time taken between transmission and the reception in the absence of gravitating object which is the well known gravitational time delay.

Now let us consider the case that the observer is at the point B instead of the point A. In that case the proper time between transmission and the reception of the signal to be measured by the observer will be [127]

$$
\begin{aligned}
c_0\Delta\tau_{AB} \simeq\ & (1-\frac{\mu}{r_B})\Delta t_{AB} \simeq 2\left(\sqrt{r_A^2-r_o^2}+\sqrt{r_B^2-r_o^2}\right) \\
& +4\mu\left(ln\frac{r_A+\sqrt{(r_A^2-r_o^2)}}{r_o}+ln\frac{r_B+\sqrt{(r_B^2-r_o^2)}}{r_o}\right)+ \\
& 2\mu\left[(\frac{r_A-r_o}{r_A+r_o})^{1/2}+(\frac{r_B-r_o}{r_B+r_o})^{1/2}\right] \\
& -2\mu(\frac{\left(\sqrt{r_A^2-r_o^2}+\sqrt{r_B^2-r_o^2}\right)}{r_B})
\end{aligned}
\tag{2.4}
$$

Due to the last term of the right hand side of the above expression, which is the dominating one among the general relativistic correction terms, the time taken between transmission and the reception will be reduced from the usual the special-relativistic time of travel when the distance between A and B exceeds certain value. This effect is known as gravitational time advancement (negative time delay) that arises because of the clock runs differently at different positions in gravitational field.

2.3 Influence of Dark energy/matter on Gravitational Time Advancement

In the presence of dark energy the exterior spacetime of spherically symmetric mass distribution is no longer described by Schwarzschild geometry, but by some modification of Schwarzschild metric. For instance if dark energy is cosmological constant, the exterior static spacetime will be Schwarzschild- de Sitter (SDS) spacetime.

Here we shall consider a general static spherically symmetric metric of the form

$$ds^2 = -B(r)dt^2 + A(r)dr^2 + r^2/d\Omega^2 \tag{2.5}$$

with

$$B(r) = 1 - 2m/r - a\Lambda r^n/3 \tag{2.6}$$

and

$$A(r) = (1 - 2m/r - \Lambda r^n/3)^{-1} \tag{2.7}$$

where a and Λ are constants. Different choices of n and a lead to different models of dark energy.

case 1: With n=1/2, a=2, $\Lambda = \pm\sqrt{GM/r_c^2}$ the model represents the gravitational field of a spherically symmetric matter distribution on the background of an accelerating universe in Dvali-Gabadadze-Porrati (DGP) braneworld gravity provided leading terms are only considered [128]. r_c is the crossover scale beyond which gravity becomes five dimensional.

case 2: For the choice n=1, a=1 and negative Λ, the model well describes the gravitational potential due to central matter distribution plus dark matter [30, 31, 117].

case 3: If n=3/2, a=2/3 and $\Lambda = -m_g^2\sqrt{\frac{2GM}{13c^2}}$, the model corresponds to the non-perturbative solution of a massive gravity theory (an alternative description of accelerating expansion of the universe) [129] where m_g is the mass of graviton.

case 4: When a=1, n=2 and $m = \mu$ the above metric describes the Schwarzschild-de Sitter (SDS) or Kotler space-time which is the exterior space time due to a static spherically symmetric mass distribution in presence of the cosmological constant Λ [130].

2.3.1 General trajectory

Now let us suppose that a light beam is moving between two points A and B in the gravitational field of equations (2.5), (2.6) and (2.7). The expression for coordinate time required for light rays to traverse the distance r_o to r, where r_o is the closest distance from the gravitating object over the trajectory can be obtained from geodesic equations which is given by

$$\delta t = \int_{r_o}^{r} \sqrt{P(r, r_o)}\, dr\,, \tag{2.8}$$

where,

$$P(r, r_o) = \frac{A(r)/B(r)}{1 - \frac{r_o^2}{r^2}\frac{B(r)}{B(r_o}} \tag{2.9}$$

For general power index (n) of Λ in equation (2.5), the above equation after integration can only be expressed in terms of hyper-geometric functions and thereby not very useful. However, for n=1 and n=2, the integral can be written in a handful form, particularly when higher order terms in M and Λ are ignored. The extra coordinate time delay (δt_1^Λ) induced by the dark sector terms in equation (2.8) is given by for n=1 and $\Lambda = -\Lambda$,

$$\begin{aligned} \delta t_1^\Lambda &= -(a+1)\frac{\Lambda}{12}\left(r\sqrt{r^2 - r_o^2} + r_o^2 ln(r + \sqrt{r^2 - r_0^2})\right) - \\ &\quad \frac{a\Lambda r_o^2}{6}\left(ln(r + \sqrt{r^2 - r_0^2}) - \sqrt{\frac{r - r_o}{r + r_o}}\right) , \end{aligned} \tag{2.10}$$

while for n=2

$$\delta t_2^\Lambda = (a+1)\frac{\Lambda}{18}\left((r^2 + 2r_o^2)\sqrt{r^2 - r_o^2}\right) - \frac{a\Lambda r_o^2}{6}\sqrt{r^2 - r_o^2}\,, \tag{2.11}$$

and for general n ($n \neq 1$) when $r_A >> r_o$ and $r_B >> r_o$,

$$\delta t_n^\Lambda \simeq \frac{(a+1)\Lambda}{6(n+1)} r^{n+1} - \frac{(a-1)\Lambda}{12(n-1)} r^{n-1} r_o^2 + O(r_o^4) \tag{2.12}$$

Hence the proper time between the transmission and the reception of the signal to be measured by the observer at point B will be for n=1

$$
\begin{aligned}
c_0\Delta\tau_1 \;\simeq\;& 2\left(\sqrt{r_A^2-r_o^2}+\sqrt{r_B^2-r_o^2}\right)+\\
& 4\mu\left(ln\frac{r_A+\sqrt{r_A^2-r_o^2}}{r_o}+ln\frac{r_B+\sqrt{r_B^2-r_o^2}}{r_o}\right)+\\
& 2\mu\left[(\frac{r_A-r_o}{r_A+r_o})^{1/2}+(\frac{r_B-r_o}{r_B+r_o})^{1/2}\right]-\\
& (a+1)\frac{\Lambda}{12}\left(r_A\sqrt{r_A^2-r_o^2}+r_o^2\,ln(r_A+\sqrt{r_A^2-r_o^2})\right)+\\
& \frac{a\Lambda r_o^2}{6}\left(\sqrt{\frac{r_A-r_o}{r_A+r_o}}-ln(r_A+\sqrt{r_A^2-r_o^2})\right)-\\
& (a+1)\frac{\Lambda}{12}\left(r_B\sqrt{r_B^2-r_o^2}+r_o ln(r_B+\sqrt{r_B^2-r_o^2})\right)+\\
& \frac{a\Lambda r_o^2}{6}\left(\sqrt{\frac{r_B-r_o}{r_B+r_o}}-ln(r_B+\sqrt{r_B^2-r_o^2})\right)\\
& -2\left(\frac{\mu}{r_B}-\frac{a\Lambda r_B}{3}\right)\left(\sqrt{r_A^2-r_o^2}+\sqrt{r_B^2-r_o^2}\right)
\end{aligned}
\tag{2.13}
$$

Usually for observing time advancement effect, $r_o = r_B$. Further for describing flat rotation curve, a has been chosen as 1. Hence the above equation reduces to

$$
\begin{aligned}
c_0\Delta\tau_1 \;\simeq\;& 2\sqrt{r_A^2-r_B^2}+4\mu\; ln\left(\frac{r_A+\sqrt{r_A^2-r_B^2}}{r_B}\right)+\\
& 2\mu\left(\frac{r_A-r_B}{r_A+r_B}\right)^{1/2}-\\
& \frac{\Lambda}{6}\left(r_A\sqrt{r_A^2-r_B^2}+r_B^2\;ln\left(r_A+\sqrt{r_A^2-r_B^2}\right)\right)-\\
& \frac{\Lambda}{6}r_B^2\left(\sqrt{\frac{r_A-r_B}{r_A+r_B}}-ln(r_A+\sqrt{r_A^2-r_B^2})\right)\\
& -2\left(\frac{\mu}{r_B}-\frac{\Lambda r_B}{3}\right)\sqrt{r_A^2-r_B^2}
\end{aligned}
\tag{2.14}
$$

When $r_A >> r_B$, the above equation transforms to

$$
\begin{aligned}
c_0\Delta\tau_1 \;\simeq\;& 2r_A-2\mu\left(\frac{r_A}{r_B}-2ln\left(\frac{2r_A}{r_B}\right)-1\right)-\\
& \frac{\Lambda}{6}\left(r_A^2+2r_B^2 ln2r_A-4r_A r_B\right)
\end{aligned}
\tag{2.15}
$$

Similarly for n=2 with $r_o = r_B$

$$\begin{aligned} c_0\Delta\tau_2 &\simeq 2\sqrt{r_A^2 - r_B^2} + \\ &4\mu\, ln\left(\frac{r_A + \sqrt{r_A^2 - r_B^2}}{r_B}\right) + 2\mu\left(\frac{r_A - r_B}{r_A + r_B}\right)^{1/2} \\ &+(a+1)\frac{\Lambda}{18}\left(r_A^2 + 2r_B^2\right)\sqrt{r_A^2 - r_B^2} - \\ &\frac{a\Lambda r_B^2}{6}\sqrt{r_A^2 - r_B^2} - 2\left(\frac{\mu}{r_B} + \frac{a\Lambda r_B^2}{3}\right)\sqrt{r_A^2 - r_B^2} \end{aligned} \tag{2.16}$$

which for $r_A >> r_B$ becomes

$$\begin{aligned} c_0\Delta\tau_2 &\simeq 2r_A + 2\mu\left(2ln\left(\frac{2r_A}{r_B}\right) + 1 - \frac{r_A}{r_B}\right) \\ &+\frac{\Lambda}{18}\left((a+1)r_A^3 + ar_A r_B^2\left(2 - 13a\right)\right) - 2\frac{ar_A r_B}{3}\Big) \end{aligned} \tag{2.17}$$

and for general n

$$\begin{aligned} c_0\Delta\tau_n &\simeq 2r_A + 2\mu\left(2ln\left(\frac{2r_A}{r_B}\right) + 1 - \frac{r_A}{r_B}\right) \\ &+\frac{(a+1)\Lambda}{6(n+1)}r^{n+1} - \frac{(a-1)\Lambda}{12(n-1)}r^{n-1}r_o^2 - \\ &\frac{2a\Lambda r_A r_B^n}{3} \end{aligned} \tag{2.18}$$

Unless Λ effect dominates over the pure Schwarzschild effect, the net time delay will be negative in all the above cases resulting time advancement.

2.3.2 Small distance travel

Let us suppose a light beam is moving from a point on the Earth surface(B) (R, θ, ϕ) where the radius of Earth is denoted as R_E, to a nearby point with coordinates C$(R + \Delta R, \theta, \phi)$ and reflects back to the transmitter position(B). The light signal will travel null curve of space-time satisfying $ds^2 = 0$. Then the proper distance between point B and point C is given by,

$$\begin{aligned}\Delta L_{BC} &= \int_R^{R+\Delta R}(1-2m/r-\Lambda r^n/3)^{-1/2}dr \\ &\simeq \Delta R[1+\frac{m}{R}-\frac{m\Delta R}{2R^2}+\frac{\Lambda R^n}{6}(1+\frac{n\Delta R}{2R}+\frac{n(n-1)\Delta R^2}{6R^2}) \\ &+\frac{3m^2}{2R^2}+\frac{m\Lambda R^{n-1}}{2}(1+\frac{(n-1)\Delta R}{2R})] \end{aligned} \tag{2.19}$$

The coordinate time interval in transmitting a light signal from B to C and back, is given by,

$$\begin{aligned}\Delta t &= 2\int_R^{R+\Delta R}(1-\frac{2m}{r}-\frac{\Lambda r^n}{3})^{-1/2}(1-\frac{2m}{r}-\frac{a\Lambda r^n}{3})^{-1/2}dr \\ &\simeq 2L_{BC}[1+\frac{m}{R}+\frac{3m^2}{2R^2}+\frac{\Lambda aR^n}{6}(1+\frac{n\Delta R}{2R}+\frac{n(n-1)\Delta R^2}{6R^2}) \\ &+m\Lambda(R^{n-1}(1+\frac{(n-1)\Delta R}{2R})(\frac{2a}{3}+\frac{1}{6}) \\ &-\frac{(a+1)R^{n-1}}{6}(1+\frac{n\Delta R}{2R})+\frac{R^{n-2}(a+1)\Delta R}{12})-\frac{m\Delta R}{2R^2}] \end{aligned} \tag{2.20}$$

The observer at B will experience that coordinate time interval in proper time to be measured by the observer at B between transmission and reception of the signal is given by,

$$\begin{aligned}\Delta\tau_1 &= (1-\frac{2m}{R}-\frac{a\Lambda R^n}{3})^{1/2}\Delta t \\ &\simeq 2L_{BC}[1+\frac{\Lambda aR^n}{6}(\frac{n\Delta R}{2R}+\frac{n(n-1)\Delta R^2}{6R^2}) \\ &+m\Lambda(R^{n-1}(1+\frac{(n-1)\Delta R}{2r})(\frac{2a}{3}+\frac{1}{6})-\frac{R^{n-1}(a+1)}{6}(1+\frac{n\Delta R}{2R}) \\ &+\frac{R^{n-2}(2a+1)\Delta R}{12}-\frac{aR^{n-1}}{6}(3+\frac{n\Delta R}{2R}))-\frac{m\Delta R}{2R^2}] \end{aligned} \tag{2.21}$$

In deriving the above equations, the higher order terms in Λ and $m^2\Lambda$, m^3, $m^2\frac{\Delta R^2}{R^2}$and higher order m terms have been neglected.

2.4 Discussion and Conclusion

Dark energy has a significantly different kind of influence on gravitational time advancement than that of pure Schwarzschild geometry. The time advancement effect is entirely due to pure Schwarzschild geometry, while dark energy leads to only time delay effect which means gravitational time advancement effect will be reduced in presence of dark energy. When $\Lambda r_A^2 > 2\mu/r_B$, there no time advancement at all. So in principle the time advancement effect should be able to identify dark matter clearly.

In contrast the conformal theory description of flat rotation curve suggests large time advancement effect. The fitting of galactic rotation curves suggest $\Lambda/3 = -(5.42\times10^{-42}\frac{M}{M_\odot}+3.06\times10^{-30})\ cm^{-1}$ [131]. Therefore, in our galaxy, dark matter potential should start dominating over the luminous matter contribution (pure Schwarzschild part) at distances larger than about 30 kpc. Hence at distances beyond $\sim$ 30 kpc time advancement effect will be quite large. The experimental realization to examine gravitational time advancement effect at such distances is a challenging issue.

Here it is worthwhile to mention that the gravitational time advancement effect has not been experimentally verified yet but it should not be very difficult to test the effect. This is because the magnitude of time advancement effect is reasonably large. In fact gravitational time advancement is a much stronger effect than gravitational time delay when large distances are involved. However, time delay has the advantage of probing stronger gravity. In the solar system tests of gravitation, time delay measurements are mainly relied on passage of radiation grazing the sun thereby solar gravitational potential at the surface of the sun comes into play. In such a situation the time delay is about 240 μsec whereas the total special relativistic travel time between the earth and the sun is about 1000 seconds which means the gravitational time delay is about 2×10^{-7} part of the total travel time. For testing gravitational time advancement from the earth or its surroundings, on the other hand, solar gravitational potential at the position of earth shall be applicable and when light propagates from the earth to say Pluto and back, the time advancement will be about 1 msec over the total propagation time of 50000 seconds i.e. here the time advancement is about 0.2×10^{-7} part of the total travel time which is just one order smaller than time delay caused by the sun and hence is detectable. Note that the above estimates need to be corrected taking into

account the variations in round-trip travel time due to the orbital motion of the target relative to the Earth by using radar-ranging or any other similar kind of data. Since gravity can not be switched off, one does not have access to a special relativistic propagation of photon against which the time delay to be measured. Therefore, variations of time delay is measured as a function of distance to verify the radial profile of equation (2.3). Similar check can be made for the time advancement also.

The future missions such as the Beyond Einstein Advanced Coherent Optical Network (BEACON) [132] or the GRACE Follow-On (GRACE-FO) mission [133] will probe the gravitational field of the Earth with unprecedented accuracy. The BEACON mission will employ four small spacecraft equipped with laser transceivers and the spaceraft will be placed in circular Earth orbit at a radius of $80,000$ km. All the six distances between the spacecraft will be measured to high accuracy ($\sim 0.1\ nm$) out of which one diagonal laser trajectory will be very close to the Earth thereby pick the gravitational time delay effect. If the distance between the spacecraft and the Earth is also measured by an Earth bound observer and compared with distances measured by the spacecraft, the time advancement effect may be revealed from the measurements. The GRACE-FO, which is scheduled for launch in 2017, will be equipped with a laser ranging interferometer and is expected to provide range with an accuracy of 1 nm and with such level of accuracy general relativistic effects may become significant [134]. It is, therefore, important to examine whether the effect of time advancement can have any significant effect on observables of GRACE-FO.

To probe dark matter through it's influence on gravitational time advancement properly, one requires to observe time advancement (delay) effect at distance ~ 30 kpc or beyond. For probing dark energy observations are to be made at even higher distances. This is currently not feasible. At present observations can be made only from the earth or from its neighborhood via a satellite/space station. So strategies to be developed for observing time advancement/delay effect at other distances, may be some indirect means. This would be very challenging task.

For small distance travel, the time advancement effect is a second order effect, unlike the long distance travel where time advancement occurs due to first order effect. However, since the time advancement effect is cumulative in nature, if a light beam is allowed to travel say from the earth surface radially upwards to a nearby point large number of times it (the light beam) should acquire time advancement

of reasonable magnitude when observed from the earth surface which should be measurable.

In summary, we investigate the influence of dark matter/energy on gravitational time advancement. We obtain analytical expression for time advancement to first order in M and Λ where Λ is the parameter describing the strength of dark matter/energy. From our results it is found that dark energy leads to gravitational time delay only whereas pure Schwarzschild metric gives both time delay and time advancement (negative effective time delay) depending on the position of the observer.

The present finding suggests that in principle the measurements of gravitational time advancement at large distances can verify the dark matter and a few dark energy models or put upper limit on the dark matter/energy parameter.

Chapter 3

Probing dark matter and dark energy through gravitational time advancement

3.1 Introduction:

Light propagation in gravitational field leads to an extra time delay over the time required for light transmission between two points in Euclidean space, which is the well known gravitational or Shapiro time delay effect [83], [135]. The observation of the time delay effect in the solar system constitutes one of the classical tests of general relativity. The difference in gravitational time delay between photon/-gravitational waves and neutrinos or any other neutral particle with non-zero mass also has been used as a probe to examine the Principle of Equivalence [136] and dark sector of the universe [84], [137]. Presently the gravitational time delay effect is often employed to measure the masses of pulsars in binary systems [138], [139].

Gravitational time delay is generally estimated by evaluating the additional coordinate time needed by a photon or a particle in a round trip journey in a gravitational field of a massive object over the coordinate time required in the absence of the gravitating object. However, the coordinate time difference is not a measurable quantity in a gravitational field; one needs to convert the coordinate time difference in to proper time difference which is a real measurable quantity. When such conversion is considered an opposite kind of effect, the so called gravitational

time advancement (GTA) (negative time delay), is taken place if the observer is situated at stronger gravitational field in respect to the gravitational field encountered by the photon during its journey [127]. The GTA effect is essentially caused by the fact that clock runs differently in gravitational field depending on the curvature. The GTA of photons has been found to be affected by dark matter and dark energy [140] and therefore, at least in principle, the measurements of GTA at large distances can verify the dark matter and a few dark energy models or put upper limit on the dark matter/energy parameters. The measurement of GTA also can be employed to discriminate the Gravity Rainbow (photons of different energies experience different gravity levels) from pure General Relativity [141].

Like photons, particles having non-zero masses should also suffer GTA when the observer is at stronger gravitational field. In this chapter, we like to derive expression of GTA for particles with non-zero mass in Schwarzschild geometry. We further wish to examine the effect of the gravitational field that describes the observed rotation curve of spiral galaxies (in this chapter we denote it as dark matter field) and the dark energy in the form of Cosmological constant on gravitational time advancement. The importance of the present investigation is many fold: It offers, at least in principle, to probe the presence of dark matter and dark energy, it constitutes a possible test of the GTA and it allows to estimate mass of a particle of unknown mass.

The plan of the chapter is the following. In the next section(3.2) we shall present the basic formulation for calculating gravitational time advancement for a particle. In section 3.3 we shall estimate the GTA in a round trip journey by a particles under the influence of Schwarzschild geometry. In section 3.4 we shall study the effect of cosmological constant and dark matter gravitational field on GTA. We shall discuss the results in section 3.5 and conclude our findings in the same section.

3.2 Methodology

Consider the following scenario: An electromagnetic/gravitational wave or a particle is moving between the points A and B in a gravitational field due to a static spherically symmetric matter distribution as depicted in figure 3.1.

We consider that the gravitational field is described by a general static spherically symmetric metric,

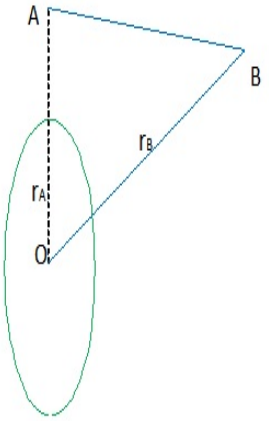

FIGURE 3.1: Geometrical configuration of time delay/advancement of photon/-particle in gravitational field. O is the Centre of the spherically symmetric mass distribution, A and B are two arbitrary points. r_A and r_B are radial distances of X and Y from O respectively.

$$ds^2 = -\kappa(r)c^2dt^2 + \sigma(r)dr^2 + r^2d\Omega^2 \ . \tag{3.1}$$

The geodesic equations for a test particle motion in equatorial plane under the influence of the space time given by equation (3.1) leads to the following relation

$$\frac{\sigma(r)}{\kappa(r)^2}\left(\frac{dr}{dt}\right)^2 + \frac{\alpha_1}{r^2} - \frac{c^2}{\kappa(r)} = -\alpha_2 c^2 \,, \tag{3.2}$$

where α_1 ($\equiv r^4\left(\frac{d\phi}{dp}\right)^2$, p is an affine parameter obeying the relation $d\tau^2 = \kappa(r)dp^2$ for particles with non-zero mass and $p = \tau$ for photon) and α_2 ($\equiv \left(\kappa(r)\frac{d(ct)}{d\tau}\right)^{-2}$) are associated with the constants of motion, α_1 is related to the angular momentum of the particle and α_2 is related to the energy ϵ of the particle. At the distance of closest approach r_o, $\frac{dr}{dt}$ must vanish, which gives

$$\alpha_1 = c^2 \left[-\alpha_2 + \frac{1}{\kappa(r_o)} \right] r_o^2 \,, \tag{3.3}$$

and $\alpha_2 = \frac{m^2 c^4}{\kappa(r_o)\epsilon^2}$, m and ϵ ($\equiv mc\sqrt{B}\frac{d(ct)}{d\tau}$) are the mass and energy of the particle. Hence the time required by a particle to traverse a distance from r_o to r is given by

$$\Delta t\,(r, r_o) = \frac{1}{c} \int_{r_o}^{r} \sqrt{P(r, \alpha_2)}\, dr \,, \tag{3.4}$$

where,

$$P(r, \alpha_2) = \frac{\sigma(r)/\kappa(r)}{\left[1 - \alpha_2\, \kappa(r) + \frac{{r_o}^2}{r^2} \left(\alpha_2\, \kappa(r) - \frac{\kappa(r)}{\kappa(r_o)} \right) \right]} \,. \tag{3.5}$$

Therefore the difference in proper time between transmission and reception in a round trip journey of the signal to be measured by the observer at r_o is

$$\Delta\tau = 2\sqrt{\kappa(r_o)} \Delta t\,(r, r_o), \tag{3.6}$$

Since the expression in equation (3.6) through equation (3.4) involves integration of the function $P(r, \alpha_2)$ which involves the metric coefficients $\sigma(r)$ and $\kappa(r)$, explicit expressions for $\sigma(r)$ and $\kappa(r)$ are required to proceed further. In the following sections we shall evaluate the proper time between transmission and reception for three different physically viable choices of $\sigma(r)$ and $\kappa(r)$.

3.3 GTA of a particle with non-zero mass in Schwarzschild geometry

In the Schwarzschild geometry i.e. when $\kappa(r) = \sigma(r)^{-1} = 1 - \frac{2\mu}{r}$ where $\mu = GM/c^2$, G is the gravitational constant and c is the speed of light, the coordinate time delay in round trip journey by a particle of mass m between A and B up to the first order accuracy of μ is given by

$$\begin{aligned}\Delta t_m^{Sch} &= \frac{2}{c\sqrt{1-\alpha_2}}\Bigg[\sqrt{r_A^2 - r_o^2} + \sqrt{r_B^2 - r_o^2} \\ &+ \frac{\mu\,(2-3\alpha_2)}{(1-\alpha_2)} \ln \frac{\left(r_A + \sqrt{r_A^2 - r_o^2}\right)\left(r_B + \sqrt{r_B^2 - r_o^2}\right)}{r_o^2} \\ &+ \frac{\mu}{(1-\alpha_2)}\left(\sqrt{\frac{r_A - r_o}{r_A + r_o}} + \sqrt{\frac{r_B - r_o}{r_B + r_o}}\right)\Bigg], \end{aligned} \tag{3.7}$$

For a particle of mass m and energy ϵ, $\alpha_2 = \frac{m^2c^4}{(1-2\mu/r_o)\epsilon^2}$. Hence the difference in proper time between transmission and reception of a particle of mass m from A to B and back to be measured by the observer at A reads

$$\begin{aligned}\Delta\tau_m^{Sch} &= \sqrt{B(r_A)}\Delta t_m^{Sch} \simeq \frac{2}{c\sqrt{1-\alpha_2}}\Bigg[\left(\sqrt{r_A^2 - r_o^2} + \sqrt{r_B^2 - r_o^2}\right)\left(1 - \frac{\mu}{r_A}\right) + \\ &\frac{\mu\,(2-3\alpha_2)}{(1-\alpha_2)} \ln \frac{\left(r_A + \sqrt{r_A^2 - r_o^2}\right)\left(r_B + \sqrt{r_B^2 - r_o^2}\right)}{r_o^2} \\ &+ \frac{\mu}{(1-\alpha_2)}\left(\sqrt{\frac{r_A - r_o}{r_A + r_o}} + \sqrt{\frac{r_B - r_o}{r_B + r_o}}\right)\Bigg]. \end{aligned} \tag{3.8}$$

Since both $\frac{\mu}{r_A}$ and Shapiro delay terms are small compare to special relativistic term, here we have ignored their higher order and cross terms. In the absence of the gravitating object (i.e. in flat space time) the time required by a particle of mass m and energy ϵ to travel between A and B is

$$\left(\sqrt{r_A^2 - r_o^2} + \sqrt{r_B^2 - r_o^2}\right) / \left(c\sqrt{1 - m^2c^4/\epsilon^2}\right).$$

Due to gravitational effect this time is shorten by a factor $(1 - \mu/r_A)$ (first term in the right hand side of the above expression). The observed time will be smaller than the special relativistic time of propagation when the distance between A and B exceeds a certain value so that μ/r_A factor overcomes the Shapiro delay. The above expression thus gives the GTA for particles with mass m. The GTA for massless particles such as photon can be readily obtained from the above equation by putting $\alpha_2 = 0$ (corresponding to $m = 0$).

If r_B is much larger than r_A and r_o, the expression for GTA of particle with mass m can be approximated as

$$\Delta\tau_m^{Sch} \approx \frac{2}{c\sqrt{1-\alpha_2}} r_B \left(1 - \frac{\mu}{r_A}\right) , \tag{3.9}$$

For relativistic particles ($\epsilon >> m$) and when $r_o \sim r_A$ the equation (3.9) reduces to

$$\Delta\tau_m^{Sch} \approx \frac{2r_B}{c} \left[\left(1 - \frac{\mu}{r_A}\right)\left(1 + \frac{m^2}{2\epsilon^2}(1 + 2\mu/r_A)\right)\right] . \tag{3.10}$$

Therefore, the difference in arrival times after a round trip journey between particle with mass m and energy ϵ and photon those emitted at the same time reads

$$\Delta\tau_m^{Sch} - \Delta\tau_\gamma^{Sch} \approx \frac{m^2c^3r_B}{\epsilon^2}\left(1 + \mu/r_A\right) , \tag{3.11}$$

The first part in the right hand side of the above expression is the special relativistic effect whereas the second part is the GR correction.

Under the same conditions the difference in arrival times between particles with the same mass but different energies ϵ_1 and ϵ_2 with $\epsilon_2 > \epsilon_1$ is given by

$$\Delta\tau_m^{Sch}(\epsilon_2) - \Delta\tau_m^{Sch}(\epsilon_1) \approx m^2c^3r_B\left(\frac{1}{\epsilon_2^2} - \frac{1}{\epsilon_1^2}\right)\left(1 + \mu/r_A\right) , \tag{3.12}$$

Here an important point to be noted by examining the equation (3.7) that the sign of the expression of Shapiro time delay does not change for traveling from a stronger field to a weaker one and back again instead of traveling from a weak gravitational field to a stronger one and return back (the Shapiro delay is the same

in both the situation). Rather a new effect, owing to the fact that that clock runs differently in gravitational field depending on the curvature, comes into play that leads to negative time delay or GTA in all the cases. The Shapiro delay mainly varies logarithmically with distance while the GTA varies linearly with distance. For a particle traveling from a weak gravitational field to a stronger one and return back magnitude of the negative time delay effect is much smaller than that of the Shapiro time delay, the resulting delay thus is a positive one. But when a particle travels from a stronger field to a weaker one and back again, the negative delay component starts dominating after a certain (small) distance, leading to a net GTA.

We have not mentioned any particular particle so far, our results are very general, applicable to any particle with non-zero mass and even with zero mass. However, charged particles also suffer electromagnetic interaction and therefore, only stable neutral particles can be exploit to examine the GTA/Shapiro time delay effect in a realistic situation. Neutrons with life time around 15 minutes in its rest frame, can be utilized to test GTA/Shapiro delay in certain astrophysical situations not involving very large distances. Neutrinos are stable but their mass is not definitely known yet. Moreover the upper limit of their mass is too small so that the mass effect on GTA of neutrinos is very small.

We would estimate the magnitude of the GTA effect for a simple situation as follows: Consider that photon and thermal neutron are simultaneously sent from the top of the Earth's atmosphere towards the Moon where they (photon and neutron) are reflected back at the originating point. To survive without decay, the kinetic energy of the neutron has to be at least around 1 MeV. The Shapiro delay of photon and 1 MeV neutron in the mentioned case are 0.07 ns and 0.07 μs respectively whereas the GTA of photon and 1 MeV neutron will be ~ 0.9 ns and 1.8 μs respectively. The difference in arrival times between two neutrons, one with kinetic energy 1 MeV and other having kinetic energy 10 MeV will be about 1.6 μs. The magnitude of the GTA effect in the mentioned situation is thus well within the reach of the modern experiments. .

The future astrometric missions Beyond Einstein Advanced Coherent Optical Network (BEACON) [132] or the GRACE Follow-On (GRACE-FO) [133] are expected to detect the GTA effect employing laser beam from space craft. The mission BEACON will put six numbers of small spacecraft in a circular orbit of radius 80000 km and each spacecraft will be equipped with laser transceivers. Introduction of

thermal neutron transceivers along with laser transceivers in such a future mission will lead to detect the GTA effect of particles.

3.4 Effect of Dark sector on GTA of a relativistic particle

A wide variety astrophysical observations suggest that ordinary baryonic matter composes only 4.9% of the matter in the Universe [107]. The rest is mainly composed of dark energy (68.3%) and dark matter (26.8%) components of unknown nature [107]. In this section we shall examine the effect of dark matter and dark energy on GTA. We shall consider the same physical scenario as depicted in figure 3.1.

The presence of dark energy and dark matter lead to some modification of the Schwarzschild metric as the exterior space-time of a spherically symmetric mass distribution. Let us consider the following functional form of $\sigma(r)$ and $\kappa(r)$ in equation (3.1)

$$\kappa(r) = 1 - 2\mu/r - \beta_1 r^n \tag{3.13}$$

and

$$\sigma(r) = 1 + 2\mu/r + \beta_2 r^n \tag{3.14}$$

where n, β_1 and β_2 are constants. We shall consider the following cases:

case 1: The choice $n = 1$, and $\beta_1 = \beta_2 = -\beta = -\left(5.42 \times 10^{-39} \frac{M_B}{M_\odot} + 3.06 \times 10^{-28}\right)$ m^{-1} (i.e. a linear potential), where M_B is mass of baryonic matter in galaxy, has been found to describe well the observed flat rotation curves (with maximum extension upto extending around 100 kpc) of a sample of 111 spiral galaxies [131],

[142]. Since the radial extension of dark matter in a galaxy is not known, maximum radial distance of validity of the model can not be stated with certainty. But in general the model should not be extended to intergalactic scale.

case 2: When $n = 2$, $\beta_1 = \beta_2 = \Lambda/3$ the above metric represents the Schwarzschild-de Sitter (SDS) or Kotler space-time which is the exterior space time due to a static spherically symmetric mass distribution in presence of the cosmological constant Λ with $\Lambda \sim 10^{-52}\mathrm{m}^{-2}$ [130].

The coordinate time required by a particle to traverse a round trip distance from r_A, which coincides with the distance of closest approach, to r_B under the influence of space time geometry defined by equation (3.1), (3.12) and (3.13) is given by [137]

$$\Delta t_n(r_B, r_A) \approx \Delta t_m^{Sch}(r_B, r_A) + \frac{1}{c\sqrt{1-\alpha_2}}\{[\beta_1 + \beta_2 - \frac{\beta_1\alpha_2}{(1-\alpha_2)}]\mathcal{I}_n^1 - \frac{\beta_1}{(1-\alpha_2)}\mathcal{I}_n^2\}, \tag{3.15}$$

where, $\mathcal{I}_n^1$ and $\mathcal{I}_n^2$ are integrals defined by

$$\mathcal{I}_n^1 = \int_{r_A}^{r_B} \frac{{r_B}^{n+1}\, dr}{\sqrt{({r_B}^2 - r_A^2)}}$$

and

$$\mathcal{I}_n^2 = r_A^2 \int_{r_A}^{r_B} \frac{r_B\,({r_B}^n - r_A^n)\; dr}{({r_B}^2 - r_A^2)\,\sqrt{({r_B}^2 - r_A^2)}}.$$

In the above equation $\alpha_2 = \frac{m^2}{(1-2\mu/r_o-\beta_1 r^n)\epsilon^2}$ which is also to be used here in Δt_m^{Sch}.

For $n = 1$ and $n = 2$ corresponding to DM and DE model respectively, we have analytical solutions of $\mathcal{I}_1^1$, $\mathcal{I}_1^2$ and $\mathcal{I}_2^1$, $\mathcal{I}_2^2$ which are given below

$$\begin{aligned} \mathcal{I}_1^1 &= \frac{r_B}{2}\sqrt{r_B^2 - r_A^2} + \frac{r_A^2}{2}\,\ln\frac{r_B + \sqrt{r_B^2 - r_A^2}}{r_A}, \\ \mathcal{I}_1^2 &= -r_A^2\sqrt{\frac{r_B - r_A}{r_B + r_A}} + r_A^2 \ln\frac{r_B + \sqrt{r_B^2 - r_A^2}}{r_A}\,. \end{aligned} \tag{3.16}$$

$$\mathcal{I}_2^1 = \frac{1}{3}\sqrt{r_B^2 - r_A^2}\left(r_B^2 + 2r_A^2\right) ,$$
$$\mathcal{I}_2^2 = r_A^2\sqrt{r_B^2 - r_A^2} . \tag{3.17}$$

Thus for the dark matter model i.e. when $n = 1$, $\beta_1 = \beta_2 = -\beta$ the proper time required for the travel by a particle with mass m and energy ϵ for the round trip travel between A to B as measured by an observer at A is given by

$$\begin{aligned}\Delta\tau_m^{\beta} \simeq\ & \Delta\tau_m^{Sch} - \frac{1}{c\sqrt{1-\alpha_2}}\Bigg[\left(\beta - \frac{\beta\alpha_2}{2(1-\alpha_2)}\right)\Bigg(r_B\sqrt{r_B^2 - r_A^2} \\ & + r_A^2 \ln\frac{r_B + \sqrt{r_B^2 - r_A^2}}{r_A}\Bigg) - \frac{\beta r_A^2}{(1-\alpha_2)}\left(\sqrt{\frac{r_B - r_A}{r_B + r_A}} + \ln\frac{r_B + \sqrt{r_B^2 - r_A^2}}{r_A}\right) \\ & + \beta r_A\sqrt{r_B^2 - r_A^2}\Bigg]\end{aligned} \tag{3.18}$$

In the above expression we have ignored the cross terms between M and β and higher order terms in β. It is noted from the above equation that β reduces the net time advancement.

In the presence of the cosmological constant ($n = 2$, $\beta_1 = \beta_2 = \Lambda/3$), the proper time required for the travel by a particle with mass m and energy ϵ for the round trip journey between A to B as measured by an observer at A reads

$$\begin{aligned}\Delta\tau_m^{\Lambda} \simeq\ & \Delta\tau_m^{Sch} + \frac{1}{3\,c\sqrt{1-\alpha_2}}\Bigg[\left(2\Lambda - \frac{\Lambda\alpha_2}{1-\alpha_2}\right)\left(\frac{1}{3}\sqrt{r_B^2 - r_A^2}\left(r_B^2 + 2r_A^2\right)\right) \\ & - \frac{\Lambda}{1-\alpha_2}\left(r_A^2\sqrt{r_B^2 - r_A^2}\right) - \Lambda r_A^2\sqrt{r_B^2 - r_A^2}\Bigg]\end{aligned} \tag{3.19}$$

When $r_B >> r_A$, considering only the leading order terms, for relativistic particles the equation (3.18) and (3.19) respectively reduce to

$$\Delta\tau_m^{\beta} \approx \frac{r_B}{c}\left[\left(1 - \frac{\mu}{r_A} - \beta r_B/2\right)\left(1 + \frac{m^2}{2\epsilon^2}(1 + 2\mu/r_A - \beta r_A)\right)\right] . \tag{3.20}$$

and

$$\Delta\tau_m^{\Lambda} \approx \frac{r_B}{c}\left[\left(1-\frac{\mu}{r_A}+\Lambda r_B^2/9\right)\left(1+\frac{m^2}{2\epsilon^2}(1+2\mu/r_A+\Lambda r_A^2/3)\right)\right]. \qquad (3.21)$$

The GTA of photons/GW can be obtained from the above expressions by putting $m = 0$. Therefore, the difference in arrival times after one way journey (half of the round trip travel time) from B to A between particle with mass m and energy ϵ and photon/GW those emitted at the same time reads

$$\Delta\tau_m^{\beta} - \Delta\tau_{\gamma}^{\beta} \approx \frac{m^2 r_B}{2c\epsilon^2}\left(1+\mu/r_A-\beta r_B/2\right), \qquad (3.22)$$

$$\Delta\tau_m^{\Lambda} - \Delta\tau_{\gamma}^{\Lambda} \approx \frac{m^2 r_B}{2c\epsilon^2}\left(1+\mu/r_A+\Lambda r_B^2/9\right), \qquad (3.23)$$

In the expressions for GTA of particles the first order effects of flat rotation curve and cosmological constant appear separately from the contribution of mass (Schwarzschild term) as revealed from equation (3.18) to (3.21). Since the contribution of dark matter and dark energy are visible only at large distance scales, neutrons are not suitable for probing the dark matter/energy through GTA effect of particles. Neutrinos seem the only option in this regards.

Another pertinent issue is that getting reflecting back a particle at the Earth from a large distance away is not a realistic idea. So instead of two way motion, we need to consider just one way motion. Measurement of GTA through one way motion can be performed, at least in principle, by sending light/particle from artificial satellite/space station to the Earth. Since the time of emission from a distant source is not known, measurement of GTA or Shapiro delay from one way travel is not possible in such cases. Instead the measurement of difference of arrival times of two particles (or a particle and a photon or two same kind of particles but with different energies) gives an opportunity to test GR and dark matter/energy models provided the relative time of emission of the particles is known within a small uncertainty.

In the next section we shall see how the GTA effect alters the prevailing result of Shapiro time delay of the neutrinos from SN-1987. We shall also estimate the magnitude of dark matter contribution on the GTA of neutrinos from SN 1987.

3.5 Discussion and conclusion:

In Schwarzschild space time particles with non-zero mass suffers GTA when the observer is at higher gravitational potential compare to the gravitational field encounter by the particle during its journey. The net GTA of particles with non-zero mass is found smaller than that of photons/GW. Due to lower speed, particles with non-zero mass should arrive later than the photon/GW if both were departed at the same instant from the source and the delay of particles with respect to photons can easily be estimated using special relativity. The gravitational time delay enhances the delay for particles with non-zero mass. The net delay in arrival time of relativistic particles, however, reduces to half of the gravitational time delay when proper time of the observer is taken into account.

The dark matter field leads to larger GTA. More importantly the GTA is influenced by the dark matter gravitational field at the source position. Thus if the source is located at large distance away (at the outskirt of the galaxy), the dark matter contribution to GTA can be quite large. Interestingly in the presence of dark matter field the prevailing condition for GTA that the observer has to be in stronger gravitational field is no more required. In the dark matter field the net GTA of particles with non-zero mass is found larger than that of photons/GW.

In contrast to dark matter field effect the cosmological constant (dark energy) is found to reduce the magnitude of GTA which could be due to the repulsive nature of cosmological constant. Similar to dark matter case the contribution of cosmological constant to time delay can be large because the gravitational field due to cosmological constant at the source position contributes in the net delay.

When the distance of the source is quite large compare to the observer distance from the gravitational object the GTA for particles with non zero mass is proportional to square of particle mass and goes inversely with the square of the energy of the particles. So measurement of GTA can be exploit to evaluate mass or put limit on the mass of particles with unknown mass, at least in principle. Another relevant issue is that how far the dark matter halo extends to? The stability criterion can severely constrain the extent of the H1 gas in a galaxy and thereby leads to some testable upper limit on the size of a galaxy [143]. The GTA effect can in principle be exploit to probe the extension of our galaxy.

To exemplify the points stated above we consider the case of photons and neutrinos from the well known supernovae 1987A in the Large Magellanic Cloud. The neutrinos from SN '1987A arrived about four hours earlier than the appearance of the optical counterpart. Since the observer at the Earth is at higher gravitational field of the galaxy for the propagation of photons and neutrinos from the supernovae 1987A to the Earth, one needs to consider the proper time for evaluating the true time delay.

The SN1987A is located at a distance about 50 Kpc [144] and the travel time of a photon from SN1987a to the Earth is about 1.62×10^5 years. Considering that the total mass of the galaxy inside 60 kpc is about $6 \times 10^{11}\ M_\odot$ and the distance between the Earth and Center of the galaxy is about 12 kpc, the gravitational time delay (without considering proper time) experienced a photon while traveling from SN1987a to the Earth is about 1.2×10^7 seconds [136], [145]. After considering the proper time interval and treating the galactic gravitational field as purely Schwarzschild in nature, the net delay will be nearly 2.85×10^6 seconds (here r_B is not much larger than r_o and hence the full expression as given in Eq. (3.9) needs to apply). So there is no time advancement in this case but the net gravitational delay is nearly an order less than that reported earlier [136], [145]. If we consider the dark matter model described by case 1 of equation (3.13) and (3.14), and assuming baryonic mass of the galaxy is about 16% of the total galactic mass the net delay for a photon will be -6.2×10^6 seconds i.e. there will be nearly half an year time advancement instead of time delay. At the distance of SN1987a, the effect of cosmological constant is quite small and its contribution ($\sim 240\ s$) to the net gravitational time delay thus can be ignored.

If we turn to SN1987a neutrinos, a major issue is that despite a huge progress in neutrino physics over the last three decades or so, the definite mass of the three neutrinos: electron, muon and tau neutrinos (and antineutrinos) are still unknown though experimental evidence of neutrino oscillations suggest that they are not massless. The cosmological observations give an upper bound on the sum of the active neutrinos $\sum m_\nu^i < 0.23$ eV, [107] here the superscript i denotes the mass eigenstate of neurinos. The Lyman alpha forest power spectrum suggests more stringent limits $\sum m_\nu^i < 0.12$ eV [146]. The energy of the detected neutrinos from SN1987a is of the order of 10 MeV. Therefore, there will be no significant difference in time of arrival between photon and neutrinos emitted at same point

of time, the correction term due to mass is less than a nano-second; much less than the intrinsic error .

In the above analysis we assumed that metric parameters are identical for all the particles following the Einstein equivalence principle. To examine a possible violation of Einstein equivalence principle one usually employ the post-parameterized Newtonian (PPN) metric i.e. $\kappa(r) = 1 - \frac{2\mu}{r}$ and $\sigma(r) = 1 + \frac{2\gamma_i\mu}{r}$, (up to the accuracy of μ) where γ_i is the first PPN parameter that can be different for different particles, the subscript i denotes species of the particle. γ is unity in general relativity, zero in the Newtonian theory. The observations suggests γ is very close to 1 [87]. For the PPN metric the difference in proper time between transmission and reception of a particle of mass m from A to B and back to be measured by the observer at A reads

$$\Delta\tau_m^{PPN} \simeq \frac{2}{c\sqrt{1-\alpha_2}}\Bigg[\left(\sqrt{r_A^2 - r_o^2} + \sqrt{r_B^2 - r_o^2}\right)\left(1 - \frac{\mu}{r_A}\right) + \frac{\mu\left(1+\gamma_i-(2+\gamma_i)\alpha_2\right)}{(1-\alpha_2)}\ln\frac{\left(r_A + \sqrt{r_A^2 - r_o^2}\right)\left(r_B + \sqrt{r_B^2 - r_o^2}\right)}{r_o^2} + \frac{\mu}{(1-\alpha_2)}\left(\sqrt{\frac{r_A - r_o}{r_A + r_o}} + \sqrt{\frac{r_B - r_o}{r_B + r_o}}\right)\Bigg]. \tag{3.24}$$

and therefore, when $r_A \simeq r_o$ the difference in arrival times after a round trip journey between a relativistic particle with mass m and energy ϵ and a photon those emitted at the same time reads

$$\Delta\tau_m^{PPN} - \Delta\tau_\gamma^{PPN} \simeq \frac{2}{c}\Bigg[\sqrt{r_B^2 - r_A^2}\left(1 - \frac{\mu}{r_A}\right)\frac{m^2c^4}{2\epsilon^2} + \mu ln\frac{r_B + \sqrt{r_B^2 - r_A^2}}{r_A}(\gamma_\mu - \gamma_\gamma) + 3\mu\sqrt{\frac{r_B - r_A}{r_B + r_A}}\frac{m^2c^4}{2\epsilon^2}\Bigg], \tag{3.25}$$

Since neutrino mass is very small, the middle term of the right hand side of the above equation will dominate and hence effectively one gets the same expression that was used in [136] to examine the Einstein equivalence principle using SN 1987A data considering neutrinos are massless particle.

The recent detection of a few gravitational wave transients from sources at large distances creates better opportunity to examine the gravitational time advancement and its consequences. The gravitational waves and neutrinos are expected to emit within a short period (few seconds at most) of time from such binary black hole/neutron star coalescence or from supernova explosions. The observation of arrival time difference between gravitational wave and neutrinos from such large distance sources may provide an independent way to constrain on the mass of the neutrinos.

In conclusion of the chapter, we have obtained expressions for GTA of particles in Schwarzschild geometry for the first time by considering proper time interval of propagation of a particle with non-zero mass between two points in a gravitational field. Out findings suggest that the gravitational time advancement may take place when the observer is situated at stronger gravitational field compare to the gravitational field encountered by the particle during its journey. Subsequently we study the effect of dark matter and dark energy on gravitational time advancement. It is found that dark matter leads to larger gravitational time advancement whereas dark energy always produces time delay. We have demonstrated how the present findings can be tested in a real observational situation. Finally after applying our findings to neutrinos (and photons) from SN 1987, we have shown that the net time delay of a photon/gravitational wave is much smaller than quoted in the prevailing chapter due to GTA effect.

Very recently ICECUBE experiment and Fermi telescope detected neutrinos and photons within a short time period from BLAZER TXS 0506+056 [147], [148]. More such kind of detection from various sources are expected in near future. The present findings will have direct application to test various underlying physics related issues of GR and particle physics from the measurement of the difference in time of arrivals of photons/gravitational wave and neutrinos from such astrophysical sources.

Chapter 4

Gravitational lensing by global monopole

4.1 Introduction:

Some quantum field theories admit formation of topological defects of different kinds during phase transitions in the early universe as a consequence of spontaneous breaking of symmetry. The topological defects are classified depending on the topology of vacuum manifold. A monopole may form when manifold contains surfaces those cannot be continuously shrunk to a point. When monopole is formed through spontaneous breaking of a gauge symmetry the resultant configuration has finite energy and its mass is condensed in a very tiny core. The produced monopole configuration thereby behaves like an elementary particle. Instead if monopole is resulted from breakdown of a global symmetry, the produced configuration has linearly divergent mass owing to the long range Nambu-Goldstone field. The typical distance between global monopole and anti-monopoles will be of the horizon size if such global monopole formed in the early universe and that gives a natural cut-off of the energy density of global monopole system.

The gravitational field due to a global monopole can be quite strong because of large energy density associated with Nambu-Goldstone field surrounding the monopole. The exterior space time metric due to global monopole is asymptotically non flat due to the long range Nambu-Goldstone field with energy density decreasing with the distance as r^{-2} [149]. Interestingly such kind of variation

(as r^{-2}) of energy density of global monopole configuration has been exploited to explain the flatness of rotation curves of stars and gases at the outer part of several galaxies [150]. An important feature of the global monopole configuration is that for minimally coupled to gravity system the effective mass in the tiny core of the system is negative that leads to a repulsive potential. As a result no bound orbits exist for the global monopole configuration those are minimally coupled to gravity [149, 151]. Such lack of bound orbits feature can be avoided by considering some nonminimal couplings of global monopole configuration to gravity [152]. Alternatively if a global monopole is swallowed by a black hole at the centre of a galaxy, the resultant configuration admits bound orbit as the effective mass of the system becomes positive and it also can describe the observed flat rotation curve of galaxies.

Gravitational lensing studies provide important clue about mass distribution of the universe including the presence of dark matter [153, 154]. It is also an important tool to probe the nature of space-time geometry of gravitational lenses [153, 155]. The theory of lensing has been developed in stages by many authors including Einstein himself [156]. The deflection angle is weak field regime is usually evaluated exploiting post-parametrized Newtonian formalism that incorporate General Relativity and many other modified theories [153, 155]. The observational consequences of weak lensing were primarily suggested by Chwolson [158] and Zwicky [157]. The lensing theory in strong field regime of Schwarzschild space time was mainly developed by Virbhadra and Ellis [159] and Frittelli and Newman [160]. The lens equation without weak-field or small angle approximations was first introduced in [159, 161] and the observational features of the strong lensing phenomena was explored in [159] by treating the massive black hole of the galactic Centre as Schwarzschild lens. A few interesting works (not exhausted) considering other static spherical symmetric lens in strong field can be found in Refs. [162–164].

The light propagation in space time of a global monopole is well studied in the chapter both weak field [164–166] and strong field [167] regime. In [165] the deflection angle is obtained from the geodesic equations exploiting standard integration method. The strong gravitational lensing of a Schwarzschild black hole with a solid deficit angle owing to a global monopole is studied in [167] applying Bozza's analytical technique [168].

Conventionally the quantum of bending of light rays due to a lens (massive deflector) is derived from null geodesic equations in the neighborhood of the lens

describing it (the lens) by an appropriate space time metric. Recently Rindler and Ishak [54] have claimed that the conventional prescription does not yield complete result of deflection angle in general, particularly when the space-time metric is asymptotically non flat. Working with the Schwarzschild-de Sitter (SDS) geometry [130], they demonstrated that contrary to the conventional result there is a small contribution of cosmological constant Λ in the bending though the orbital equation for light in SDS space-time is free from Λ. In their prescription (for obtaining bending angle) the contribution of Λ to the bending angle comes from the space-time metric itself. Note that according to Rindler and Ishak [54] null geodesic equation and its integral are only the 'half story 'in estimating the bending angle, the space-time metric itself constitutes the remaining part of the story.

While estimating gravitational bending due to global monopole the effect of asymptotically non-flat geometry of global monopole space-time is usually not considered in the chapter, which is precisely our objective of the present study. In this target we shall apply the Rindler-Ishak method for estimation of bending angle and thereby the influence of asymptotically non-flat geometry, if any, on gravitational lensing by global monopole space-time will be examined. Consequently we shall look for proper detectable signature of global monopole through gravitational lensing studies. We shall employ our findings to examine the consistency of global monopole hypothesis as an alternative to dark matter in galaxies.

The plan of the chapter is the following. In the next section(4.2) we would present the exterior Barriola-Vilenkin space-time due to a global monopole. In section 4.3 we briefly describe the technique to be adopted for estimation of bending angles. In section 4.4 we would estimate gravitational bending due to global monopole metric. In section 4.5 we shall investigate gravitational bending for space-time due to a Schwarzschild black hole that swallowed a global monopole. The image position and magnification of images in weak gravitational lensing due to a Schwarzschild black hole that swallowed a global monopole will be described in section 4.6. We shall discuss our findings in section 4.7 and we shall conclude in the same section.

4.2 The space-time metric due to global monopole

A simplest model that gives rise to a global monopole consists of a self-coupling scalar field triplet φ^a ($a = 1, 2, 3$ the internal O(3) index) whose original global $O(3)$ symmetry is spontaneously broken to $U(1)$. The Lagrangian of the model is described by (we are working in units such that $G = c = \hbar = 1$)

$$L = \frac{1}{2}\partial_\mu \varphi^a \partial^\mu \varphi^a - \frac{\lambda}{4}\left(\varphi^a \varphi^a - \eta^2\right)^2 \tag{4.1}$$

where η represents the scale of symmetry breaking and λ is a constant of the model. The configuration describing a monopole is given by the ansatz

$$\varphi^a = \eta f(r)\frac{x^a}{r} \tag{4.2}$$

with $x^a x^a = r^2$. In flat space $f(r) = 1 - (\lambda\eta^2 r^2)^{-1}$. Hence outside the core of a global monopole $f(r) \approx 1$. Accordingly the energy momentum tensor can be approximated as $T_t^t \approx T_r^r \approx \eta^2/r^2$ and $T_\theta^\theta \approx T_\phi^\phi \approx 0$. Barriola and Vilenkin [149] derive the gravitational field for the configuration from the Einstein equations which is given by

$$\begin{aligned} ds^2 &= -\left(1 - 8\pi\eta^2 - \frac{2M}{r}\right)dt^2 + \\ &\quad \left(1 - 8\pi\eta^2 - \frac{2M}{r}\right)^{-1} dr^2 + r^2\left(d\theta^2 + \sin^2\theta d\phi^2\right) \end{aligned} \tag{4.3}$$

with $M = M_{GM}$, $M_{GM} \sim -\frac{16\pi}{3}\lambda^{-1/2}\eta$ denotes the effective mass of the global monopole.

Interestingly for $M = 0$ (in equation (4.3)), the curvature tensor components are $R_0^0 = R_1^1 = R_{01} = 0$, $R_2^2 = \frac{1-8\pi\eta^2}{r^2}$ and hence the curvature of the space time remains non-zero.

Since the effective mass M is negative, the gravitational potential due to global monopole is repulsive. Consequently the space-time does not admit any bound orbit for test particles [149, 151]. For reasonable values of λ and η, M is very small

on the astrophysical scale. Thus neglecting the tiny negative mass at the core the global monopole metric reads as

$$\begin{aligned} ds^2 &= -\left(1-8\pi\eta^2\right)dt^2+\left(1-8\pi\eta^2\right)^{-1}dr^2 \\ &\quad +r^2\left(d\theta^2+\sin^2\theta d\phi^2\right) \end{aligned} \tag{4.4}$$

that can be recast as

$$ds^2=-dt^2+dr^2+\left(1-8\pi\eta^2\right)r^2\left(d\theta^2+\sin^2\theta d\phi^2\right) \tag{4.5}$$

which describes a space with a deficit angle $\Delta = 8\pi\eta^2$; in this configuration the surface area of a sphere of radius r is $4\pi\Delta r^2$ instead of $4\pi r^2$.

If we restrict to the equatorial plan ($\theta = \pi/2$), the metric (4.5) reduces to $ds^2 = -dt^2+dr^2+(1-\Delta)\,r^2d\phi^2$ which becomes locally Minkowskian under a coordinate transformation $\phi' = \sqrt{1-\Delta}\phi$. Thus light path should remain unperturbed by the presence of global monopole space time. The space time geometry around global monopole in equatorial plan, however, is not globally Minkowskian because ϕ' changes from 0 to $\sqrt{1-\Delta}2\pi$. Therefore, light rays while propagating in the equatorial plan of the metric 4.4 would suffer a bending by $\sim \Delta\pi/2$.

The spherically symmetric gravitational collapse of the matter around a global monopole leads to formation of a black hole [165] (alternatively a black hole can swallow a global monopole) and thereby a black hole can possess 'hair' in the form of topological charge.

4.3 Methodology for estimation of bending angle

Before addressing the deflection of light rays in the case of asymptotically non-flat space-time let us first quickly review the basic approach of calculating bending of light due to gravity in asymptotically flat space-time.

The geometrical configuration for the phenomenon of gravitational bending of light is given in Figure (4.1). The light emitted by the distant source S is deviated by the

gravitational source (Lens) L and reaches the observer O. The angle of deflection (α) is the difference between the angle of emission (from the source) and the angle of reception (by the observer) minus π. The angles are to be measured with respect to a common polar axis which is usually taken as the line joining the observer and the center of the lens (OL), the so called optic axis or a line perpendicular to it that passes through the Centre of the lens. If both the observer and the source are situated in the flat space-time region and if tangents are drawn to the null geodesic at the source and image positions, which are represented by SQ and IO in Figure (4.1)(considering the space-time away from the lens is flat), and if C is their point of intersection (if there were no lensing object present) then $\angle OCJ$ will be the angle of deflection (α) by the lens.

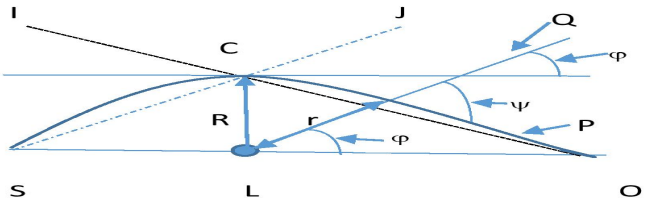

FIGURE 4.1: Lensing diagram - the source S emits light rays which reach the observer O after being gravitationally deflected by the lens L.

The null geodesic equation of light in flat space time is $\frac{d^2u}{d\phi^2}+u=0$, where $u=1/r$. Hence the orbit equation of undeflected (straight line) light ray in flat space not containing the pole (the centre of the lens in the lensing configuration) is given by $u=u_o sin(\phi-\phi_o)$, where $r_o=1/u_o$ is the perpendicular distance from the Centre of the lens to the path of the light rays and ϕ_o is the angle that the light rays made with the polar axis at the point of intersection. For simplicity of calculations the direction of the polar axis is normally taken either parallel or perpendicular to the undeflected light rays which corresponds to $\phi_o=0$ or $-\pi/2$ respectively. In the

case of weak gravitational field one expects that the light path will be deviated by a small amount from the straight line path and one explores for a solution of the orbit on that (perturbation) basis [56].

For asymptotically flat space-time and when the source and observers are far away (in compare to the length scale of the impact parameter which is the perpendicular distance from the center of the lens to the tangent to the null geodesic at the source) from the lens, the direction of light orbit at source position (observer) may be taken as the same to the direction of asymptotic light rays in the source (observer) region. Exploiting this feature one conventionally estimates the emission (reception) angle from the null geodesic equation by letting the radial distance to be infinitely large.

For asymptotically non-flat space time letting $r \to \infty$ to obtain the asymptotes of the orbit is not proper. This is because the direction of light rays at the source (observer) position may not be the same to the direction of asymptotic light rays. For instance, in the case of Schwarzschild-de Sitter space time the direction of light rays at the source (observer) position will not be the same to that at any other (distant) points owing to the non-flat character of the asymptotic space time. Hence the conventional approach is not strictly applicable for estimating bending angle in such a situation.

Rindler and Ishak prescribe a method for obtaining bending angle in asymptotically non-flat space time [54]. Their method is based on the invariant formula for the cosine of the angle between two coordinate directions P and Q

$$\cos(\psi) = \frac{g_{ij}P^iQ^j}{(g_{ij}P^iP^j)^{1/2}(g_{ij}Q^iQ^j)^{1/2}} \tag{4.6}$$

If P is taken as the direction of the orbit and Q is taken as that of the coordinate line $\phi =$ constant (Figure (4.1)), then one may write $P \equiv (dr, d\phi) = (dr/d\phi, 1)d\phi$, $(d\phi < 0)$ and $Q \equiv (dr, 0) = (1, 0)dr$. Consequently for the general spherically symmetric space time metric $ds^2 = -f(r)dt^2 + f(r)^{-1}dr^2 + r^2\left(d\theta^2 + \sin^2\theta d\phi^2\right)$ the angle between P and Q directions becomes [55]

$$\tan(\psi) = \frac{rf(r)^{1/2}}{|dr/d\phi|} \tag{4.7}$$

The one-sided bending angle is then given by $\epsilon = \psi - \phi$.

4.4 Gravitational deflection of light due to global monopole

First we follow the conventional approach of calculating the bending angle. In the equatorial plane ($\theta = \pi/2$) the orbital equation for photon in monopole space-time (4.4) as obtained from the null geodesic equations is

$$\frac{d^2u}{d\phi^2} + (1 - \Delta)u = 0 \tag{4.8}$$

where $u = 1/r$. The exact solution of the above equation reads

$$u = u_o \sin\left[(1 - \Delta)^{1/2}\phi\right] \tag{4.9}$$

where u_o is a constant, related to the closest distance parameter (r_o) through the relation $u_o = 1/r_o$. The asymptotes of the orbit can be obtained letting $r \to \infty$ which gives $\phi^1_\infty = 0$ and $\phi^2_\infty = \pi(1 - \Delta)^{-1/2}$. Hence the total bending (angle between the two asymptotes) is given by

$$\delta\phi = \left[(1 - \Delta)^{-1/2} - 1\right]\pi \tag{4.10}$$

For small Δ, the deflection angle becomes $\Delta\pi/2$, which was expected in view of the other form of the monopole metric (4.5).

Because of the asymptotically non-flat nature of global monopole space time we will now follow the prescription of Rindler and Ishak [54].

For the metric given by equation (4.4) we get from equation (4.9)

$$\frac{dr}{d\phi} = -u_o r^2 (1 - \Delta)^{1/2} \cos\left[(1 - \Delta)^{1/2}\phi\right] \tag{4.11}$$

Let us consider the situation that the source, lens and observer are perfectly aligned. So first we take $\phi = 0$ (corresponding to the source) as prescribed by Rindler and Ishak [54]. The equation (4.9) immediately implies $r \to \infty$ which means that the source has to be at infinity for an admissible photon trajectory

from the source with non-zero distance of closest approach. Because of asymptotically non-flat behavior of the space time geometry we don't prefer the choice of source at infinity. Let for the time being we consider that the source is at infinity. Consequently $\psi_o = 0$ as follows from the equation (4.7). Next consider $\phi = \pi$ for the observer which leads to $r = R/\sin\left[(1-\Delta)^{1/2}\pi\right]$ where $R = 1/u_o$. The equation (4.7) then gives $\psi_\pi = (1-\Delta)^{1/2}\pi$. Thus the total bending angle is

$$\begin{aligned} \delta\epsilon &= \psi_o - \phi_o + \psi_\pi - \phi_\pi \\ &= \left[(1-\Delta)^{1/2} - 1\right]\pi \\ &\simeq -\Delta\pi/2 \end{aligned} \tag{4.12}$$

which clearly differs from what we obtained in equation (4.10) using the conventional method. More importantly the deflection angle is negative. For small Δ the difference of deflection angle between two approaches becomes $\Delta\pi$. The difference in bending angle in two approaches appears to be due to asymptotic non-flat characteristics of the space time. The observer position differs in the two cases; in the conventional case the source and observers (asymptotes) are placed at $(r = \infty, \phi = 0)$ and $(r = \infty, \phi = \pi(1-\Delta)^{-1/2})$ (otherwise the observer cannot see the deflected ray) respectively whereas the points $(r = \infty, \phi = 0)$ and $(r = R/\sin((1-\Delta)^{1/2})\pi), \phi = \pi)$ are chosen in the Rindler-Ishak approach as coordinates of the source and observer. The tangent to the light orbit at the observer point, which is at finite distance away from the lens, makes a finite angle that leads the difference in the two estimates. Since the position of source and observer are pre-fixed in any real observations, it is rational to apply Rindler-Ishak method over the conventional method for estimation of deflection angle.

Now we shall estimate the bending angle also considering general position of source (ϕ_s, d_s) and observer (ϕ_o, d_o) [55, 169] without demanding a perfect alignment of the source, lens and observer. In such a case, we get from equation (4.7) through equations (4.9) and (4.11)

$$\begin{aligned} \delta\epsilon_k &= \psi_k - \phi_k \\ &= \left[(1-\Delta)^{1/2} - 1\right]\phi_k \\ &\simeq -\Delta\phi_k/2 \end{aligned} \tag{4.13}$$

where k stands for s and o (denoting respectively source and observer), so that the total deflection angle becomes

$$\begin{aligned} \delta\epsilon &= \epsilon_s + \epsilon_o \\ &= \left[(1-\Delta)^{1/2} - 1\right](\phi_s + \phi_o) \\ &\simeq -\Delta/2\,(\phi_s + \phi_o) \end{aligned} \tag{4.14}$$

The expression for equation (4.12) can be retrieved from the above equation by putting $\phi_s = 0$ and $\phi_o = \pi$.

In view of the negative bending angle the lensing diagram for an isolated global monopole essentially looks like that given in the figure (4.2) below:

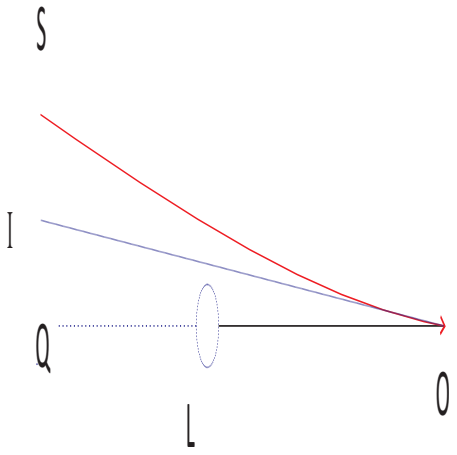

FIGURE 4.2: Lensing diagram - the source S emits light rays which reach the observer O after being gravitationally deflected by the lens L which is an isolated global monopole. The image position is denoted as I.

4.5 Bending of light due to a Schwarzschild black hole that swallowed a global monopole

The space time described by the global monopole metric does not have any event horizon around the monopole. It also does not admit any bound orbit [149, 151]. However, there will be an event horizon if a Schwarzschild black hole of mass greater than the effective (negative) mass of a global monopole swallows the monopole. This configuration also allows bound orbits. The metric that represents the configuration is that given by equation (4.3) with $M = M_{bh} - M_{GM}$ is the difference of the mass (M_{bh}) of the Schwarzschild black hole and the effective (negative) mass (M_{GM}) of the monopole. We will now consider bending of light exploiting both the conventional and the Rindler-Ishak methods [54].

Proceeding exactly the same way as in the preceding section the orbital equation for photon in this case is given by

$$\frac{d^2u}{d\phi^2} + (1-\Delta)u = 3Mu^2 \tag{4.15}$$

Adopting usual perturbation approach, the solution of the above equation to the first order in M reads

$$\begin{aligned} u &= u_o \sin\left[(1-\Delta)^{1/2}\phi\right] + \\ &\quad \frac{3Mu_o^2}{2(1-\Delta)}\left(1 + \frac{1}{3}\cos\left[2(1-\Delta)^{1/2}\phi\right]\right) \end{aligned} \tag{4.16}$$

At the distance of closest approach r_o, $dr/d\phi$ vanishes which gives the relation

$$\frac{1}{r_o} = \frac{1}{R}\left(1 + \frac{M}{R(1-\Delta)}\right) \tag{4.17}$$

For the asymptotes of the orbit we let $r \to \infty$ and consequently the above equation gives $\phi_\infty^1 \approx -\frac{2M}{R}(1-\Delta)^{-3/2}$ and $\phi_\infty^2 \approx \pi(1-\Delta)^{-1/2} - \frac{2M}{R}(1-\Delta)^{-3/2}$. Hence the total bending in the first of $\frac{M}{R}$ is given by

$$\begin{aligned}\delta\phi &= \left[(1-\Delta)^{-1/2}-1\right]\pi + \frac{4M}{R}(1-\Delta)^{-3/2} \\ &\simeq \Delta\pi/2 + \frac{4M}{R(1-\Delta)^{3/2}} \\ &\simeq \Delta\pi/2 + \frac{4M}{R} + \frac{6\Delta M}{R} \end{aligned} \tag{4.18}$$

which is what obtained in [165]. Now we will estimate the bending following the prescription of Rindler and Ishak i.e. vide equation (4.7). Differentiating equation (4.16) we get

$$\begin{aligned}\frac{dr}{d\phi} &= -u_o r^2(1-\Delta)^{1/2}\cos(1-\Delta)^{1/2}\phi - \\ &\quad Mr^2u_o^2(1-\Delta)^{-1/2}\sin\left[2(1-\Delta)^{1/2}\phi\right] \end{aligned} \tag{4.19}$$

When $\phi = 0$, the equation (4.16) suggests that it occurs when $r = \frac{R^2}{2M}(1-\Delta)$. Consequently the equation (4.7) gives that to the first order in M, $\psi_o = \frac{2M}{R(1-\Delta)}$. On the other hand when $\phi = \pi$, $1/r \approx \frac{1}{R}\sin((1-\Delta)^{1/2})\pi) + \frac{2M}{R^2(1-\Delta)}$. When Δ is small, the equation (4.7) gives $\psi_{pi} = \pi - \Delta\pi/2 + \frac{2M}{R(1-\Delta)}$. Thus the total bending angle is

$$\delta\epsilon = \psi_o + \psi_\pi - \pi = -\Delta\pi/2 + \frac{4M}{R(1-\Delta)} \tag{4.20}$$

One can recover the usual bending expression for the Schwarzschild space time from the above equation for $\Delta = 0$. Again it has been noted that the above expression of bending is not equal to that obtained by the conventional approach as given by equation (4.18).

4.6 Image position and magnification in weak lensing by global monopole space time

The angular position of the images (ζ) can be obtained from the lens equation as given below [159]

$$\tan\zeta - \tan\beta = \frac{d_{ls}}{d_{os}}\left[\tan\zeta + \tan(\delta\epsilon - \zeta)\right] \tag{4.21}$$

where β denotes the angular source position, α is the deflection angle, d_{ls} and d_{os} are the distances between lens and source and observer and source respectively. For positive β, the above relation only gives images on the same side ($\zeta > 0$) of the source. Images on the other side can be obtained by taking negative values of β.

When the source, lens and observer are aligned i.e. when β is small, the lens equation in the weak lensing scenario ($\delta\epsilon$small) reduces to

$$\beta = \zeta - \frac{d_{ls}}{d_{os}}\delta\epsilon \tag{4.22}$$

The image positions can be obtained from the above equation after inserting the expression for bending angle from equation (4.20) which leads to

$$\zeta_{\pm} = \frac{1}{2}\left(\beta' \pm \sqrt{4\alpha_0' + \beta'^{\,2}}\right) \tag{4.23}$$

where the indices $\pm$ denote the parities of the images, where

$$\beta' = \beta - \frac{d_{ls}}{d_{os}}\Delta\frac{\pi}{2}\ , \tag{4.24}$$

and

$$\alpha_0' \equiv \sqrt{\frac{d_{ls}}{d_{ol}d_{os}}\frac{4M}{1-\Delta}}\ . \tag{4.25}$$

The form of the equation (4.23) is exactly same to the expression of image position in lensing by Schwarzschild black hole. When $\Delta = 0$, the equation (4.23) reduces to the expression of the image positions due to Schwarzschild lens. It appears that the role of the second term in the right side of equation (4.24) is just of an off-set angle. A point to be noted that for formation of Einstein-Chwolson ring in the present case the source has to be at $\beta = \frac{d_{ls}}{d_{os}}\Delta\frac{\pi}{2}$ instead of $\beta = 0$.

The magnification of the image (the ratio of the flux of the image to the flux of the unlensed source) when the lens is a Schwarzschild black hole that swallowed a global monopole is given by

$$\mu_{\pm} = \frac{1}{(\beta/\zeta_{\pm})\partial\beta/\partial\zeta_{\pm}} = \frac{1}{4}\left[\frac{\beta'}{\sqrt{\beta'^{\,2}+4\alpha_0'^{\,2}}} + \frac{\sqrt{\beta'^{\,2}+4\alpha_0'^{\,2}}}{\beta'} \pm 2\right] \tag{4.26}$$

The form of the above expression is again the same to that of Schwarzschild lensing case. In figure (4.3) the image magnifications are shown as a function of normalized source position in gravitational lensing by a Schwarzschild black hole that swallowed a global monopole considering $\frac{d_{ls}}{d_{os}} = 0.9$. The results are compared with magnification in lensing by a Schwarzschild black hole.

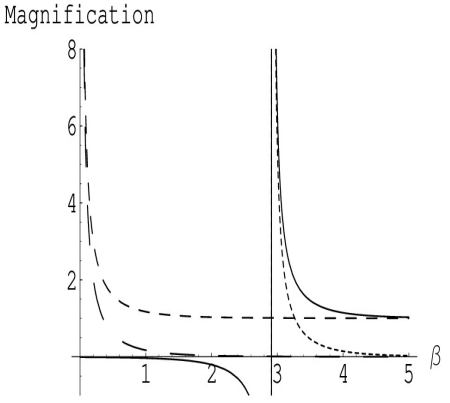

FIGURE 4.3: Magnification in weak gravitational lensing - the solid line and dotted line respectively denote μ_+ and μ_- due to lensing by a Schwarzschild black hole that swallowed a global monopole, the dashed line and long dashed line respectively denote μ_+ and μ_- due to lensing by a Schwarzschild black hole.

The ratio of magnifications of two images is given by

$$\frac{\mu_+}{\mu_-} = \left[\frac{\sqrt{\beta'^{\,2}+4\alpha_0'^{\,2}}+\beta'}{\sqrt{\beta'^{\,2}+4\alpha_0'^{\,2}}-\beta'}\right]^2 \tag{4.27}$$

4.7 Discussion & Conclusion

We have estimated gravitational deflection angle due to a global monopole and a Schwarzschild black hole that swallowed a global monopole using Rindler-Ishak prescription. The signatures of gravitational bending due to global monopoles

as obtained from the present analysis include i) the deflection angle is negative, ii) the magnitude of the angle is nearly constant iii) it is independent of impact parameter.

Clearly for the stated space time geometries the quantum of bending angles obtained with Rindler-Ishak method differ significantly from those obtained with conventional technique owing to asymptotic non-flat characteristics of the stated space times. The Rindler-Ishak method appears to be more flexible; it reproduces the results obtained in conventional approach when source and observer are placed at large distances when the space time metrics are asymptotically flat. However, when source and/or observer are at finite distance away from the lens or if the space time is not flat asymptotically, Rindler-Ishak technique offers a way to estimate the true bending angle and consequently to obtain the image positions.

Global monopole or rather a Schwarzschild black hole that swallowed a global monopole at the center of a galaxy has been proposed in the chapter as an alternative to dark matter hypothesis owing to inverse square of distance variation of the energy density of the global monopole configuration that correctly describe the observed flat rotation curve of galaxies. Interestingly for a symmetry breaking scale of $\eta \sim 10^{16}$ GeV the equivalent Newtonian mass contained within typical galactic radius of $r_{gal} \sim 15$ kpc turns out to be $\Delta r_{gal} \sim 10^{69}$ GeV which is an order higher than the luminous mass of the galaxy [150]. The presence of dark matter is already indicated by several gravitational lensing measurements; several lensing observations such as the Sloan Digital Sky Survey [170], the Hubble Space Telescope [171] missions indicate the presence of an order larger extra mass over the luminous mass of the lensing object particularly when galaxy clusters are considered as lenses. The dark matter candidature of global monopole system is not consistent with such lensing observations as is explained below citing the case of Abell 370 cluster.

The 'giant luminous arcs'were first observed in rich galaxy cluster Abell 370 [172, 173] at redshift 0.374. The details analysis of the observed luminous arcs suggested that they were gravitationally lensed images of background galaxies [174–178]. Here our objective is to estimate the mass of the lensing galaxy Abell 370 from a giant luminous arc using equation (4.23) and compare the estimated mass with the luminous mass obtained independently from photometric study

TABLE 4.1: Estimated mass of Abell 370

Object	z_l	z_s	r_E in arcsecs	$M/M_\odot \times 10^{-11}$ Global monopole	$M/M_\odot \times 10^{-11}$ Schwarzschild
*Abel*370	0.374	0.724	25	923.06	923.07

[172, 173]. Generally galaxy clusters have complex matter distributions and cannot be considered to be either point masses or spherically symmetric but a spherically symmetric lens model can be employed as a first approximation to extract the same order of magnitude results as the more realistic case analyzing the large arcs that are observed in clusters [177, 178]. We have considered the longest arc, A0, which has a radius of curvature of about $25''$ [174] and treat it as an Einstein ring. The observed redshift (z_s) of A0 is 0.724 which gives the distance of the background galaxy. A concordance cosmological model of $(\Omega_m, \Omega_\Lambda, \Omega_k) = (0.3; 0.7; 0)$ is applied for distance estimation from redshifts of lens and source. Our findings are given in Table (4.1).

It is found that estimated mass of Abell 370 from the above stated simplified model is consistent, of the same order of magnitude, with Subaru weak-lensing measurements [179] and Hubble Space Telescope (HST) observations [180]. The estimated mass by treating the lens Abell 370 as a Schwarzschild space time that swallowed a global monopole does not differ significantly from that obtained by modeling the lens as pure a Schwarzschild space time. But when the global monopole system is considered as an alternative to dark matter, the estimated total mass of the lens Abell 370 will represent the mass of only the luminous matter in the cluster. This is in contrast to the GR case (pure Schwarzschild geometry) where the estimated total mass of Abell 370 is the sum of the luminous and presumed dark matter. The photometric measurement suggests that mass of the luminous matter in Abell 370 is at least two orders smaller than the total mass of Abell 370 [174]. Thus the lensing observations of Abell 370 does not support the alternative dark matter hypothesis of global monopole system.

It is worthwhile to mention that for lensing galaxy system of smaller luminous mass the contribution of global monopole (Δ) can be significant as may be seen from the figure (4.4) below where the variation of deflection angle with luminous mass

is shown for both pure Schwarzschild geometry and global monopole swallowed Schwarzschild geometry taking the closest distance parameter 100 kpc.

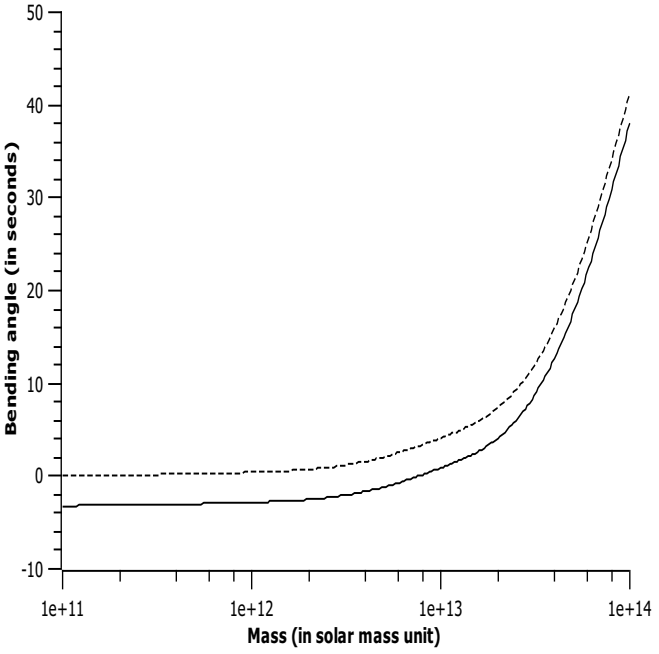

FIGURE 4.4: Variation of deflection angle with mass due to a pure Schwarzschild model (dotted line) and a global monopole swallowed Schwarzschild model (solid line). The closest distance parameter is taken 100 kpc.

The global monopole is an interesting class of topological defects and to look for possible observable effects of global monopole is important irrespective of its success/failure as an alternative to dark matter. In this chapter we have investigated about gravitational lensing signature of global monopole space time and improve the prevailing theoretical formulation of gravitational lensing by global monopole space time. The present findings should be useful in the search for global monopole through gravitational lensing observations.

Chapter 5

Space-time geometry of spiral galaxy halo

5.1 Introduction:

The astrophysical observations reveal that after the termination of luminous disk the expected Keplerian fall-off is absent in rotation curves (variation of angular velocity of test particles with distance from the galactic center) of spiral galaxies [181–185]. The frequency shift of the 21 cm HI emission line from neutral hydrogen cloud at large distances from the galactic center rotating in circular orbits allow to construct rotation curve of galaxies involving distances up to a few tens of kpc or even few hundreds of kpc in few cases. The observed flatness of galactic rotation curves implies that either the Galaxy contains far more matter than contributed by the luminous matters such as stars, planets and the gas or the laws of gravity is different at large distances. The velocity dispersion of galaxies in the galactic clusters [186, 187], gravitational lensing by galaxies [187–192, 192] also support the existence of invisible matter which is commonly referred as dark matter.

The dark matter hypothesis has also received support from the cosmological observations. The ΛCDM model, where Λ is the cosmological constant and CDM stands for cold dark matter, fits the cosmological observations well and is quite successful in describing the formation and evolution of the large scale structure in the Universe (see for instance [193, 194]). In cosmology the cold dark matter hypothesis draws from two phenomena - inflation and big-bang nucleosynthesis.

The inflationary idea suggests that the Universe is nearly flat with matter density equals to critical density which receives support from the observed anisotropy features in the cosmic microwave background radiation (CMBR) [195]. The baryon density inferred from nucleosynthesis suggests that ordinary matter can contribute at most 15% of the critical density [196]. Hence if the inflationary picture is correct, then most of the matter in the Universe must be nonbaryonic. The ΛCDM model interprets that the gravitational attraction of cold dark matters leads to formation of cosmic structures and it also plays important role in holding the structures together.

The space time geometry of galactic halo in presence of dark matter is a very relevant issue. Besides study of the effects of gravitational interactions in the galactic halo region it also offers possibility of cross-verification of existence of dark matter itself through different local gravitational phenomena such as gravitational lensing, gravitational time delay [137], time advancement [127, 140, 197] etc. A naive Newtonian analysis suggests that the tangential velocity (v_φ) of rotation $\beta_\varphi = \sqrt{\frac{GM}{c^2 r}}$, where $\beta_\varphi = v_\varphi/c$, c is the speed of light, G is the gravitational constant(CMBR), M is the total mass inside the radius r of the galaxy and r is the distance from the galactic center. The observed flatness of galactic rotation curves implies that M is a function of r that increases linearly with r. In Newtonian analysis the galactic gravitational potential is expressed accordingly as $\frac{GM(r)}{r}$. Newtonian treatment is, however, inadequate to describe the true and complete gravitational field of galactic halo as required for gravitational lensing and similar other local gravitational phenomena.

Several attempts were made to model dark matter halos in the general relativistic framework. In the Newtonian approach gravitational field is solely represented by gravitational potential. In Newtonian concept the matter density solely plays the role of generation of the gravitational potential which can be completely determined by the observed rotation curve in the galactic halo region. In contrast, even in the spherically symmetric situation general relativistic analysis requires knowledge of two metric coefficients (g_{tt} and g_{rr}), to completely describe the gravitational field of galactic halo. One of the underlying reasons for such a difference is that in the general relativistic framework pressure also contributes to gravitational field unlike in the Newtonian approach. While the g_{tt} can be obtained from the features of rotation curve, additional input about the equation of state of dark matter is required to determine g_{rr}. Applying general relativistic prescription and

invoking observed flat rotation curve feature, several researchers proposed space time geometry of galactic halo considering dark matter as minimally coupled scalar field with potential [150, 152, 198, 199], as scalar field in Brans-Dicke theory [200], as perfect fluid [201], as quintessential matter [202], in Brane world scenario [203] etc. The metric coefficient g_{rr} in the mentioned works [150, 152, 198–203] are different, depending on the choice of the equation of state of dark matter, but g_{tt} is the same in all the cases, proportional to $r^{\beta_\varphi^2}$ as obtained from the flat rotation curve feature. In all the stated works, a non-zero pressure of dark matter particles was considered for deriving the gravitational field.

Under the context the objective of this chapter is to explore for a general relativistic solution of space time geometry of galactic halo in presence of CDM which will be consistent with the observed flatness of rotation curve and will respect the basic principles of general relativity. Note that our objective is not to model the dark matter of galaxy, rather we shall derive the space time metric in the galactic halo region taking the observed feature of galactic rotation curve as an input and assuming the presence of cold dark matter in galaxy. The gravitational lensing observations provide another compelling evidence for existence of dark matter in galactic halo. We shall study the gravitational lensing due to the space time metric of galactic halo as derived in this chapter.

The organization of the chapter is as the following. In the next section (5.2) we shall evaluate the gravitational potential at galactic halo exploiting observed flat rotation curve feature and considering the presence of cold dark matter. We shall discuss other relevant issues like stability of circular geodesics in the same section. In section 5.3 we shall study gravitational lensing due to the derived space time metric. We shall discuss our results in section 5.4 and finally conclude in the same section.

5.2 Galactic potential in presence of cold dark matter invoking observed flat rotation curve feature:

In Newtonian gravity the tangential velocity of a test particle in circular orbits around the central mass distribution is obtained simply by equating the centripetal

acceleration with the gravitational acceleration due to central mass that leads to $v_\varphi = \sqrt{\frac{GM}{r}}$, The determination of tangential velocity in GR framework is slightly complex. Assuming that the galactic halo is spherically symmetric, the general static space time metric of the halo can be written in curvature coordinates as [204]

$$ds^2 = -e^{2\lambda(r)}dt^2 + \frac{dr^2}{1-\frac{2m(r)}{r}} + r^2(d\theta^2 + sin^2\theta d\phi^2), \tag{5.1}$$

where $\lambda(r)$ and $m(r)$ are functions of r only. We are expressing quantities in natural units i.e. c and G are taken as 1. The function $\lambda(r)$ is known as the "potential" and $m(r)$ is the shape function which essentially reflects the effective gravitational mass. Assuming that test particles move on the equatorial plane ($\theta = \pi/2$) the tangential velocity of a non-relativistic test particle in a circular orbit can be obtained from the study of geodesics for the above space-time metric which is given by [198, 199, 201]

$$\beta_\varphi^2 = r\lambda'(r) \tag{5.2}$$

where prime denotes the derivative with respect to r. Since observations suggests that β_φ is nearly constant at large galactic distances, the above equation immediately gives at halo region $e^{2\lambda(r)} \propto r^{2\beta_\varphi^2}$. This form of g_{tt} is adopted in the several previous works [150, 152, 198–203] for galactic halo.

Here we look for a form of g_{tt} that can be recast as perturbation of Minkowski metric as expected in the weak gravitational field regime. Since the gravitational field is weak in the halo region we consider the metric in the halo region can be written as $g_{\mu\nu} = \eta_{\mu\nu} + h_{\mu\nu}$, where $h_{\mu\nu}$ is the small perturbation over the Minkowski metric $\eta_{\mu\nu}$. Accordingly we write g_{tt} of equation (5.1) as

$$e^{2\lambda(r)} = 1 - \frac{2M_B}{r} + f(r)\ , \tag{5.3}$$

where $f(r)(\equiv h_{tt})$ is a function of r that arises due to presence of dark matter and M_B is the total baryonic matter of the galaxy within radius r. The observations suggest that after the galactic bulge the density of baryonic matter is very small and M_B may be taken as a constant. When r is small, $f(r)$ is smaller than

$\frac{2M_B}{r}$ and vice versa for large r. In the galactic halo region we may approximate $e^{2\lambda(r)} \simeq 1 + f(r)$. Since the magnitude of β_φ^2 is very small we shall keep only the leading order terms in β_φ^2 in the solution of halo metric ignoring higher order terms. When flat rotation curve feature is invoked, the equation (5.2) leads to the following solution

$$f(r) \simeq 2\beta_\varphi^2 lnr + C1 \tag{5.4}$$

where $C1$ is an integration constant which may be fixed from the boundary conditions. Note that the above solution does not necessarily require the presence of dark matter; it follows from the observed flatness feature of galactic rotation curve at outskirt of spiral galaxies. At present one cannot rule out the possibility that some modification of general relativity could be the origin of the logarithmic form in the potential.

5.2.1 Space time geometry of halo for cold dark matter

For complete understanding of space-time geometry in the halo region the knowledge about g_{rr} is also required. Additional input in the form of dark matter equation of state is needed to determine g_{rr}. The nature of dark matter is an unanswered issue of contemporary astrophysics. The only information available about dark matter is that it has not shown any interaction with the baryonic matter except the gravitational interaction.

Numerical simulations of structure growth suggests that dominant part of the dark matter in the universe is preferably "cold" i.e. velocity of dominant part of the dark matter particles is much less than the speed of light. Though the ΛCDM model receives an indisputable success on large scales, validity of the CDM scenario on galactic scales has been questioned in several works. It is found from N-body numerical simulations that CDM halos and sub-halos should have a high density (cuspy) profile at the centre [205–207]. The CDM model also gives overabundance of dwarf galaxies in the Milky Way and other similar galaxies/local groups against the observations, which is the so called missing satellites problem [208–210]. There are other issues like the so called too-big-to-fail problem [211, 212]. However, recent studies claim that except the core-cusp problem, other discrepancies between observations and CDM based simulations are removed when baryonic effects are properly taken into consideration in the simulation [213]. The warm cold matter

(WDM) has been proposed in the literature as an alternative to CDM [214, 215] but the WDM model also shares the core-cusp problem in galactic scale [216]. Besides, high redshift Lyman-α forest data disfavors the WDM model [217]. There is also a possibility that the core-cusp problem originated due to our poor understanding of galaxy formation or due to improper underlying assumptions in the N-body simulations [218, 219]. Theoretically weakly-interacting massive particles is the most attractive dark-matter candidates from particle physics point of view which falls under the cold dark matter category. Considering all the aspects and the overall performance over large scales and galactic scales CDM model still remains the most favored dark matter model. We shall, therefore, derive g_{rr} from Einstein field equation considering that the pressure of dark matter is negligibly small i.e. considering essentially the energy momentum tensor of cold dark matter.

Considering that the dark matter as a fluid with energy density $\rho(r)$, radial pressure $p_r(r)$, and tangential pressure $p_T(r)$, the Einstein field equations for dark matter halo read (we shall take $c = 1$ through out the manuscript) :

$$\frac{2m'(r)}{r^2} = 8\pi\rho \tag{5.5}$$

$$\frac{2}{r^2}\left[r\lambda'(r)\left(1-\frac{2m(r)}{r}\right)-\frac{m(r)}{r}\right] = 8\pi p_r \tag{5.6}$$

$$\begin{aligned}&\left(1-\frac{2m(r)}{r}\right)\left(\lambda''(r)+\lambda'^{\,2}(r)+\frac{\lambda'(r)}{r}\right)\\&-\frac{1}{r^3}\left[m'(r)-m(r)\right]\left[1+r\lambda'(r)\right] = 8\pi p_T.\end{aligned} \tag{5.7}$$

Now we consider the followings: In the galactic halo region $m(r) >> M_B$. For cold dark matter $p_r = p_T = 0$. Inserting the flat rotation curve led metric coefficient e^{λ} i.e. expression given in equation (5.4) in equations (5.6) and (5.7) we get to the accuracy of β_{φ}^2

$$m(r) \simeq \beta_{\varphi}^2 r \tag{5.8}$$

The above equation together with equation (5.4) completely specify the halo space time geometry.

5.2.2 Matching with the exterior Schwarzschild space time

In general relativity the Schwarzschild metric is the unique static vacuum solution and thus represents the exterior space time of galaxies with mass parameter equals to total mass M_T content of the galaxy. The solution derived above must match the exterior Schwarzschild metric at galactic boundary. We consider the junction conditions given by given by O'brien and Synge [220, 221] i.e. the metric tensor and all the first order partial derivatives $\frac{\partial g_{\mu\nu}}{\partial x^{\varsigma}}$ except possibly $\frac{\partial g_{r\nu}}{\partial r}$ should be continuous at the junction. Note that a solution satisfying the junction conditions of O'brien and Synge always can be transformed to one satisfying the conditions of Lichnerowicz [222] and vice versa [223, 224].

The matching of metric tensor g_{tt}, g_{ii} (i=1,3) and $\frac{\partial g_{tt}}{\partial r}$ at galactic boundary ($r = R_G$, where R_G is the radius of the galaxy) consistently suggest that $C1 = 2\beta_{\varphi}^2(1 - lnR_G)$ and

$$M_T = M_B + \beta_{\varphi}^2 R_G. \tag{5.9}$$

The matching of $\frac{\partial g_{rr}}{\partial r}$ at galactic boundary can be achieved by a coordinate transformation as demonstrated in [224] for general class of solutions.

5.2.3 The space time geometry of galactic halo

Thus finally the space-time metric of galactic halo(CMBR) appears as

$$\begin{aligned} ds^2 &= -\left(1 - 2\beta_{\varphi}^2 - \frac{2M_B}{r} + 2\beta_{\varphi}^2 ln(r/R_G)\right) dt^2 \\ &\quad + \frac{dr^2}{1 - 2\beta_{\varphi}^2 - \frac{2M_B}{r}} + r^2(d\theta^2 + sin^2\theta d\phi^2) \ . \end{aligned} \tag{5.10}$$

For the metric given in equation (5.1) circular orbits will exist when $0 < r\lambda' < 1$ which is indeed the case for the solution given in equation (5.10). The time-like circular geodesics has to be stable for a viable space time geometry of the galactic halo. The condition for stable circular orbit for the metric given in equation (5.1)

is [225]

$$3\lambda' + r\lambda'' > 2r\lambda'^{\,2} \tag{5.11}$$

As $\beta < 1$, the above condition satisfies for the derived metric.

Inserting the solution of $m(r)$ in equation (5.5), the density of dark matter is readily obtained as

$$\rho \simeq \frac{1}{4\pi}\frac{\beta_\varphi^2}{r^2} \tag{5.12}$$

At least in the outer parts of galaxies dark matter has a mass density profile closely resembling that of an isothermal sphere.

The total gravitational energy E_G between two fixed radii, say r_i and r_o in the halo region can be estimated for the metric (5.10) following [226] which is given by

$$E_G = M_{DM} - E_M = 4\pi \int_{r_i}^{r_o} \left[1 - \left(1 - \frac{2m(r)}{r}\right)^{-1/2}\right] \rho r^2 dr \tag{5.13}$$

where M_{DM} is the dark matter mass (we have ignored the contribution of luminous matter) which is given by

$$M_{DM} = 4\pi \int_{r_i}^{r_o} \rho r^2 dr \simeq \beta_\varphi^2 \,(r_o - r_i) \tag{5.14}$$

The gravitational energy E_G is, therefore, given by

$$E_G \simeq -\beta_\varphi^4 \,(r_o - r_i) \tag{5.15}$$

which is negative as expected owing to positive ρ and the gravitational field of the halo is, thereby, attractive.

5.3 Gravitational lensing due to gravitational field of galactic halo

It is often argued that combined observations of galaxy rotation curves and gravitational lensing can provide better insight of the gravitational field of the galactic halo [227, 228]. In [228] it was shown that the form of gravitational potential extracted from rotation curve $\lambda_{RC}(r)$ and lensing observations $\lambda_{Lens}(r)$ are not the same in general:

$$\begin{aligned} \lambda_{RC}(r) &= \lambda(r), \\ \lambda_{Lens}(r) &= \frac{1}{2}\lambda(r) + \frac{1}{2}\int \frac{m(r)}{r^2} dr \end{aligned} \tag{5.16}$$

For the halo metric given in (5.10), $\lambda_{RC}(r) = \lambda_{Lens}(r) = \lambda(r)$ owing to pressure less fluid.

In gravitational lensing scenarios when photon trajectories are outside the galaxy, which is the case in most of the observations involving external galaxies/galaxy clusters as lens, the gravitational deflection will be that due to Schwarzschild geometry with total mass as given by equation (5.9). In such cases the gravitational lensing phenomenon can provide information about the total mass of the galaxy, check the validity of equation (5.9) and thereby the halo metric. When the null geodesics are through galactic halo the lensing phenomenon may additionally probe the space time geometry of halo.

When source and observer are at large distance away compare to the distance of closest approach (r_o), for the metric given in equation (5.1) the gravitational bending angle over the journey from r_o to infinity may be written as

$$\phi(r_o) - \phi(r_\infty) = \int_{r_o}^{\infty} \frac{dr\sqrt{\left(1 - \frac{2m(r)}{r}\right)^{-1}}}{r\sqrt{\left[\frac{r^2}{r_o^2}\left(\frac{e^{2\lambda(r_o)}}{e^{2\lambda(r)}} - 1\right) - 1\right]}} \tag{5.17}$$

For the halo metric given in equation (5.10), the total bending angle to the leading order in m/r and β_φ will be

$$\alpha \simeq \frac{4M_B}{r_o} + 2\beta_\varphi^2\pi \ . \tag{5.18}$$

Therefore, the deflection angle will be enhanced by a constant factor $2\beta_\varphi^2$ over the Schwarzschild value for light trajectory from source to observer. Note that the conventional dark matter model (Newtonian) also gives constant bending angle when distance of closest approach of photon trajectories are within the galaxy. Usually Schwarzschild deflection angle is employed to interpret lensing observations. The Schwarzschild deflection angle ($\frac{4M(r)}{r_o}$) becomes a constant when (dark matter) mass increases linearly with halo radius. Here a point to be noted: the expression for Schwarzschild deflection angle is evaluated under the assumption that mass parameter M_T is a constant, independent of radial coordinate. So application of Schwarzschild deflection angle for dark matter radial dependent mass is not proper if distance of closest approach is within the galaxy.

The angular position of the images (ζ) can be obtained from the lens equation in the weak lensing scenario is given by [229]

$$\zeta = \beta + \frac{d_{ls}}{d_{os}}\alpha \tag{5.19}$$

where β denotes the angular source position, d_{ls} and d_{os} are the distances between lens and source and observer and source respectively. The image positions can be obtained from the above equation after inserting the expression for bending angle either from equation (5.18) or the Schwarzschild deflection angle depending on whether the distance of closest approach is inside or outside the galaxy.

If mass of baryonic matter in galaxy is known independently by some other method such as through photometry, the prediction of halo space time metric can be tested observationally through lensing observations.

The expression of image position in weak field Schwarzschild lensing is given by

$$\zeta_\pm = \frac{1}{2}\left(\beta \pm \sqrt{4\alpha_0 + \beta^2}\right) \tag{5.20}$$

where the indices $\pm$ denote the parities of the images, and

$$\alpha_0 \equiv \sqrt{\frac{d_{ls}}{d_{ol}d_{os}}4M_T}\ . \tag{5.21}$$

An important question at this stage is that whether the halo space time geometry can be verified from observational lensing data or not. Since the presence of dark matter is clearly revealed in galaxy clusters, here we have considered the case of gravitational lensing by cluster Abell 370 in which the 'giant luminous arcs'were first observed [172, 173]. Our objective is to first estimate M_T from the lensing observation and subsequently we shall compare the so evaluated M_T with that given by equation (5.9).

Galaxy clusters have complex matter distributions in general and cannot be considered to be either point masses or spherically symmetric mass distribution. However, a spherically symmetric lens model can be employed as a first approximation to extract the same order of magnitude results as the more realistic case analyzing the large arcs that are observed in clusters [177, 178]. We have considered the luminous arc, A0, which has a radius of curvature of about $25''$ [176] and treat the arc as an Einstein ring [174, 176]. The observed redshift (z_s) of A0 is 0.724 which gives the distance of the background galaxy and the lens distance is obtained from the redshift 0.374 of Abell 370. A concordance cosmological model of $(\Omega_m, \Omega_\Lambda, \Omega_k)$ $= (0.3; 0.7; 0)$ is applied for distance estimation from redshifts of lens and source. Our estimated total mass from lensing observations is given in Table 5.1.

The estimated mass of the luminous matter in Abell 370 from photometric measurement is found at least two orders smaller than the total mass of Abell 370 [176]. We use β_φ as velocity of dispersion for Abell 370 which is 1367 $km\ s^{-1}$ [176, 230]. The radius of the galaxy is an unknown parameter which we have taken equal to Einstein radius as a first approximation i.e. about 200 kpc which is consistent with the findings from Hubble imaging observations [180]. The total mass obtained from equation (5.9) is also given in Table 5.1. We find that the mass obtained from equation (5.9) agrees reasonably well with the lensing observations.

Interestingly the lensing results also can be utilized to check the validity of baryonic Tull-Fisher relation [231]. Tully & Fisher first demonstrated that an empirical power law relation exists between luminosity and rotation velocity of galaxies [232]. However, the optical Tully-Fisher relation exhibits a break; the power law index differs for fainter and brighter galaxies [231]. The rotational velocity of galaxies is found to exhibit a single power law relation with total baryonic disk mass, which is

TABLE 5.1: Estimated baryonic mass of Abell 370

Object	z_l	z_s	r_E in arcsecs	$M_T/M_\odot \times 10^{-11}$ from lensing data	$M_B/M_\odot \times 10^{-11}$ from equation (5.9)
*Abel*370	0.374	0.724	25	923.06	873.3

the sum of stellar mass and gas mass of galaxy, instead of luminosity. The baryonic Tully-Fisher relation is given by $M_B \propto \beta_\varphi^4$. We would like to replace rotational velocity by baryonic mass. A sample of rotational velocity data for galaxies with large variation in mass are shown in Table 2 which are taken from [233–235]. The variation of β_φ^4 with M_B from the observed data is shown in Fig. (5.1). Expressing the rotational velocity as $\beta_\varphi^4 = a_{tf}^2 M_B$ where a_{tf}^2 is a proportionality constant, we get by the least square fitting of the data $a_{tf}^2 = 2.43 \times 10^{-24}\ M_\odot^{-1}$. Accordingly the equation (5.9) reduces to

$$M_T = M_B + a_{tf} R_G M_B^{1/2}. \tag{5.22}$$

Using M_T as obtained from gravitational lensing observation of Abell 370 we can estimate M_B which turns out to be $\sim 2 \times 10^{14}$ which is not consistent with the estimated baryonic mass of Abell 370 from photometric study. It seems that baryonic mass in baryonic Tully-Fisher relation should be replace by total mass that contains both luminous and dark matter mass.

5.4 Discussion and Conclusion

In this chapter the form of gravitational potential of galactic halo led by the flat rotation curve features is derived. The mass function is obtained considering the presence of cold dark matter in galaxy. The mass function will alter from that derived here if any other form of dark matter such as perfect fluid, or scalar field inspired dark matter state is considered. However, gravitational potential derived from lensing observations for a different choice of dark matter state instead of cold dark matter in general does not consistently match with that obtained from the flat rotation curve feature [228].

TABLE 5.2: Rotational velocity and baryonic mass data of different galaxies

Galaxy	$v(kms^{-1})$	$M_{stellar}(10^{10}M_{\odot})$	$M_{gas}(10^{10}M_{\odot})$
UGC 2885	300	30.8	5
NGC 2841	287	32.3	1.7
NGC 5533	250	19	3
NGC 6674	242	18	3.9
NGC 3992	242	15.3	0.92
NGC 7331	232	13.3	1.1
NGC 3953	223	7.9	0.27
NGC 5907	214	9.7	1.1
NGC 2998	213	8.3	3
NGC 801	208	10	2.9
NGC 5371	208	11.5	1
NGC 5033	195	8.8	0.93
NGC 3893	188	4.2	0.56
NGC 4157	185	4.83	0.79
NGC 2903	185	5.5	0.31
NGC 4217	178	4.25	0.25
NGC 4013	177	4.55	0.29
NGC 3521	175	6.5	0.63
NGC 4088	173	3.3	0.79
NGC 3877	167	3.35	0.14
NGC 4100	164	4.32	0.3
NGC 3949	164	1.39	0.33
NGC 3726	162	2.62	0.62
NGC 6946	160	2.7	2.7
NGC 4051	159	3.03	0.26
NGC 3198	156	2.3	0.63
NGC 2683	155	3.5	0.05
NGC 3917	135	1.4	0.18
NGC 4085	134	1	0.13
NGC 2403	134	1.1	0.47
NGC 3972	134	1	0.12
UGC 128	131	0.57	0.91
NGC 4010	128	0.86	0.27
F568-V1	124	0.66	0.34
NGC 3769	122	0.8	0.53
NGC 6503	121	0.83	0.24
F568-3	120	0.44	0.39
NGC 4183	112	0.59	0.34
F563-V2	111	0.55	0.32
F563-1	111	0.4	0.39
NGC 1003	110	0.3	0.82
UGC 6917	110	0.54	0.2
UGC 6930	110	0.42	0.31
M 33	107	0.48	0.13
UGC 6983	107	0.57	0.29
NGC 247	107	0.4	0.13
NGC 7793	100	0.41	0.1
NGC 300	90	0.22	0.13
NGC 5585	90	0.12	0.25
NGC 55	86	0.1	0.13
UGC 6667	86	0.25	0.08
UGC 2259	86	0.22	0.05
UGC 6446	82	0.12	0.3
UGC 6818	73	0.04	0.1
NGC 1560	72	0.034	0.098
IC 2574	66	0.01	0.067
DDO 170	64	0.024	0.061
NGC 3109	62	0.005	0.068
DDO 154	56	0.004	0.045
DDO 168	54	0.005	0.032

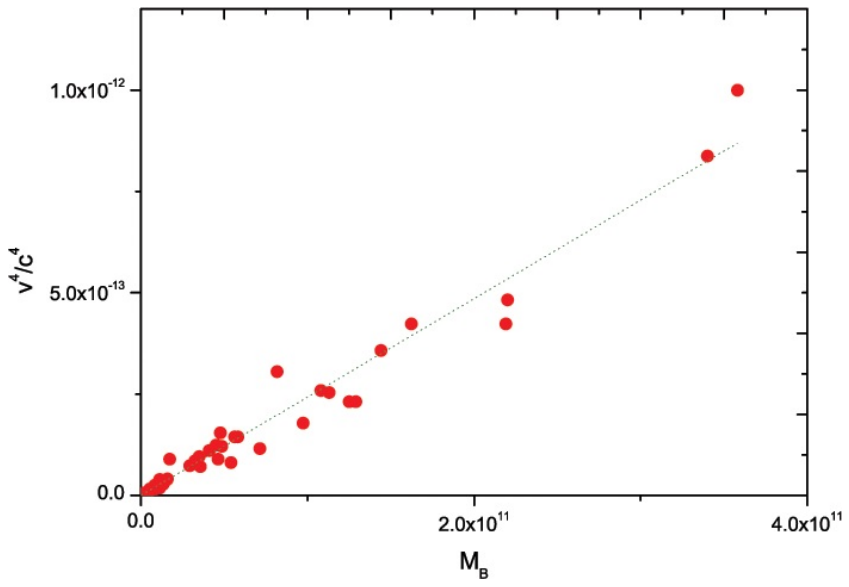

FIGURE 5.1: The variation of β_φ^4 with M_B for several galaxies. The dotted line represents the least squared fit of the data.

Instead of exactly flat rotation curve i.e. instead of constant β_φ if we use universal halo velocity profile as given below [236, 237]

$$\beta_\varphi^2 = k\frac{r_a^2}{r_a^2 + r^2} \tag{5.23}$$

where $\frac{\rho_o}{4\pi}$, ρ_o is the central density and r_a is a constant, the potential f(r) will become

$$f(r) \simeq kln[(r_a^2 + r^2)/R^2] \tag{5.24}$$

which reduces to Eq.(5.4) when $r >> r_a$, with $k = \beta_\varphi^2$.

Numerical simulations suggest an approximate universality for the density profile of cold dark matter halos [238]. The density profile of dark matter prescribed by Navarro, Frenk and White (NFW) is widely used which is given by [238]

$$\rho(r) = \frac{\rho_s}{r/r_s(1 + r/r_s)^2} \tag{5.25}$$

The mass function corresponds to the NFW density profile will be

$$m_{NFW}(r) = 4\pi r_s^3 \rho_s \left(\frac{r_s}{r + r_s} + Log(r + r_s)\right) \tag{5.26}$$

However, for $m_{NFW}(r)$ (together with λ) the radial and transverse pressure of dark matter fluid do not vanish as expected for cold dark matter. The assumption of exactly flat rotation curve in deriving metric potential can be the reason for such an inconsistency.

The radial extension of a galaxy i.e. dark matter is so far not known which is one of the unanswered questions of modern astrophysics. Some alternative theories to GR, particularly conformal gravity can explain the galactic rotation curve without invoking any dark matter component [131]. However, the radial extent of galaxies in conformal theory [143] are not the same to the GR prediction and hence this feature is also a testable observable to differentiate the two models. In the present model the total mass of dark matter is proportional to the radius of galaxy. So if total mass is obtained say from lensing measurements and if baryonic mass is estimated from say photometric study, one can readily estimate the radial extension of a galaxy from equation (5.9) under the present framework and hence is an important testable parameter for the model.

In summary, we have derived gravitational field at halo of spiral galaxies in presence of cold dark matter considering observed flat rotation curve feature as an input. The gravitational lensing formulation have been derived for the halo metric. The lensing observation of Abell 370 is found to validate the derived halo space time. As a corollary the baryonic mass in baryonic Tully-Fisher relation seems to be replaced by total mass of a galaxy for consistent explanation of Abell 370 lensing observation.

In recent years few studies on dark matter distribution in galaxies have been made from lensing observations particularly using the Sloan Digital Sky Survey (SDSS) Data [239] and the Hubble Space Telescope observations [171]. However, the weak lensing signal in SDSS survey imaging is very noisy [154] and interpreted dark matter distribution in galaxies suffer from significant uncertainties. Future precise measurements of dark matter content within galactic halo independently from gravitational lensing and other methods should provide opportunity to further validate the derived halo metric.

Chapter 6

Baryonic Tully-Fisher test of Grumiller's modified gravity model

6.1 Introduction

Several astrophysical observations and specially the observation of flat rotation curve of galaxies lead to the hypothesis of dark matter. However, despite several efforts so far there is no direct evidence of dark matter particles, nor their existence is predicted by any standard theoretical model of particle physics. Consequently many alternative explanations of flat rotation curve of galaxies exist in the chapter including modification of gravitational law at large distances [240], [241] or even modification of Newton's laws of dynamics [29].

Grumiller proposed a quantum motivated theory of gravity that aims to explain the galactic flat rotation in terms of a Rindler acceleration term without the need of any dark matter [31], [242]. Assuming spherical symmetry, Grumiller considered the most general form of metric in four dimensions

$$ds^2 = g_{\alpha\beta}(x^\mu)dx^\alpha dx^\beta + \Phi^2(x^\mu)\left(d\theta^2 + sin^2\theta d\varphi^2\right),\ \alpha,\beta,\mu = 0,1 \tag{6.1}$$

where $g_{\alpha\beta}(x^\mu)$ is a two dimensional metric and the surface radius $\Phi^2(x^\mu)$ is a 2-dimensional dilaton field. To obtain $g_{\alpha\beta}(x^\mu)$ and $\Phi^2(x^\mu)$ Grumiller considered the most general two dimensional renormalizable gravitational theory of the form

$$S = -\int \sqrt{-g}[\Phi^2 R + 2\partial\Phi^2 - 6\Lambda\Phi^2 + 8a\Phi + 2]d^2x\,, \tag{6.2}$$

which contains two fundamental constants, Λ and a, the cosmological constant and a Rindler acceleration, respectively. The specialty of the gravitational theory driven by the above action is that it gives a standard Newtonian kind of potential, and the theory has no curvature singularities at large $\Phi(x^\mu)$. The solution of the two dimensional fields $g_{\alpha\beta}(x^\mu)$ and $\Phi(x^\mu)$ are given by

$$g_{\alpha\beta}dx^\alpha dx^\beta = -B(r)dt^2 + \frac{dr^2}{B(r)}, \tag{6.3}$$

$$\Phi^2(x^\mu) = r^2, \tag{6.4}$$

where

$$B(r) = 1 - \frac{2M}{r} - \Lambda r^2 + 2ar, \tag{6.5}$$

M is a constant of motion. When $\Lambda = a = 0$, the above solution reduces to the Schwarzschild solution and for $M = \Lambda = 0$ the solution becomes the 2-dimensional Rindler metric. The above solutions are mapped into the four dimensional world through equation (6.1).

The theory has found to explain the rotation curves of spiral galaxies well [243]. By fitting the rotation curves of eight galaxies of The HI Nearby Galaxy Survey (THINGS) [244] the Rindler acceleration term was found as $a \sim 3 \times 10^{-11}\ m\ s^{-2}$ [243]. When a larger sample (thirty galaxies) of rotation curves were considered the fitting of the data by the Rindler acceleration was found not very good [246], [247] but the goodness of fitting with the Grumiller's theory was still found comparable to that using standard Navarro-Frenk-White (NFW) profile [238], [245]. The fitted Rindler acceleration parameter, however, exhibit considerably large spread, at least one order of magnitude with mean around $3 \times 10^{-11}\ m\ s^{-2}$ [247].

The rotation velocity of galaxies is known to relate with their (galaxies) luminosity [232]. The optical Tully-Fisher relation, however, shows break; the relation is not universal for bright and faint galaxies [231]. Instead galactic rotation velocity is found to exhibit universal relation with the total baryonic mass (M) of the galaxy with the form $M \propto v_{rot}^4$ [231].

In this chapter we would like to test the Grumiller theory against baryonic Tully-Fisher relation and subsequently we shall estimate the Rindler acceleration parameter in the framework of Grumiller's model using observed total baryonic mass versus rotation velocity data for a sample of sixty galaxies.

6.2 Rotation velocity as a function of baryonic matter in Grumiller theory

For the metric given by equation (6.1) with equation (6.3) the expression of rotation velocity (v_{rot}) of galaxies is given by,

$$v_{rot}^2 = \frac{rB'(r)}{2B(r)} \tag{6.6}$$

where $B'(r)$ signifies the derivative with respect to r, r is the co-ordinate distance from galactic centre. For the solution of B(r) given by equation (6.5) the rotation velocity becomes

$$v_{rot}^2 \approx (\frac{m}{r} - \Lambda r^2 + ar)^{1/2} \tag{6.7}$$

Because of very small magnitude of Λ we henceforth ignore the corresponding term in the expression of rotation velocity. The observed rotation velocity in galaxies is in general not strictly constant even at large distances but often has some weak dependence on radial distance. The rotation velocity in Grumiller gravity is also not exactly flat (constant) at large r but slowly increases with r. So an obvious question is what value of rotation velocity will be considered for testing the Tully-Fisher relation. For Grumillers theory we consider (local) extremum value of rotation velocity. The radial distance (r_e) at which rotation velocity reaches its extremum value can be obtained by differentiating equation (6.7) with respect to r and equating it to zero which gives

$$r_e^2 \simeq \frac{m}{a} \tag{6.8}$$

Inserting it to equation (6.7), we get,

$$v_{rot}'^4 = 4am, \tag{6.9}$$

where v') denotes the extremum rotation velocity. The above expression shows that Grumiller's theory correctly describe the baryonic Tully-Fisher relation, at least at the theoretical level.

To match with the observed rotation curve feature a power-law generalization of the Rindler modified Newtonian potential ($-M/r+ar^n$) is proposed in the chapter [247]. Such a power law generalization modifies the equation (6.9) as

$$v_{rot}'^4 \propto m^{\frac{n}{n+1}} \tag{6.10}$$

In the above case baryonic mass is not strictly proportional to fourth power of rotation velocity but varies as $m \propto v_{rot}'^{4(n+1)/2n}$.

6.3 Estimation of Rindler acceleration parameter from observed rotation velocity vs Mass data

In this section our objective is to estimate the Rindler acceleration parameter from observed rotation velocity vs baryonic mass data for a sample of disk galaxies. We use the compiled data of Sanders and MacGaugh [235] as given in Table 6.1 that include the early works of many good astronomer.

The major luminous matter components in a typical spiral galaxy are stars and gas. Accordingly the total mass of the galaxy is considered as sum of the stellar mass and gas mass. In the used sample the mass is estimated through photometry, particularly using redder passbands as tracer. The HI thickness method was used for measuring the rotation velocity. The details of the data used and procedure of estimation of mass and rotating velocity are discussed in [231], [235].

The equation (6.9) is used to estimate the Rindler acceleration parameter a from the observed data. We fit the observed rotation velocity versus baryonic mass data by the Tully-Fisher relation (equation (6.9)) using the χ^2 goodness-of-fit test. The

fitting gives $a = (3.81 \pm 0.01) \times 10^{-11}\ ms^{-2}$ with reduced $\chi^2 = 2.0$. The fitted curve is shown in figure (6.1).

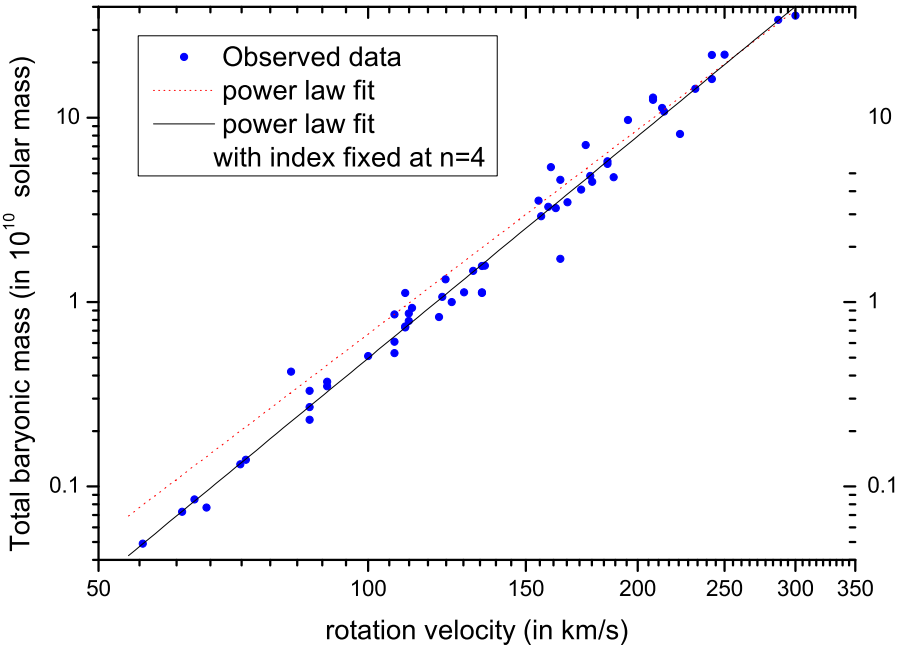

FIGURE 6.1: Variation of observed total baryonic mass with rotation velocity. The filled (blue) circle represent the observed data, solid (black) line gives the fitting of the data for standard Rindler acceleration (power index fixed at 4) and the dotted (red) line shows the fitting of the data with generalized Rindler acceleration under Grumiller's modified gravity model.

The estimated values of a for individual galaxies are given in the last column of the Table 6.1. It has a small spread, ranges from $1.99 \times 10^{-11}\ ms^{-2}$ for UGC 6446 to $7.79 \times 10^{-11}\ ms^{-2}$ for NGC 3949 with mean value $3.8 \times 10^{-11}\ ms^{-2}$ and standard deviation 0.90. The frequency distribution of estimated a for the sample of sixty galaxies is shown in figure (6.2).

We also fit the observed rotation velocity versus baryonic mass data for the modified Tully-Fisher relation (equation (6.10)) led by power-law generalization of the Rindler modified Newtonian potential using the χ^2 goodness-of-fit test which is also depicted in figure (6.2). In this case the fitted value of the parameters are found $n = 1.19$ and $a = 9.08 \times 10^{-11}\ ms^{-2}$ with reduced $\chi^2 = 1.77$.

TABLE 6.1: Galaxy data

Galaxy	$V_{rot}(km\,s^{-1})$	$M_{stellar}(10^{10}M_{\odot})$	$M_{gas}(10^{10}M_{\odot})$	$a(10^{-11})(ms^{-2})$
UGC 2885	300	30.8	5	4.19
NGC 2841	287	32.3	1.7	3.70
NGC 5533	250	19	3	3.29
NGC 6674	242	18	3.9	2.90
NGC 3992	242	15.3	0.92	3.92
NGC 7331	232	13.3	1.1	3.73
NGC 3953	223	7.9	0.27	5.61
NGC 5907	214	9.7	1.1	3.60
NGC 2998	213	8.3	3	3.37
NGC 801	208	10	2.9	2.69
NGC 5371	208	11.5	1	2.77
NGC 5033	195	8.8	0.93	2.75
NGC 3893	188	4.2	0.56	4.86
NGC 4157	185	4.83	0.79	3.86
NGC 2903	185	5.5	0.31	3.73
NGC 4217	178	4.25	0.25	4.13
NGC 4013	177	4.55	0.29	3.76
NGC 3521	175	6.5	0.63	2.44
NGC 4088	173	3.3	0.79	4.06
NGC 3877	167	3.35	0.14	4.13
NGC 4100	164	4.32	0.3	2.90
NGC 3949	164	1.39	0.33	7.79
NGC 3726	162	2.62	0.62	3.94
NGC 6946	160	2.7	2.7	2.25
NGC 4051	159	3.03	0.26	3.60
NGC 3198	156	2.3	0.63	3.74
NGC 2683	155	3.5	0.05	3.01
NGC 3917	135	1.4	0.18	3.89
NGC 4085	134	1	0.13	5.28
NGC 2403	134	1.1	0.47	3.80
NGC 3972	134	1	0.12	5.33
UGC 128	131	0.57	0.91	3.68
NGC 4010	128	0.86	0.27	4.40
F568-V1	124	0.66	0.34	4.38
NGC 3769	122	0.8	0.53	3.08
NGC 6503	121	0.83	0.24	3.71
F568-3	120	0.44	0.39	4.63
NGC 4183	112	0.59	0.34	3.13
F563-V2	111	0.55	0.32	3.23
F563-1	111	0.4	0.39	3.56
NGC 1003	110	0.3	0.82	2.42
UGC 6917	110	0.54	0.2	3.66
UGC 6930	110	0.42	0.31	3.71
M 33	107	0.48	0.13	3.98
UGC 6983	107	0.57	0.29	2.82
NGC 247	107	0.4	0.13	4.58
NGC 7793	100	0.41	0.1	3.63
NGC 300	90	0.22	0.13	3.47
NGC 5585	90	0.12	0.25	3.28
NGC 55	86	0.1	0.13	4.40
UGC 6667	86	0.25	0.08	3.07
UGC 2259	86	0.22	0.05	3.75
UGC 6446	82	0.12	0.3	1.99
UGC 6818	73	0.04	0.1	3.76
NGC 1560	72	0.034	0.098	3.77
IC 2574	66	0.01	0.067	4.56
DDO 170	64	0.024	0.061	3.66
NGC 3109	62	0.005	0.068	3.75
DDO 154	56	0.004	0.045	3.72
DDO 168	54	0.005	0.032	4.26

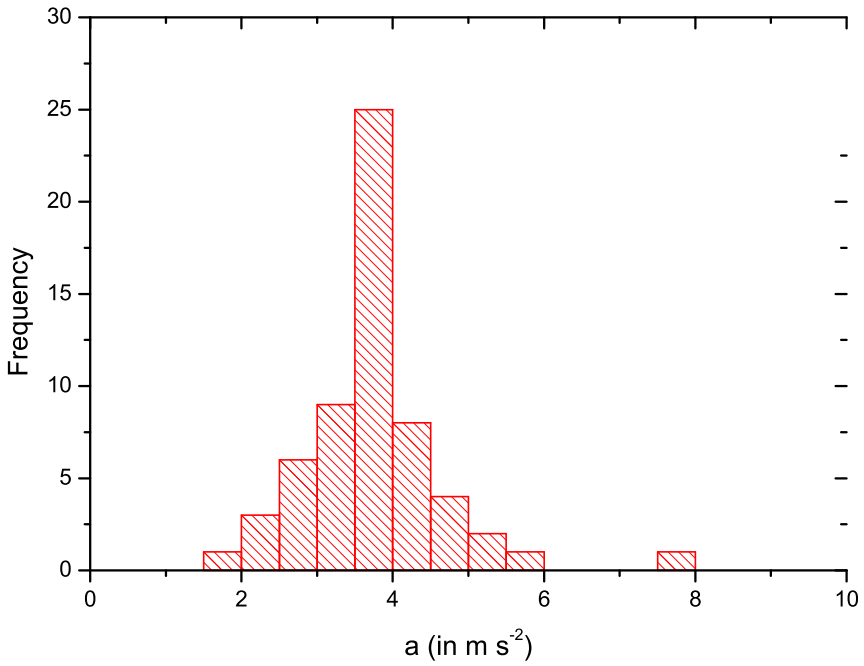

FIGURE 6.2: Frequency distribution of estimated Rindler acceleration parameter.

6.4 Discussion and conclusion

The Rindler parameter was estimated in [243] by fitting rotation curves of eight galaxies of The HI Nearby Galaxy Survey (THINGS) and the fitted mean value of the Rindler acceleration parameter was found $a \sim 3 \times 10^{-11}\ ms^{-2}$. However, when a larger sample of galaxies were considered for analysis the spread in the value of acceleration parameter becomes quite large and thereby the validity of the Grumiller model is questioned [247]. In contrast the Rindler acceleration parameter as estimated in the present chapter using the rotation velocity versus total baryonic mass data of a sample of sixty galaxies exhibits relatively small spread. The mean value is, however, nearly the same to that obtained by fitting rotation curves [247]. As stated already the rotation velocity in Grumiller's theory (equation (6.7)) is not flat but slowly diverges asymptotically which is not in accordance with the observed behaviour in typical rotation curves where rotation velocity is found to decrease slowly at large radial distances [237]. This seems the main reason of poor description of rotation velocity curves by the Grumiller's model. While describing the observed rotation velocity versus baryoinc mass data

we have considered extrema values of rotation velocity thereby taking out the radial dependence of rotation velocity.

It was found in [247] that the goodness of fits of rotation curves are better in the generalized Rindler acceleration model than that of the standard Rindler acceleration model. However, the power law index n was found to vary substantially (from 0.2 to 3.3) to describe the observer rotation curves [247], which is against the universality of the baryonic Tully-Fisher relation as may be noted from equation (6.10). The power law generalization is thus not suitable for Tully-Fisher feature unless power law index is kept fixed and universal for all galaxies. Since the form of the Grumiller's solution (equation (6.3) and (6.5)) is the same to the vacuum (static spherically symmetric) solution of Weyl gravity [30], [117] the present findings are also applicable to Weyl gravity.

The criterion of the stability of orbits in Grumiller's modified gravity/conformal gravity leads to testable upper limit on the size of the galaxies [143]. Future observations on last stable orbit in galaxies is expected to provide an important test of the Grumiller's model/conformal gravity prediction.

In conclusion we demonstrate that Grumiller's modified gravity model correctly reproduces the baryonic Tully-Fisher relation at theoretical level. We fit the observed total baryonic mass versus rotation velocity data for a sample of sixty galaxies by Grumiller's model and estimate the value of Rindler acceleration parameter. The mean value of so obtained Rindler parameter is found consistent with that estimated from fitting of rotation velocity curves of disk galaxies.

Chapter 7

Conclusion

7.1 Conclusion:

The present thesis has presented different theoretical studies of influences of dark sector on few local gravitational phenomena with the objective to explore theoretically possibilities of testing dark sector and discriminating different models of dark sector, at least in principle.

The influence of dark matter/energy on gravitational time advancement has been studied and analytical expressions for the time advancement has been obtained which is found to depend on the strength of dark matter/energy. The results of the present investigation suggest that in principle the measurements of gravitational time advancement at large distances can verify the dark matter and a few dark energy models or put an upper limit on the dark matter/energy parameter. The findings demonstrated that dark energy gives only a (positive) gravitational time delay, irrespective of the position of the observer. Consequently, there will be no time advancement effect at all at radial distances where the gravitational field due to dark energy is stronger than the gravitational field of the Schwarzschild geometry. In the alternative dark matter models like conformal gravity model or Grumiller's modified gravity the time advancement take place irrespective of gravitational field of the observer if dark matter field is stronger than the gravitational field of luminous matter.

The expressions for gravitational time advancement of particles with non-zero mass has been deduced in Schwarzschild geometry. Subsequently the effect of dark

matter and dark energy on gravitational time advancement for particles with non-zero mass have been studied. It has been proposed that comparison of gravitational time advancement for a photon and a relativistic particle of a non-zero mass can be used, at least in principle, as a tool to verify the presence of dark matter and dark energy.

Gravitational lensing studies have been performed for global monopole space time. The bending angle is found negative when lensed by an isolated global monopole system which is a clear signature of the global monopole system. The present study suggests that the global monopole description of dark matter is not compatible with gravitational lensing observations.

Grumiller's modified gravity theory and conformal gravity theory can describe flat rotation curve of galaxies without invoking dark matter. After confronting the theoretical predictions with the observations involving the rotation velocities at large distances from the galactic centre for a sample of sixty galaxies the Grumiller's modified gravity theory and conformal gravity theory are found consistent with baryonic Tully-Fisher feature.

Considering observed flat rotation curve feature as an input and assuming presence of cold dark matter a new space-time metric has been obtained by solving Einstein field equations. The gravitational lensing for the derived space time has been studied and it is found that the model correctly describes the lensing observation for the cluster Abell 370.

The problem of dark matter and dark energy, particularly their origin and nature are very challenging. Further detailed studies on various aspects and on various directions are needed to progress in understanding the outstanding problems of dark sector. In near future the author will take up gravitational lensing studies for alternative dark matter and dark energy models.

In summary the works presented in the thesis explore the possible signature of dark matter and dark energy on gravitational time advancement phenomenon, has questioned the viability of global monopole model of dark matter through gravitational lensing studies, the consistency of two notable alternative models of dark matter, the Grumiller's modified gravity theory and the conformal gravity theory, with baryonic Tully-Fisher feature is established. The gravitational lensing features of a general static spherically symmetric spacetime metric, which is

deduced assuming flat feature of galactic rotation curve and the presence of cold dark matter, are studied.

Bibliography

[1] P. A. R. Ade et al., (Planck Collaboration), Astron. Astrophys., 571, A16 (2014);

[2] Newton, I., Philosophiae Naturalis Principia Mathematica. Auctore Js. Newton, doi:10.3931/e-rara-440 (1687);

[3] Einstein, A., Annalen der Physik 17, 1, pp. 891-921, (1905); pp. 910-911, (1905);

[4] Einstein. A, Annalen der Physik 354 (7), 769-822, (1916);

[5] Weinberg, S.: Gravitation and Cosmology: Principles and Applications of The General Theory of Relativity.John Wiley Press, New York (1972);

[6] Friedman, A., Zeitschrift fur Physik, 10(1), 377-386 (1922);

[7] Lemaitre, G. , Annales de la Societe Scientifique de Bruxelles, 47, 49 (1927);

[8] Weinberg, S., Cosmology, Oxford University Press, NY. (2008);

[9] Riess, A. et al., AJ, 116, 1009 (1998); Perlmutter, S. et al., Astrophysical Journal, 517, 565 (1999);

[10] Kapteyn, Jacobus Cornelius., Astrophysical Journal. 55: 302-327 (1922);

[11] Zwicky, F., Helvetica Physica Acta. 6: 110-127 (1933);

[12] Rubin, V. C. and Ford, W. K. J., Astrophysical Journal, 159, 379 (1970);

[13] Taylor, A. N. et al. Astrophysical Journal. 501 (2): 539-553 (1998);

[14] Ratra, P., Peebles, L., Physical Review D. 37 (12): 3406 (1988);

[15] Caldwell, R., Dave, R., Steinhardt, P. J., Phys. Rev. Lett. 80, 1582 (1998);

[16] Zlatev, I., Wang, L.-M., Steinhardt, P.J., Phys. Rev. Lett. 82, 896 (1999);

[17] Caldwell. R. R., Phys. Lett. B 545, 23 (2002);

[18] Hoyle, F., Mon. Not. R. Astron. Soc. 108, 372 (1948);

[19] Armendariz-Picon, C., Damour, T., Mukhanov, V. F., Phys. Lett. B , 458, 209 (1999);

[20] Armendariz-Picon, C., Mukhanov, V. and Steinhardt, P. J., Phys. Rev. Lett. 85, 4438 (2000);

[21] Armendariz-Picon, C., Mukhanov, V. and Steinhardt, P. J., Phys. Rev. D 63, 103510 (2001);

[22] Garriga, J., Mukhanov, V. F., Phys. Lett. B 458, 219 (1999);

[23] Bento, M., Bertolami, O., Sen, A., Phys. Rev. D 66, 043507 (2002);

[24] Kamenshchik, A. Y., Moschella, U., Pasquier, V., Phys. Lett. B 511, 265 (2001);

[25] De Felice, A., Tsujikawa, S., Living Rev. Relativ. 13, 3 (2010);

[26] Sotiriou, T., Faraoni, V., Rev. Mod. Phys,82,451 (2008);

[27] Dvali, G., Gabadadze, G. and Porrati, M., Phys. Lett. B 485, 208 (2000) Lue, A. and Starkman, G. Phys. Rev. D 67, 064002 (2003);

[28] Gorbunov, D., Koyama, K., Sibiryakov, S., Physical Review. D73 (4): 044016 (2006);

[29] Milgrom, M., Astrophysical Journal. 270: 365-370 (1983);

[30] Mannheim, P. D. and Kazanas, D., Astrophys. J. 342, 635 (1989);

[31] Grumiller, D., Phy. Rev. Let., 105, 211303 (2010);

[32] Buchdahl H. A., Mon. Not. Roy. Astron. Soc., 150, 1 (1970);

[33] Rindler, W. Oxford: Oxford University Press, p. 305 (2001);

[34] Will, C.M., Living Rev Relativ 17:4, (2014);

[35] Islam, J. N., Phys. Lett. A 97, 239 (1983);

[36] Cardona, J. F. and Tejeiro, J. M., Astrophys. J. 493, 52 (1998);

[37] Kagramanova, V., Kunz, J. and *Lämmerzahl*, C., Phys. Lett. B 634, 465 (2006);

[38] Sereno, M and Jetzer, Ph., Phys. Rev. D 73, 063004 (2006);

[39] Hackmann, E. and Lammerzahl, C. Phys. Rev. Lett. 100, 171101 (2008);

[40] Miraghaei, H., Nouri-Zonoz, M.: Gen. Relativ. Gravit. 42, 2947-2956 (2010);

[41] Kerr, A. W., J. C. Hauck, J. C. , and Mashhoon, B., Classical Quantum Gravity 20, 2727 (2003);

[42] Arakida, H., Int. J. Theor. Phys. 52, 1408 (2013);

[43] Sultana, J., Kazanas, D., Said, J. L., Physical Review D, 86(8), 084008 (2012);

[44] Yu F., Liu M. L. and Gui Y. X., Eur. Phys. J. C 60, 175-179 (2009);

[45] Krisher T.P., Astrophys. J., 331, L135 (1988);

[46] Schmidt, H.-J., Phys.Rev. D 78, 023512 (2008);

[47] Hu. Y.-P., et al., Adv. High Energy Phys., 604321,7 (2014);

[48] Farrugia, G., Said, J. L. and Ruggiero, M. L., Phys. Rev. D. 93, 104034 (2016);

[49] Mecheri, R., Abdelatif, T., Irbah, A., Provost, J. and Berthomieu, G., Solar Phys., 222, 191-197 (2004); Antia, H. M., Chitre, S. M. and Gough, D. O., Astron. Astrophys., 477, 657-663 (2008);

[50] Nordtvedt, K., Phys. Rev. D 61, 122001 (2000);

[51] Iorio, L., International Journal of Modern Physics D, 15, 473 (2006);

[52] Liang, S., Xie, Y. Res. Astron. Astrophys. 14, 527-532 (2014);

[53] Lake, K., Phys. Rev. D 65 087301 (2002);

[54] Rindler,W., Ishak, M. Phys. Rev. D 76 043006 (2007);

[55] Bhadra, A., Biswas. S., and Sarkar, K. Phys. Rev. D , 82, 063003 (2010);

[56] Bhadra, A., arXiv:1007.1794 (2010);

[57] Sereno, M., Phys.Rev.D77, 043004 (2008);

[58] Sereno, M., Phys.Rev.Lett. 102, 021301 (2009);

[59] Schucker, T., Gen. Relativ. Gravit. 41, 67 (2009);

[60] Lake, K., arXiv:0711.0673 (2007);

[61] Bhattacharya, A., Garipova, G, M., Laserra, E., Bhadra, A. and Nandi, K. K. JCAP 1102, 028 (2011);

[62] Khriplovich, Pomeransky, I. A., Int. J. Mod. Phys. D 17, 2255 (2008);

[63] Park, M., Phys. Rev. D.78, 023014 (2008);

[64] Ishak, M., Phys. Rev. D 78, 103006, 1-6 (2008);

[65] Arakida, H. and Kasai, M., Phys. Rev. D 85, 023006 (2012);

[66] Aghili, M. E., Bolen, B. and Bombelli, L., Gen. Rel. Grav. 49,10 (2017);

[67] Biressa, T. and de Freitas Pacheco, J. A., Gen. Rel. Grav. 43, 2649 (2011);

[68] Butcher, L. M., Phys. Rev. D 94, 083011 (2016);

[69] Guenouche, M.; Zouzou, S. R., Phys. Rev. D.98, 123508 (2018);

[70] Liu, M., Lu, J. and Gui, Y., Eur. Phys. Jour. C 59, 107 (2009);

[71] Fernando, S., Gen. Relativ. Gravit. 44, 1857 (2012);

[72] Quin, Wu, and Zou, The gravitational deflection of light in MOND, A and A, arXiv:astro-ph/9406051 (1994);

[73] Bekenstein, Sanders., The Astr. Jour, 429: 480-490 (1994);

[74] Mortlock, Turner., Mon. Not. R. Astron. Soc. 327, 557-566 (2001);

[75] Milgrom, M. and Braun, E., Astrophys. J. 334, 130 (1988);

[76] Edery, A. and Paranjape, M. B., Phys. Rev. D 58, 024011, pp. 1-8 (1998);

[77] Sultana, J. and Kazanas, D., Phys. Rev. D 81: 127502 (2010);

[78] Cattani, C., Scalia, M., Laserra, E., Bochicchio, I. and Nandi, K. K. , Phys. Rev. D 87 047503 (2013);

[79] Sultana, J., Journal of Cosmology and Astroparticle Physics, 048 (2013);

[80] Lim, Y. K. and Wang, Q. H., Phys. Rev. D 95, no. 2, 024004 (2017);

[81] Nzioki, A.M., Dunsby, P.K.S., Goswami, R., Carloni, S., Phys. Rev. D 83, 024030 (2011);

[82] Kennefick, D., Phys. Today, 62(3), 37 (2009);

[83] Shapiro, I. I., Phys. Rev. Letters,13, 789 (1964);

[84] Asada, H., Physics Letters B 661, 78-81, (2008);

[85] Schucker, T. and Zaimen, N., AA 484, 103 (2008);

[86] Liu, M., Yu, B., Yu, F., and Gui, Y., European Physical Journal C, 67, 507 (2010);

[87] Bertotti, B., Iess, L. and Tortora, P., Nature, 425, 374 (2003);

[88] Chen, J. H. and Wang, Y. J., Chin. Phys. 16, 3212 (2007);

[89] Vessot, R. F. C., et. al., Phys. Rev. Lett. 45 2081 (1980);

[90] Abbott, B. P., et al. (Virgo, LIGO Scientific), Phys. Rev. Lett. 116, 061102, 1602.03837 (2016);

[91] Abbott, B. P., et al. (Virgo, LIGO Scientific), Phys. Rev. Lett. 116, 241103, 1606.04855 (2016);

[92] Abbott, B. P., et al. (VIRGO, LIGO Scientific), Phys. Rev. Lett. 118, 221101, 1706.01812 (2017);

[93] Abbott, B. P., et al. (Virgo, LIGO Scientific), Astrophys. J. 851, L35 1711.05578 (2017);

[94] Abbott, B. P., et al. (Virgo, LIGO Scientific), Phys. Rev. Lett. 119, 141101, 1709.09660 (2017);

[95] Abbott, B. P., et al. (Virgo, LIGO Scientific), Phys. Rev. Lett. 119, 161101, 1710.05832 (2017);

[96] Abbott, B. P., et al. (LIGO Scientific, VINROUGE, Las Cumbres Observatory, DES, DLT40, Virgo, 1M2H,Dark Energy Camera GW-E, MASTER), Nature 551, 85, 1710.05835 (2017);

[97] Arvanitaki, A., Baryakhtar, M., Dimopoulos, S., Dubovsky, S., and Lasenby, R., Phys. Rev. D95, 043001, 1604.03958 (2017);

[98] Hicken, M., Wood-Vasey, W. M., Blondin, S., et al., ApJ, 700, 1097 (2009);

[99] Suzuki, N., Rubin, D., Lidman, C., et al., ApJ, 746, 85 (2012);

[100] Kowalski, M., Rubin, D., Aldering, G. et al., ApJ, 686, 749 (2008);

[101] de Blok, W. J. G., Walter, F., Brinks, E., Trachternach, C., Oh, S.-H. and Kenni-cutt, R. C., Astron. J. 136, 2648 (2008);

[102] Trimble, V., Annual Rev. Astron. Astrophys. 25, 425, (1987);

[103] D'Amico, G., Kamionkowski, M. and Sigurdson, K., arXiv: 0907.v1 (1912);

[104] de Bernardis, P., Ade, P. A. R., Bock, J. J., et al., Nature, 404, 955 (2000);

[105] Komatsu, E., Dunkley, J., Nolta, M. R., et al., ApJS, 180, 330 (2009);

[106] Ade, P. A. R., Aghanim, N., Armitage-Caplan, C., et al. (Planck Collaboration), Astron. Astrophys. 571, A16 (2014);

[107] Ade, P. A. R., Aghanim, N., Armitage-Caplan, C., et al. (Planck Collaboration), Astron. Astrophys. 571, A23 (2014);

[108] Eisenstein, D.J., Zehavi, I., Hogg, D. W., et al., ApJ, 633, 560 (2005);

[109] Anderson, L., Aubourg, E., Bailey, S., et al., MNRAS, 427, 3435 (2012);

[110] Slosar, A., et al., J. Cosmology Astropart. Phys., 4, 26 (2013);

[111] Allen, S. W., Rapetti,D. A., Schmidt, R. W. et al., MNRAS, 383, 879 (2008);

[112] Schrabback, T., Hartlap, J., Joachimi. B. et al., Astron. Astrophys, 516, A63 (2010);

[113] Carroll, S. M., Living Rev.Rel. 4, 1 (2001);

[114] Peebles, P. and Ratra, B., Rev.Mod.Phys. 75, 559 (2003);

[115] Weinberg, S., Rev.Mod.Phys. 61, 1 (1989);

[116] Damour, T., and $Esposito - Farèse$, G., Class. Quantum Grav., 9, 2093 (1992);

[117] Kazanas, D. and Mannheim, P. D., Astrophys. J. Suppl. 76, 431 (1991);

[118] de Rham, Claudia., Living Rev. Relativity, 17, 7 (2014);

[119] Lue, A., Phys.Rept. 423, 1 (2006);

[120] Feng, J. L., Annu. Rev. Astron. Astrophys. 48, 495 (2010);

[121] Bekenstein, J. D. and Milgrom M., Astrophys. J. 286, 7 (1984);

[122] Bekenstein, J.D., Contemporary Physics 47, 387 (2006);

[123] Ferreira, P.G., Starkmann, G., Science 326, 812 (2009);

[124] Chen, B., Kantowski, R. and Dai, X., Phys. Rev. D 82, 043005 (2010);

[125] Khriplovich, I. B. and Pitjeva, E. V., Int. J. Mod. Phys. D 15, 615 (2006);

[126] Bertone, G. and Merritt, D., Mod. Phys. Lett., A 20, 1021 (2005);

[127] Bhadra, A and Nandi, K. K., Gen Relativ Gravit 42, 293 (2010);

[128] Lue, A. and Starkman, G., Phys. Rev. D 67, 064002 (2003);

[129] Vainshtein, A. I., Phys. Lett. B 39, 393 (1972);

[130] Kottler, F., Ann. Phys. (Leipzig) 361, 401 (1918);

[131] Mannheim, P. D. and O'Brien, J. G., Phys. Rev. Letts, 106, 121101 (2011);

[132] Turyshev , S. G., Lane , B., Shao, M. and Girerd, A., Int. J. Mod. Phys. D 18, 1025 (2009);

[133] Pierce, R., Leitch, J., Stephens, M., Bender, P. and Nerem, R., Applied Optics 47, 5007 (2008);

[134] Turyshev, S. G., Sazhin, M.V. and Toth, V.T., Phys Rev. D 89, 105029 (2014);

[135] Shapiro, I. I., Ash, M. E., and Tausner, M. J., Phys. Rev. Lett. 17, 933 (1966);

[136] Longo, M. J., Phys. Rev. Lett. 60, 173 (1988);

[137] Sarkar, T., Ghosh, S., and Bhadra, A., Eur. Phys. J. C 76, 405 (2016);

[138] Demorest, P.B., Pennucci, T., Ransom, S.M., Roberts, M. S. E. and Hessels, J. W. T., Nature 467, 1081 (2010);

[139] Corongiu, A., Burgay, M., Possenti, A., Camilo, F., D'Amico, N., Lyne, A. G., Manchester, R. N., Sarkissian, J. M., Bailes, M., Johnston, S., et al., Astrophys. J. 760, 100; arXiv:1210.1167 (2012);

[140] Ghosh, S., Bhadra, A., Eur. Phys. J. C 75, 494 (2015);

[141] Deng, Xue-Mei and Xie, Yi. Phys. Lett. B 772, 152 (2017);

[142] Mannheim, P. D., OBrien, J. G., Phys. Rev. D 85, 124020 (2012);

[143] Nandi, K. K. and Bhadra, A., Phys. Rev. letts. 109, 079001 (2012);

[144] Panagia, N., Memorie della Societa Astronomia Italiana. 69, 225 (1998);

[145] Bose, S. K., McGlinn, W. D., Phys. Rev. D 38, 2335 (1988);

[146] Palanque-Delabrouille, N., et al., Phys. 11, 011 (2015);

[147] IceCube Collaboration et al., Science 361, 146 (2018);

[148] IceCube Collaboration, Science 361, 147 (2018);

[149] Barriola, M., Vilenkin, A, Phys. Rev. Lett. 63, 341 (1989);

[150] Nucamendi, U., Salgado, M., Sudarsky, D., Phys. Rev. D 63, 125016 (2001);

[151] Harari, D. and Lousto, C., Phys. Rev. D 42, 2626 (1990);

[152] Nucamendi, U., Salgado, M. and Sudarsky, D., Phys. Rev. Lett. 84, 3037 (2000);

[153] Schneider, P., Ehlers, J., Falco, E. E., Gravitational Lenses, Springer-Verlag, Berlin, 1992; Blandford, R. D., Narayan, R., Annu. Rev. Astron. Astrophys. 30, 311 (1992);

[154] Massey, R., Kitching, T., Richard, J., Rep. Prog. Phys. 73, 086901 (2010);

[155] Bhadra, A., Sarkar, K. and Nandi, K. K., Phys. Rev. D 75, 123004 (2007);

[156] Einstein, A., Science. 84, 506 (1936);

[157] Zwicky, F., Phys. Rev., 51, 290 (1937); F. Zwicky, Phys. Rev., 51, 679 (1937);

[158] Chwolson, O., Astr. Nachrichten, 221,329 (1924);

[159] Virbhadra, K. S. and Ellis, G. F. R., Phys. Rev. D, 62, 084003 (2000);

[160] Frittelli, S. and Newman, E. T., Phys. Rev. D 59, 124001 (1999);

[161] Virbhadra, K. S., Narasimha, D. and Chitre, S. M., Astron. Astrophys. 337, 1 (1998);

[162] Virbhadra, K. S. and Ellis, G. F. R., Phys. Rev. D 65, 103004 (2002); Eiroa, E. F., Romero, G. E., and Torres, D. F., Phys. Rev. D 66, 024010 (2002); Bhadra, A., Phys. Rev. D 67, 103009 (2003); Sarkar, K. and Bhadra, A., Class.Quant.Grav.23, 6101 (2006); Nandi, K. K., Zhang, Y. -Z. and Zakharov, A. V., Phys. Rev. D 74, 024020 (2006);

[163] Sereno, M., Phys. Rev. D 69, 023002 (2004); Whisker, R., Phys. Rev. D 71, 064004 (2005); Eiroa, E. F., Phys. Rev. D 73, 043002 (2006); Mukherjee, N. and Majumdar, A. S., Gen. Relativ. Gravit. 39, 583 (2007); Gyulchev, G. N. and Yazadjiev, S. S., Phys. Rev. D 75, 023006 (2007); Chen, S. and Jing, J., Phys. Rev. D 80, 024036 (2009); Virbhadra, K. S., Phys. Rev. D 79, 083004 (2009); Liu, Y., Chen, S. and Jing, J., Phys. Rev. D 81, 124017 (2010);

[164] Ding, C., Kang, S., Chen, C. -Y., Chen, S. and Jing, J., Phys. Rev. D 83, 084005 (2011); Nakajima, K. and H. Asada, H., Phys. Rev. D 85, 107501 (2012); Gyulchev, G. N. and Stefanov, I. Z., Phys. Rev. D 87, 063005 (2013); Eiroa, E. F. and Sendra, C. M., Phys. Rev. D 88, 103007 (2013); Sadeghi, J., Naji, J. and Vaez, H., Phys. Lett. B 728, 170 (2014); Younas, A., Jamil, M., Bahamonde, S. and Hussain, S., Phys. Rev. D 92, 084042 (2015); Zhao, S. -S. and Xie, Y., Cosmol, J., Astropart. Phys. 07, 007 (2016); Chakraborty, S. and SenGupta, S., Cosmol. J., Astropart. Phys. 07, 045 (2017); Sendra, C. M., Gen. Relativ. Gravit. 51, 83 (2019); Ovgun, A., Phys. Rev. D 99, 104075 (2019);

[165] Dadhich, N., Narayan, K. and Yajnik, U A, Pramana J. Phys. 50, 307 (1998);

[166] Perlick, V., Phys. Rev. D 69, 064017 (2004);

[167] Cheng, H., Man, J., Class Quant Grav. 28, 015001 (2011); Man, J. and Cheng, H., Phys. Rev. D, 92, 024004 (2015);

[168] Bozza, V., Phys. Rev. D 66, 103001 (2002);

[169] Ishak, M., Rindler, W., Dossett, J., Moldenhauer, J. and Allison, C., Mon. Not. Roy. Astron. Soc. 388, 1279 (2008);

[170] Mandelbaum, R., Seljak, U., Kauffmann, G., Hirata, C., Brinkmann, J., Mon. Not. Roy. Astron. Soc. 368, 715 (2006); Mandelbaum, R., Seljak, U., Cool, R. J., Blanton, M., Hirata, C. M. and Brinkmann, J., Mon. Not. Roy. Astron. Soc. 372, 758 (2006);

[171] Gavazzi, R., et al. Astrophys. J. 667, 176 (2007);

[172] Lynds, R., Petrosian, V., Bull. Am. Astron. Soc., 18, 1014 (1986);

[173] Soucail, G., The Messenger, 48, 43 (1987);

[174] Paczynski, B. P., Nature, 325, 572 (1987);

[175] Narasimha, D. and Chitre, S. M. ApJ., 332,75 (1988);

[176] Grossman, S. and Narayan, R., ApJ 344, 637 (1989);

[177] Bergmann, A. G., Petrosian, V. and Lynds, R., ApJ 350, 23 (1990);

[178] Pellio, R., Le Borgne, J.F., Soucail, G., Mellier, Y. and Sanahuja, B., ApJ 366, 405 (1991);

[179] Broadhurst, T. J., Barkana, R., Mon. Not. R. Astron. Soc., 390, 1647 (2008);

[180] Richard, J., Kneib, J.-P., Limousin, M., Edge, A. and Jullo, E., Mon. Not. R. Astron. Soc. 402, L44 (2010);

[181] Roberts, M. S., Rots, A. H., Astron. Astrophy., 26, 483 (1973);

[182] Rubin, V. C., Thonnard, N., Ford, W. K. Jr., Astrophys. J., 225, L107 (1978);

[183] Rubin, V. C., Roberts, M. S., Ford, W. K. Jr., Astrophys. J., 230,35 (1979);

[184] Persic, M., Salucci, P. and Stel, F., Mon. Not. Roy. Astron. Soc. 281, 27 (1996);

[185] Sofue, Y., Rubin, V. C., Ann. Revs. Astron. Astrophy. 39, 137 (2001);

[186] Zwicky, F., Helv. Phys. Acta, 6, 110 (1933);

[187] Lukovic, V., Cabella, P. and Vittorio, N., Int J. Mod. Phys. A, 29, 1443001 (2014);

[188] Belokurov, V., et al., Astrophys. J. 671, L9 (1992);

[189] Maoz, D. et al., Astrophys. J. 409, 28 (1993);

[190] King, L., Jackson, N., Blandford, R., et al., Mon. Not. Roy. Astron. Soc. 295, L41(1998);

[191] Markevitch, M., Gonzalez, A. H., et al., Astrophys. J. 606, 819 (2004);

[192] Waerbeke, L. Van., et al., Astron. Astrophy. 358, 30 (2000);

[193] Ade, P. A. R., et al. (Planck collab.), Astron. Astrophy. 594, A13 (2016);

[194] Patrignani, C., et al. (Particle Data Group), Chin. Phys. C, 40, 100001 (2016);

[195] Spergel, D. N., Astrophys. J. Suppl., 148, 175 (2003);

[196] Olive, K. A., Steigman, G., Walker,T. P., Phys. Rep., 333, 389 (2000);

[197] Ghosh, S., Bhadra, A and Mukhopadhyay, A., Gen. Rel. Grav 51, 54 (2019);

[198] Matos, T., Guzman, F. S., Nunez, D., Phys.Rev. D 62 061301 (2000);

[199] Matos, T., Guzman, F. S. and Urena-Lopez, L. A., Class. Quant. Grav. 17, 1707 (2000);

[200] Fay, S., Astron. Astrophys. 413, 799 (2004);

[201] Rahaman, F., Nandi, K. K., Bhadra, A., Kalam, M., Chakraborty, K., Phys. Lett. B, 694, 10 (2010);

[202] Arbeya, A., Lesgourgues, J. and Salatia, P., Phys. Rev. D 64, 123528 (2001);

[203] Rahaman, F., Kalam, M., DeBenedictis, A., Usmani, A. A., Ray, Saibal, Mon. Not. R. Astron. Soc. 389, 27 (2008);

[204] Misner, C. W., Thorne, K. S., Wheeler, J. A., Gravitation. Freeman & C ., San Francisco (1973);

[205] Moore, B., Nature 370, (1994) 629;

[206] Flores, R., Primack, J., Astrophys. J., 427, L1 (1994);

[207] de Blok, W., Adv. Astron. 2010, 789293 (2010);

[208] Moore, B., Ghigna, S., Governato, F., Lake, G., Quinn, T., Stadel, J., Tozzi, P., Astrophys. J., 524, L19 (1999);

[209] Klypin, A., Kravtsov, A., Valenzuela, O., Prada, F., Astrophys. J., 522, 82 (1999);

[210] Zavala, J., Jing, Y., Faltenbacher, A., Yepes, G. et al., Astrophys. J., 700, 1779 (2009);

[211] Boylan-Kolchin, M., Bullock, J., Kaplinghat, M., Mon. Not. Roy. Astron. Soc., 415, L40 (2011);

[212] Papastergis, E., Giovanelli, R., Haynes, M. P. and Shankar, F., Astron. Astrophy. 574, A113 (2015);

[213] Sawala, T., Frenk, C., Fattahi. A., et al., Mon. Not. Roy. Astron. Soc. 448, 2941 (2015);

[214] Bode, P., Ostriker, J. P. and Turok, N., Astrophys. J. 556, 93 (2001);

[215] Hansen, S. H., Lesgourgues, J., Pastor, S. and Silk, J., Mon. Not. Roy. Astron. Soc. 333, 544 (2002);

[216] Schneider, A., Anderhalden, D., Macci'o, A. and Diemand, J., Mon. Not. Roy. Astron. Soc. 441, L6 (2014);

[217] Viel, M., Becker, G. D., Bolton, J. S., Haehnelt, M. G., Phys. Rev. D 88, 043502 (2013);

[218] Weinberg, D., Bullock, J., Governato, F., Kuzio de Naray, R., Peter, A., arXiv:1306.0913 (2013);

[219] Baushev, A. N. and Pilipenko, S. V., arXiv:1808.03088v1 (2018);

[220] O'Brien, S. and Synge, J. L., Commun. Dublin Inst. Adv. Stud. A. 9 , (1952);

[221] Synge, J. L., Relativity: The General Theory (North-Holland Publishing Company, Amsterdam, 1960);

[222] Lichnerowicz, A., Theories Relativistes de la Gravitation et de E Electromagnetisme (Paris, 1955);

[223] Israel, W., Proc. Roy. Soc. A (London), 248, 404 (1958);

[224] Robson, E. H., Ann. Inst. Henri Poincare. 16A 41 (1972);

[225] Lake, K., Phys. Rev. Lett., 92, 051101 (2004);

[226] Lynden-Bell, D., Katz, J. and Bicak, J., Phys. Rev. D 75, 024040 (2007) ; Erratum, ibid, D 75, 044901 (2007);

[227] Bharadwaj, S., Kar, S., Phys. Rev. D, 68, 023516 (2003);

[228] Faber, T. and Visser, M., Mon. Not. Roy. Astron. Soc. 372, 136 (2006);

[229] Schneider, P., Ehlers, J., Falco, E. E., Gravitational Lenses, Springer-Verlag, Berlin (1992);

[230] Henry, J. P. and Lavery, R. J., Astrophys. J, 323 473 (1987);

[231] McGaugh, S. S., Schombert, J. M., Bothun, G. D. and de Blok, W. J. G., Astrophys. J. 533 L99 (2000);

[232] Tully, R. B., & J. R. Fisher, Astron. Astrophys, 54 661 (1977);

[233] Bothun, G. D., Aaronson, M., Schommer, B., Mould, J., Huchra, J., Sullivan, W. T., Astrophys. J. Suppl., 57 423(1985);

[234] Schombert, J. M., Pildis, R. A., & Eder, J. A., Astrophys. J. Suppl., 111 233 (1997);

[235] Sanders, R. H. and McGaugh, S. S., Annual Rev. Astron. Astrophys., 40 263 (2002);

[236] Persic, M and Salucci, P., Astrophys. J., 368, 60 (1991);

[237] Salucci, P., Lapi, A., Tonini, C., Gentile, G., Yegorova, I. and Klein, U. Mon. Not. R. Astron. Soc. 378, 41 (2007);

[238] Navarro, J. F., Frenk, C. S., White, S. D. M., Astrophys. J., 462, 563 (1996);

[239] Mandelbaum, R., Seljak, U., Kauffmann, G., Hirata, C., Brinkmann, J., Mon. Not. Roy. Astron. Soc. 368, 715 (2006);

[240] Capozziello, S. & Laurentis, M. De Phys. Rept. 509, 167 (2011)

[241] Clifton, T., Ferreira, P. G., Padilla, A. and Skordis, C., Phys. Rept., 513, 1 (2012) [arXiv:1106.2476 [astro-ph.CO]].

[242] Grumiller, D. and Preis, F., Int. J. Mod. Phys. D, 20, 2761 (2011)

[243] Lin, H.-N., Li, M. -H., Li, X., Chang, Z., Mon. Not. Roy. Astron. Soc. 430, 450 (2013) [arXiv:1209.3532 [astro-ph.CO]]

[244] Walter, F. et al., Astron. J., 136 , 2563 (2008)

[245] Navarro, J. F., Frenk, C. F., White, S.D.M., Astrophys. J. 490, 493 (1997)

[246] Mastache, J., Cervantes-Cota, J. L. and la Macorra, A. de, Phys. Rev. D 87, 063001 (2013) [arXiv:1212.5167 [astro-ph.GA]].

[247] Cervantes-Cota, J. L. and Gómez-López, J. A., Phys Lett B, 728, 537 (2014)

Index

Eur. Phys. J. C (2015) 75:494
DOI 10.1140/epjc/s10052-015-3719-8

THE EUROPEAN PHYSICAL JOURNAL C

Regular Article - Theoretical Physics

Influences of dark energy and dark matter on gravitational time advancement

Samrat Ghosh[a], **Arunava Bhadra**[b]

High Energy and Cosmic Ray Research Center, University of North Bengal, Siliguri 734013, India

Received: 25 August 2015 / Accepted: 4 October 2015

Abstract The effect of dark matter/energy on the gravitational time advancement (negative effective time delay) has been investigated considering a few dark energy/matter models including cosmological constant. It is found that dark energy gives only a (positive) gravitational time delay, irrespective of the position of the observer, whereas a pure Schwarzschild geometry leads to a gravitational time advancement when the observer is situated at a relatively stronger gravitational field point in the light trajectory. Consequently, there will be no time advancement effect at all at radial distances where the gravitational field due to dark energy is stronger than the gravitational field of the Schwarzschild geometry.

1 Introduction

The discovery of the acceleration of the universe's expansion [1–5] has led to the inclusion of a new component into the energy-momentum tensor of the universe having a negative pressure, the so-called dark energy component. On the other hand data from rotation curve surveys [6] and a few other observations [7,8] require there to be a dominating component of matter in galaxies which is non-luminous or dark. Several other observations, which include the cosmic microwave background (CMB) measurements [9–12], baryon acoustic oscillations (BAO) [13–15], and lensing in clusters [16,17], support the existence of dark energy as well as the presence of a dark matter halo surrounding the Galactic disc. Consequently on large distance scales, astrophysical and cosmological phenomena are governed mainly by dark matter and dark energy.

The simplest candidate for dark energy is the cosmological constant (Λ): a constant energy density with equation-of-state parameter $w = -1$ and the ΛCDM model where CDM refers to cold dark matter, which is in accordance with all the existing cosmological observations [18,19] such as the cosmic microwave background (CMB) anisotropies, the large scale structure, the scale of the baryonic acoustic oscillation in the matter power spectrum, and the luminosity distance of the supernovae type Ia; but it has a big theoretical problem—its size ($\sim 10^{-52}\,\mathrm{m}^{-2}$) is many orders of magnitudes below the expected vacuum energy density in the standard model of particle physics [20]. Hence many other theoretical explanations for the DE have been proposed in the literature in which the parameter w evolves with time or is different from -1 such as the quintessence [21–23], k-essence [24–27], phantom field [28,29], and Chaplygin gas [30,31] models. There are also proposals for a modification of general relativity, which include scalar tensor theories [32] or f(R) gravity models [33], conformal gravity models [34,35], massive gravity theories [36] including Dvali–Gabadadze–Porrati (DGP) braneworld gravity [37,38] models etc., which lead to late-time accelerated expansion without invoking any dark energy.

Like dark energy, there are also several candidates for dark matter [39] such as WIMPs, axions, sterile neutrinos etc. There are proposals for the modifications at the fundamental theoretical level as well, which include MOND [40–43], that suggest modifications in Newtonian dynamics. The evidence of the presence of non-baryonic dark matter from the CMB data, however, questions the MOND-like schemes. The conformal gravitational theory [34,35], which is based on Weyl symmetry, also can explain flat rotation curves of galaxies without the need of dark matter.

Dark energy/matter is likely to affect the gravitational phenomena on all distance scales including the local scales. Several investigations have so far been made to estimate the influence of dark energy (mainly through cosmological constant) on different local gravitational phenomena, which include the three classical observables—the perihelion shift of planets [44,45], gravitational bending of light [45–49], and grav-

[a] e-mail: samrat.ghosh003@gmail.com
[b] e-mail: aru_bhadra@yahoo.com

Published online: 16 October 2015

itational time delay (or Shapiro time delay) [45,50,51]. Due to the tiny value of Λ, the influence of dark energy has been to be found very small, not detectable by the ongoing experiments. Out of the local gravitational phenomena the effect of Λ is found to be maximum in the case of perihelion precession of planets and the observations on perihelion precession of Mercury put an upper bound of $\Lambda \leq 10^{-42}\,\mathrm{m}^{-2}$ [52]. On the other hand analysis of the perihelion precession of Mercury, Earth, and Mars also lead to a upper bound 3×10^{-19} g/cm^3 for dark matter density ($\rho_{\rm dm}$) [53], whereas the rotation curve data implies that $\rho_{\rm dm}$ in the Milky Way at the location of the solar system is $\rho_{\rm dm} = 0.5 \times 10^{-24}$ g/cm^3 [54].

In this work we would like to examine the influence of dark energy and dark matter on gravitational time advancement. The gravitational time advancement effect takes place when the observer is situated at a stronger gravitational field with respect to the gravitational field encountered by the photon while traversing a certain path [55]. We found that dark energy and dark matter do affect the gravitational time advancement and though the magnitude of the effect is small, it induces an interesting observational consequence, at least in principle.

The organization of the paper is as follows. In the next section we discuss briefly the gravitational time advancement effect. The influence of dark energy and dark matter on gravitational time advancement are evaluated in Sect. 3. The results are discussed and finally we conclude in Sect. 4.

2 Gravitational time advancement

The gravitational time delay is one of the classical solar system tests of general relativity. The general perception as regards the gravitational time delay is that due to the influence of a gravitating object the average global speed of light is reduced from its special-relativistic value c_0 and hence the signal always suffers an additional time delay. But depending upon the position of the observer, the delay can as well be negative, which was called a gravitational time advancement [55]. To exemplify the effect let us consider light propagating in a gravitational field between two points A and B. Assuming the standard Schwarzschild geometry, i.e.

$$\mathrm{d}s^2 = -(1-2\mu/r)\mathrm{d}t^2 + (1-2\mu/r)\mathrm{d}r^2 + r^2/\mathrm{d}\Omega^2, \quad (1)$$

the total coordinate time required for the round-trip journey between the points A and B (or between the points B to A and back) to the first order in $\mu = GM/c_0^2$ is given by [53]

$$c_0\Delta t_{\rm AB} = 2\left(\sqrt{r_{\rm A}^2 - r_o^2} + \sqrt{r_{\rm B}^2 - r_o^2}\right) + 4\mu\left(\ln\frac{r_{\rm A} + \sqrt{r_{\rm A}^2 - r_o^2}}{r_o} + \ln\frac{r_{\rm B} + \sqrt{r_{\rm B}^2 - r_o^2}}{r_o}\right) + 2\mu\left[\left(\frac{r_{\rm A} - r_o}{r_{\rm A} + r_o}\right)^{1/2} + \left(\frac{r_{\rm B} - r_o}{r_{\rm B} + r_o}\right)^{1/2}\right] \quad (2)$$

where $r_{\rm A}$ and $r_{\rm B}$ are the radial coordinates of the point A and B, respectively, and r_o is the closest distance to the gravitating object in the photon path.

Suppose the point A is located at a relatively much weaker gravitational field due to a mass M than the point B i.e. $r_{\rm A} >> r_{\rm B}$ where $r_{\rm A}$ and $r_{\rm B}$ are the values of coordinate r evaluated at the position A and B, respectively. Hence the proper time for transmission and the reception of the signal to be measured by the observer at the point A is

$$c_0\Delta\tau_{\rm AB} \simeq \left(1 - \frac{\mu}{r_{\rm A}}\right)\Delta t_{\rm AB} \simeq 2\left(\sqrt{r_{\rm A}^2 - r_o^2} + \sqrt{r_{\rm B}^2 - r_o^2}\right) + 4\mu\left(\ln\frac{r_{\rm A} + \sqrt{r_{\rm A}^2 - r_o^2}}{r_o} + \ln\frac{r_{\rm B} + \sqrt{r_{\rm B}^2 - r_o^2}}{r_o}\right) + 2\mu\left[\left(\frac{r_{\rm A} - r_o}{r_{\rm A} + r_o}\right)^{1/2} + \left(\frac{r_{\rm B} - r_o}{r_{\rm B} + r_o}\right)^{1/2}\right]. \quad (3)$$

In the above expression the first term on the right hand side is the usual special-relativistic time of travel. The remaining two terms are general-relativistic corrections. As a result the observed time will be higher than the time taken between transmission and the reception in the absence of a gravitating object, which is the well-known gravitational time delay.

Now let us consider the case that the observer is at the point B instead of the point A. In that case the proper time between transmission and the reception of the signal to be measured by the observer will be [55]

$$c_0\Delta\tau_{\rm AB} \simeq \left(1 - \frac{\mu}{r_{\rm B}}\right)\Delta t_{\rm AB} \simeq 2\left(\sqrt{r_{\rm A}^2 - r_o^2} + \sqrt{r_{\rm B}^2 - r_o^2}\right) + 4\mu\left(\ln\frac{r_{\rm A} + \sqrt{(r_{\rm A}^2 - r_o^2)}}{r_o} + \ln\frac{r_{\rm B} + \sqrt{(r_{\rm B}^2 - r_o^2)}}{r_o}\right) + 2\mu\left[\left(\frac{r_{\rm A} - r_o}{r_{\rm A} + r_o}\right)^{1/2} + \left(\frac{r_{\rm B} - r_o}{r_{\rm B} + r_o}\right)^{1/2}\right] - 2\mu\left(\frac{\left(\sqrt{r_{\rm A}^2 - r_o^2} + \sqrt{r_{\rm B}^2 - r_o^2}\right)}{r_{\rm B}}\right). \quad (4)$$

Due to the last term of the right hand side of the above expression, which is the dominating one among the general-relativistic correction terms, the time taken between trans-

mission and the reception will be reduced from the usual special-relativistic time of travel when the distance between A and B exceeds a certain value. This effect is known as the gravitational time advancement (negative time delay), which arises because of the clock running differently at different positions in the gravitational field.

3 Influence of dark energy/matter on gravitational time advancement

In the presence of dark energy the exterior space-time of a spherically symmetric mass distribution is no longer described by the Schwarzschild geometry, but by some modification of the Schwarzschild metric. For instance if dark energy is the cosmological constant, the exterior static space-time will be the Schwarzschild–de Sitter (SDS) space-time.

Here we shall consider a general static spherically symmetric metric of the form

$$\mathrm{d}s^2 = -\mathrm{B}(r)\mathrm{d}t^2 + A(r)\mathrm{d}r^2 + r^2/\mathrm{d}\Omega^2 \tag{5}$$

with

$$\mathrm{B}(r) = 1 - 2m/r - a\Lambda r^n/3 \tag{6}$$

and

$$A(r) = (1 - 2m/r - \Lambda r^n/3)^{-1} \tag{7}$$

where a and Λ are constants. Different choices of n and a lead to different models of dark energy.

Case 1: With $n = 1/2, a = 2$, and $\Lambda = \pm\sqrt{GM/r_c^2}$, the model represents the gravitational field of a spherically symmetric matter distribution on the background of an accelerating universe in the Dvali–Gabadadze–Porrati (DGP) braneworld gravity, provided only leading terms are considered [56]. r_c is the crossover scale beyond which gravity becomes five dimensional.

Case 2: For the choice $n = 1, a = 1$, and negative Λ, the model well describes the gravitational potential due to a central matter distribution plus dark matter [34,35,57].

Case 3: If $n = 3/2, a = 2/3$, and $\Lambda = -m_g^2\sqrt{\frac{2GM}{13c^2}}$, the model corresponds to the non-perturbative solution of a massive gravity theory (an alternative description of accelerating expansion of the universe) [58] where m_g is the mass of graviton.

Case 4: When $a = 1, n = 2$, and $m = \mu$ the above metric describes the Schwarzschild–de Sitter (SDS) or Kotler space-time, which is the exterior space-time due to a static spherically symmetric mass distribution in the presence of the cosmological constant Λ [59].

3.1 General trajectory

Now let us suppose that a light beam is moving between two points A and B in the gravitational field of Eqs. (5–7). The expression for the coordinate time required for light rays to traverse the distance r_o to r, where r_o is the closest distance from the gravitating object over the trajectory can be obtained from the geodesic equations, given by

$$\delta t = \int_{r_o}^{r} \sqrt{P(r, r_o)}\mathrm{d}r, \tag{8}$$

where

$$P(r, r_o) = \frac{\mathrm{A}(r)/\mathrm{B}(r)}{1 - \frac{r_o^2}{r^2}\frac{\mathrm{B}(r)}{\mathrm{B}(r_o)}}. \tag{9}$$

For a general power index (n) of Λ in Eq. (5), the above equation after integration can only be expressed in terms of hyper-geometric functions and thereby are not very useful. However, for $n = 1$ and $n = 2$, the integral can be written in a handy form, particularly when higher order terms in M and Λ are ignored. The extra coordinate time delay (δt_1^{Λ}) induced by the dark sector terms in Eq. (8) is given, for $n = 1$ and $\Lambda = -\Lambda$, by

$$\delta t_1^{\Lambda} = -(a+1)\frac{\Lambda}{12}\left(r\sqrt{r^2 - r_o^2} + r_o^2\ln(r + \sqrt{r^2 - r_0^2})\right) - \frac{a\Lambda r_o^2}{6}\left(\ln(r + \sqrt{r^2 - r_0^2}) - \sqrt{\frac{r - r_o}{r + r_o}}\right), \tag{10}$$

while for $n = 2$ we have

$$\delta t_2^{\Lambda} = (a+1)\frac{\Lambda}{18}\left((r^2 + 2r_o^2)\sqrt{r^2 - r_o^2}\right) - \frac{a\Lambda r_o^2}{6}\sqrt{r^2 - r_o^2}, \tag{11}$$

and for general n ($n \neq 1$) when $r_{\mathrm{A}} >> r_o$ and $r_{\mathrm{B}} >> r_o$,

$$\delta t_n^{\Lambda} \simeq \frac{(a+1)\Lambda}{6(n+1)}r^{n+1} - \frac{(a-1)\Lambda}{12(n-1)}r^{n-1}r_o^2 + O(r_o^4). \tag{12}$$

Hence the proper time between the transmission and the reception of the signal to be measured by the observer at point B will be for $n = 1$

$$c_0\Delta\tau_1 \simeq 2\left(\sqrt{r_{\mathrm{A}}^2 - r_o^2} + \sqrt{r_{\mathrm{B}}^2 - r_o^2}\right) + 4\mu\left(\ln\frac{r_{\mathrm{A}} + \sqrt{r_{\mathrm{A}}^2 - r_o^2}}{r_o} + \ln\frac{r_{\mathrm{B}} + \sqrt{r_{\mathrm{B}}^2 - r_o^2}}{r_o}\right)$$

$$+2\mu\left[\left(\frac{r_A-r_o}{r_A+r_o}\right)^{1/2}+\left(\frac{r_B-r_o}{r_B+r_o}\right)^{1/2}\right]$$
$$-(a+1)\frac{\Lambda}{12}\left(r_A\sqrt{r_A^2-r_o^2}+r_o^2\ln\left(r_A+\sqrt{r_A^2-r_o^2}\right)\right)$$
$$+\frac{a\Lambda r_o^2}{6}\left(\sqrt{\frac{r_A-r_o}{r_A+r_o}}-\ln\left(r_A+\sqrt{r_A^2-r_o^2}\right)\right)$$
$$-(a+1)\frac{\Lambda}{12}\left(r_B\sqrt{r_B^2-r_o^2}+r_o\ln\left(r_B+\sqrt{r_B^2-r_o^2}\right)\right)$$
$$+\frac{a\Lambda r_o^2}{6}\left(\sqrt{\frac{r_B-r_o}{r_B+r_o}}-\ln(r_B+\sqrt{r_B^2-r_o^2})\right)$$
$$-2\left(\frac{\mu}{r_B}-\frac{a\Lambda r_B}{3}\right)\left(\sqrt{r_A^2-r_o^2}+\sqrt{r_B^2-r_o^2}\right). \quad (13)$$

Usually for observing a time advancement effect, $r_o = r_B$. Further for describing a flat rotation curve, a has been chosen as 1. Hence the above equation reduces to

$$c_0\Delta\tau_1 \simeq 2\sqrt{r_A^2-r_B^2}+4\mu\, ln\left(\frac{r_A+\sqrt{r_A^2-r_B^2}}{r_B}\right)$$
$$+2\mu\left(\frac{r_A-r_B}{r_A+r_B}\right)^{1/2}$$
$$-\frac{\Lambda}{6}\left(r_A\sqrt{r_A^2-r_B^2}+r_B^2\ln\left(r_A+\sqrt{r_A^2-r_B^2}\right)\right)$$
$$-\frac{\Lambda}{6}r_B^2\left(\sqrt{\frac{r_A-r_B}{r_A+r_B}}-\ln\left(r_A+\sqrt{r_A^2-r_B^2}\right)\right)$$
$$-2\left(\frac{\mu}{r_B}-\frac{\Lambda r_B}{3}\right)\sqrt{r_A^2-r_B^2}. \quad (14)$$

When $r_A >> r_B$, the above equation transforms to

$$c_0\Delta\tau_1 \simeq 2r_A-2\mu\left(\frac{r_A}{r_B}-2\ln\left(\frac{2r_A}{r_B}\right)-1\right)$$
$$-\frac{\Lambda}{6}\left(r_A^2+2r_B^2\ln 2r_A-4r_Ar_B\right). \quad (15)$$

Similarly for $n = 2$ with $r_o = r_B$

$$c_0\Delta\tau_2 \simeq 2\sqrt{r_A^2-r_B^2}$$
$$+4\mu\ln\left(\frac{r_A+\sqrt{r_A^2-r_B^2}}{r_B}\right)+2\mu\left(\frac{r_A-r_B}{r_A+r_B}\right)^{1/2}$$
$$+(a+1)\frac{\Lambda}{18}\left(r_A^2+2r_B^2\right)\sqrt{r_A^2-r_B^2}$$
$$-\frac{a\Lambda r_B^2}{6}\sqrt{r_A^2-r_B^2}-2\left(\frac{\mu}{r_B}+\frac{a\Lambda r_B^2}{3}\right)\sqrt{r_A^2-r_B^2}, \quad (16)$$

which for $r_A >> r_B$ becomes

$$c_0\Delta\tau_2 \simeq 2r_A+2\mu\left(2\ln\left(\frac{2r_A}{r_B}\right)+1-\frac{r_A}{r_B}\right)$$
$$+\frac{\Lambda}{18}\left((a+1)r_A^3+ar_Ar_B^2(2-13a))-2\frac{ar_Ar_B}{3}\right), \quad (17)$$

and for general n

$$c_0\Delta\tau_n \simeq 2r_A+2\mu\left(2\ln\left(\frac{2r_A}{r_B}\right)+1-\frac{r_A}{r_B}\right)$$
$$+\frac{(a+1)\Lambda}{6(n+1)}r^{n+1}-\frac{(a-1)\Lambda}{12(n-1)}r^{n-1}r_o^2$$
$$-\frac{2a\Lambda r_Ar_B^n}{3}. \quad (18)$$

Unless the Λ effect dominates over the pure Schwarzschild effect, the net time delay will be negative in all the above cases resulting in time advancement.

3.2 Small distance travel

Let us suppose a light beam is moving from a point on the Earth surface (B) (R,θ,ϕ), where the radius of Earth is denoted as R_E, to a nearby point with coordinates C$(R+\Delta R,\theta,\phi)$ and reflects back to the transmitter position (B). The light signal will travel a null curve of space-time, satisfying $ds^2 = 0$. Then the proper distance between point B and point C is given by

$$\Delta L_{BC} = \int_R^{R+\Delta R}(1-2m/r-\Lambda r^n/3)^{-1/2}dr$$
$$\simeq \Delta R\Bigg[1+\frac{m}{R}-\frac{m\Delta R}{2R^2}$$
$$+\frac{\Lambda R^n}{6}\left(1+\frac{n\Delta R}{2R}+\frac{n(n-1)\Delta R^2}{6R^2}\right)$$
$$+\frac{3m^2}{2R^2}+\frac{m\Lambda R^{n-1}}{2}\left(1+\frac{(n-1)\Delta R}{2R}\right)\Bigg]. \quad (19)$$

The coordinate time interval in transmitting a light signal from B to C and back, is given by

$$\Delta t = 2\int_R^{R+\Delta R}\left(1-\frac{2m}{r}-\frac{\Lambda r^n}{3}\right)^{-1/2}\left(1-\frac{2m}{r}-\frac{a\Lambda r^n}{3}\right)^{-1/2}dr$$
$$\simeq 2L_{BC}\Bigg[1+\frac{m}{R}+\frac{3m^2}{2R^2}+\frac{\Lambda aR^n}{6}\left(1+\frac{n\Delta R}{2R}+\frac{n(n-1)\Delta R^2}{6R^2}\right)$$
$$+m\Lambda\left(R^{n-1}\left(1+\frac{(n-1)\Delta R}{2R}\right)\left(\frac{2a}{3}+\frac{1}{6}\right)\right.$$
$$\left.-\frac{(a+1)R^{n-1}}{6}\left(1+\frac{n\Delta R}{2R}\right)+\frac{R^{n-2}(a+1)\Delta R}{12}\right)-\frac{m\Delta R}{2R^2}\Bigg]. \quad (20)$$

The observer at B will experience that coordinate time interval in proper time to be measured by the observer at B between transmission and reception of the signal as given by

$$\begin{aligned}\Delta\tau_1 &= \left(1-\frac{2m}{R}-\frac{a\Lambda R^n}{3}\right)^{1/2}\Delta t\\ &\simeq 2L_{\rm BC}\Bigg[1+\frac{\Lambda a R^n}{6}\left(\frac{n\Delta R}{2R}+\frac{n(n-1)\Delta R^2}{6R^2}\right)\\ &\quad+m\Lambda\left(R^{n-1}\left(1+\frac{(n-1)\Delta R}{2r}\right)\left(\frac{2a}{3}+\frac{1}{6}\right)\right.\\ &\quad-\frac{R^{n-1}(a+1)}{6}\left(1+\frac{n\Delta R}{2R}\right)+\frac{R^{n-2}(2a+1)\Delta R}{12}\\ &\quad\left.-\frac{aR^{n-1}}{6}\left(3+\frac{n\Delta R}{2R}\right)\right)-\frac{m\Delta R}{2R^2}\Bigg].\end{aligned}\tag{21}$$

In deriving the above equations, the higher order terms in Λ and $m^2\Lambda, m^3, m^2\frac{\Delta R^2}{R^2}$, and terms of higher order in m have been neglected.

4 Discussion and conclusion

Dark energy has a significantly different kind of influence on gravitational time advancement than that of pure Schwarzschild geometry. The time advancement effect is entirely due to the pure Schwarzschild geometry, while dark energy leads only to a time delay effect, which means the gravitational time advancement effect will be reduced in the presence of dark energy. When $\Lambda r_{\rm A}^2 > 2\mu/r_{\rm B}$, there no time advancement at all. So in principle the time advancement effect should be able to identify dark matter clearly.

In contrast the conformal theory description of a flat rotation curve suggests a large time advancement effect. The fitting of galactic rotation curves suggests $\Lambda/3 = -(5.42\times 10^{-42}\frac{M}{M_\odot} + 3.06\times 10^{-30})\,{\rm cm}^{-1}$ [60]. Therefore, in our galaxy, the dark matter potential should start dominating over the luminous matter contribution (pure Schwarzschild part) at distances larger than about 30 kpc. Hence at distances beyond the ∼30 kpc time advancement effect will be quite large. The experimental realization to examine the gravitational time advancement effect at such distances is a challenging issue.

Here it is worthwhile to mention that the gravitational time advancement effect has not been experimentally verified yet, but it should not be very difficult to test the effect. This is because the magnitude of the time advancement effect is reasonably large. In fact, gravitational time advancement is a much stronger effect than gravitational time delay when large distances are involved. However, time delay has the advantage of probing stronger gravity. In the solar system tests of gravitation, time delay measurements mainly rely on the passage of radiation grazing the sun, and thereby the solar gravitational potential at the surface of the sun comes into play. In such a situation the time delay is about 240 μs, whereas the total special-relativistic travel time between the earth and the sun is about 1000 s, which means the gravitational time delay is about a 2×10^{-7} part of the total travel time. For testing gravitational time advancement from the earth or its surroundings, on the other hand, the solar gravitational potential at the position of earth will be applicable and when light propagates from the earth to say Pluto and back, the time advancement will be about 1 ms over a total propagation time of 50,000 s i.e. here the time advancement is about a 0.2×10^{-7} part of the total travel time, which is just one order smaller than the time delay caused by the sun and hence is detectable. Note that the above estimates need to be corrected taking into account the variations in round-trip travel time due to the orbital motion of the target relative to the Earth by using radar-ranging or any other similar kind of data. Since gravity cannot be switched off, one does not have access to a special-relativistic propagation of a photon against which the time delay is to be measured. Therefore, the variation of the time delay is measured as a function of distance to verify the radial profile of Eq. (3). A similar check can be made for the time advancement also.

The future missions, such as the Beyond Einstein Advanced Coherent Optical Network (BEACON) [61] or the GRACE Follow-On (GRACE-FO) mission [62], will probe the gravitational field of the Earth with unprecedented accuracy. The BEACON mission will employ four small spacecraft equipped with laser transceivers and the spacecraft will be placed in a circular Earth orbit at a radius of 80,000 km. All the six distances between the spacecraft will be measured to high accuracy (∼0.1 nm), out of which one diagonal laser trajectory will be very close to the Earth and thereby pick up the gravitational time delay effect. If the distance between the spacecraft and the Earth is also measured by an Earth bound observer and compared with distances measured by the spacecraft, the time advancement effect may be revealed from the measurements. The GRACE-FO, which is scheduled for launch in 2017, will be equipped with a laser ranging interferometer and is expected to provide a range with an accuracy of 1 nm. With such a level of accuracy general-relativistic effects may become significant [63]. It is, therefore, important to examine whether the time advancement can have any significant effect on the observables of GRACE-FO.

To probe dark matter through its influence on the gravitational time advancement properly, one is required to observe a time advancement (delay) effect at distance ∼30 kpc or beyond. For probing dark energy, observations are to be made at even higher distances. This is currently not feasible. At present, observations can be made only from the Earth

or from its neighborhood via a satellite/space station. So strategies to be developed for observing the time advancement/delay effect at other distances may be some indirect means. This would be a very challenging task.

For small distance travel, the time advancement effect is a second order effect, unlike the long distance travel where the time advancement occurs due to first order effect. However, since the time advancement effect is cumulative in nature, if a light beam is allowed to travel, say, from the Earth surface radially upwards to a nearby point large number of times it (the light beam), this should acquire a time advancement of reasonable magnitude when observed from the Earth surface and should be measurable.

In summary, we investigate the influence of dark matter/energy on gravitational time advancement. We obtain analytical expressions for the time advancement to first order in M and Λ where Λ is the parameter describing the strength of the dark matter/energy. From our results it is found that dark energy leads to a gravitational time delay only, whereas a pure Schwarzschild metric gives both a time delay and a time advancement (negative effective time delay) depending on the position of the observer.

The present finding suggests that in principle the measurements of gravitational time advancement at large distances can verify the dark matter and a few dark energy models or put an upper limit on the dark matter/energy parameter.

Acknowledgments The authors are thankful to an anonymous reviewer for encouraging comments and drawing attention to few useful references.

Funded by SCOAP[3].

References

1. A. Riess et al., Astron. J. **116**, 1009 (1998)
2. S. Perlmutter et al., ApJ **517**, 565 (1999)
3. M. Hicken, W.M. Wood-Vasey, S. Blondin et al., ApJ **700**, 1097 (2009)
4. N. Suzuki, D. Rubin, C. Lidman et al., ApJ **746**, 85 (2012)
5. M. Kowalski, D. Rubin, G. Aldering et al., ApJ **686**, 749 (2008)
6. W.J.G. de Blok, F. Walter, E. Brinks, C. Trachternach, S.-H. Oh, R.C. Kenni-cutt, Astron. J. **136**, 2648 (2008)
7. V. Trimble, Annu. Rev. Astron. Astrophys. **25**, 425 (1987)
8. G. D'Amico, M. Kamionkowski, K. Sigurdson, arXiv:0907.1912v1 (2009)
9. P. de Bernardis, P.A.R. Ade, J.J. Bock et al., Nature **404**, 955 (2000)
10. E. Komatsu, J. Dunkley, M.R. Nolta et al., ApJS **180**, 330 (2009)
11. P.A.R. Ade, N. Aghanim, C. Armitage-Caplan et al. (Planck Collaboration), Astron. Astrophys. **571**, A16 (2014)
12. P.A.R. Ade, N. Aghanim, C. Armitage-Caplan et al. (Planck Collaboration), Astron. Astrophys. **571**, A23 (2014)
13. D.J. Eisenstein, I. Zehavi, D.W. Hogg et al., ApJ **633**, 560 (2005)
14. L. Anderson, E. Aubourg, S. Bailey et al., MNRAS **427**, 3435 (2012)
15. A. Slosar et al., J. Cosmol. Astropart. Phys. **4**, 26 (2013)
16. S.W. Allen, D.A. Rapetti, R.W. Schmidt et al., MNRAS **383**, 879 (2008)
17. T. Schrabback, J. Hartlap, B. Joachimi et al., Astron. Astrophys. **516**, A63 (2010)
18. S.M. Carroll, Living Rev. Relativ. **4**, 1 (2001)
19. P. Peebles, B. Ratra, Rev. Mod. Phys. **75**, 559 (2003)
20. S. Weinberg, Rev. Mod. Phys. **61**, 1 (1989)
21. B. Ratra, P. Peebles, Phys. Rev. D **37**, 3406 (1988)
22. R. Caldwell, R. Dave, P.J. Steinhardt, Phys. Rev. Lett. **80**, 1582 (1998)
23. I. Zlatev, L.-M. Wang, P.J. Steinhardt, Phys. Rev. Lett. **82**, 896 (1999)
24. C. Armendariz-Picon, T. Damour, V.F. Mukhanov, Phys. Lett. B **458**, 209 (1999)
25. C. Armendariz-Picon, V.F. Mukhanov, P.J. Steinhardt, Phys. Rev. Lett. **85**, 4438 (2000)
26. C. Armendariz-Picon, V.F. Mukhanov, P.J. Steinhardt, Phys. Rev. D **63**, 103510 (2001)
27. J. Garriga, V.F. Mukhanov, Phys. Lett. B **458**, 219 (1999)
28. R.R. Caldwell, Phys. Lett. B **545**, 23 (2002)
29. F. Hoyle, Mon. Not. R. Astron. Soc. **108**, 372 (1948)
30. A.Y. Kamenshchik, U. Moschella, V. Pasquier, Phys. Lett. B **511**, 265 (2001)
31. M. Bento, O. Bertolami, A. Sen, Phys. Rev. D **66**, 043507 (2002)
32. T. Damour, G. Esposito-Farèse, Class. Quantum Gravity **9**, 2093 (1992)
33. A. De Felice, S. Tsujikawa, Living Rev. Relativ. **13**, 3 (2010)
34. P.D. Mannheim, D. Kazanas, Astrophys. J. **342**, 635 (1989)
35. D. Kazanas, P.D. Mannheim, Astrophys. J. Suppl. **76**, 431 (1991)
36. C. de Rham, Living Rev. Relativ. **17**, 7 (2014)
37. G. Dvali, G. Gabadadze, M. Porrati, Phys. Lett. B **485**, 208 (2000)
38. A. Lue, Phys. Rep. **423**, 1 (2006)
39. J.L. Feng, Annu. Rev. Astron. Astrophys. **48**, 495 (2010)
40. M. Milgrom, Astrophys. J. **270**, 365 (1983)
41. J.D. Bekenstein, M. Milgrom, Astrophys. J. **286**, 7 (1984)
42. J.D. Bekenstein, Contemp. Phys. **47**, 387 (2006)
43. P.G. Ferreira, G. Starkmann, Science **326**, 812 (2009)
44. J.N. Islam, Phys. Lett. A **97**, 239 (1983)
45. V. Kagramanova, J. Kunz, C. Lämmerzahl, Phys. Lett. B **634**, 465 (2006)
46. A. Bhadra, S. Biswas, K. Sarkar, Phys. Rev. D **82**, 063003 (2010)
47. W. Rindler, M. Ishak, Phys. Rev. D **76**, 043006 (2007)
48. M. Sereno, Phys. Rev. D **77**, 043004 (2008)
49. M. Sereno, Phys. Rev. Lett. **102**, 021301 (2009)
50. H. Asada, Phys. Lett. B **661**, 78 (2008)
51. B. Chen, R. Kantowski, X. Dai, Phys. Rev. D **82**, 043005 (2010)
52. S. Liang, Y. Xie, Res. Astron. Astrophys. **14**, 527 (2014)
53. I.B. Khriplovich, E.V. Pitjeva, Int. J. Mod. Phys. D **15**, 615 (2006)
54. G. Bertone, D. Merritt, Mod. Phys. Lett. A **20**, 1021 (2005)
55. A. Bhadra, K.K. Nandi, Gen. Relativ. Gravity **42**, 293 (2010)
56. A. Lue, G. Starkman, Phys. Rev. D **67**, 064002 (2003)
57. D. Grumiller, Phys. Rev. Lett. **105**, 211303 (2010)
58. A.I. Vainshtein, Phys. Lett. B **39**, 393 (1972)
59. F. Kottler, Ann. Phys. (Leipzig) **361**, 401 (1918)
60. P.D. Mannheim, J.G. O'Brien, Phys. Rev. Lett. **106**, 121101 (2011)
61. S.G. Turyshev, B. Lane, M. Shao, A. Girerd, Int. J. Mod. Phys. D **18**, 1025 (2009)
62. R. Pierce, J. Leitch, M. Stephens, P. Bender, R. Nerem, Appl. Opt. **47**, 5007 (2008)
63. S.G. Turyshev, M.V. Sazhin, V.T. Toth, Phys Rev. D **89**, 105029 (2014)

General Relativity and Gravitation (2019) 51:54
https://doi.org/10.1007/s10714-019-2538-x

RESEARCH ARTICLE

Probing dark matter and dark energy through gravitational time advancement

Samrat Ghosh[1] · Arunava Bhadra[1] · Amitabha Mukhopadhyay[2]

Received: 8 August 2018 / Accepted: 2 April 2019

Abstract

The expression of gravitational time advancement (negative time delay) for particles with non-zero mass in Schwarzschild geometry has been obtained. The influences of the gravitational field that describes the observed rotation curves of spiral galaxies and that of dark energy (in the form of cosmological constant) on time advancement of particles have also been studied. The present findings suggest that in presence of dark matter gravitational field the time advancement may take place irrespective of gravitational field of the observer, unlike the case of pure Schwarzschild geometry where gravitational time advancement takes place only when the observer is situated at stronger gravitational field compare to the gravitational field encountered by the particle during its journey. When applied to the well known case of SN 1987a, it is found that the net time delay of a photon/gravitational wave is much smaller than quoted in the literature. In the presence of dark matter field, the photon and neutrinos from SN 1987a should have been suffered gravitational time advancement rather than the delay.

Keywords Gravitational time advancement · Particle · Dark matter

✉ Arunava Bhadra
abhadra@nbu.ac.in

Samrat Ghosh
samrat.ghosh003@gmail.com

Amitabha Mukhopadhyay
amitabha_62@rediffmail.com

[1] High Energy and Cosmic Ray Research Centre, University of North Bengal, Siliguri, West Bengal 734013, India

[2] Department of Physics, University of North Bengal, Siliguri, West Bengal 734013, India

Published online: 23 April 2019

1 Introduction

Light propagation in gravitational field leads to an extra time delay over the time required for light transmission between two points in Euclidean space, which is the well known gravitational or Shapiro time delay effect [21,22]. The observation of the time delay effect in the solar system constitutes one of the classical tests of general relativity. The difference in gravitational time delay between photon/gravitational waves and neutrinos or any other neutral particle with non-zero mass also has been used as a probe to examine the Principle of Equivalence [14]and dark sector of the universe [2,20]. Presently the gravitational time delay effect is often employed to measure the masses of pulsars in binary systems [6,7].

Gravitational time delay is generally estimated by evaluating the additional coordinate time needed by a photon or a particle in a round trip journey in a gravitational field of a massive object over the coordinate time required in the absence of the gravitating object. However, the coordinate time difference is not a measurable quantity in a gravitational field; one needs to convert the coordinate time difference in to proper time difference which is a real measurable quantity. When such conversion is considered an opposite kind of effect, the so called gravitational time advancement (GTA) (negative time delay), is taken place if the observer is situated at stronger gravitational field in respect to the gravitational field encountered by the photon during its journey [4]. The GTA effect is essentially caused by the fact that clock runs differently in gravitational field depending on the curvature. Note that when an observer is at weaker gravity field and is exploring time delay effect due to stronger gravity, such as time delay effect due to gravitational field of the Sun, the difference in coordinate time is roughly the same to the difference in proper time. That is why Shapiro effect is experimentally verified without any issue till now.

The GTA of photons has been found to be affected by dark matter and dark energy [9] and therefore, at least in principle, the measurements of GTA at large distances can verify the dark matter and a few dark energy models or put upper limit on the dark matter/energy parameters. The measurement of GTA also can be employed to discriminate the Gravity Rainbow (photons of different energies experience different gravity levels) from pure General Relativity [8].

Like photons, particles having non-zero masses should also suffer GTA when the observer is at stronger gravitational field. Here we like to derive expression of GTA for particles with non-zero mass in Schwarzschild geometry. We further wish to examine the effect of the gravitational field that describes the observed rotation curve of spiral galaxies (in this paper we denote it as dark matter field) and the dark energy in the form of Cosmological constant on gravitational time advancement. The importance of the present investigation is many fold: It offers, at least in principle, to probe the presence of dark matter and dark energy, it constitutes a possible test of the GTA and it allows to estimate mass of a particle of unknown mass.

The plan of the paper is the following. In the next section we shall present the basic formulation for calculating gravitational time advancement for a particle. In Sect. 3 we shall estimate the GTA in a round trip journey by a particles under the influence of Schwarzschild geometry. In Sect. 4 we shall study the effect of cosmological constant

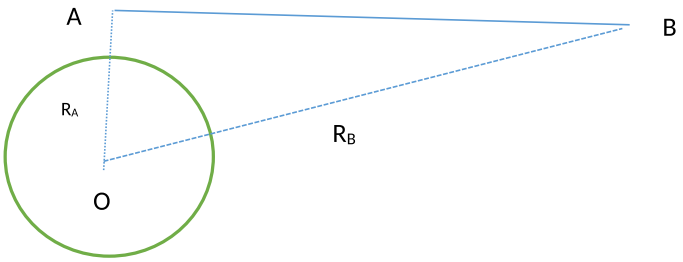

Fig. 1 Geometrical configuration of time delay/advancement of photon/particle in gravitational field. O is the Centre of the spherically symmetric mass distribution, A and B are two arbitrary points. r_A and r_B are radial distances of X and Y from O respectively

and dark matter gravitational field on GTA. We shall discuss the results in Sect. 4 and conclude our findings in the same section.

2 Methodology

Consider the following scenario: An electromagnetic/gravitational wave or a particle is moving between the points A and B in a gravitational field due to a static spherically symmetric matter distribution as depicted in Fig. 1.

We consider that the gravitational field is described by a general static spherically symmetric metric,

$$ds^2 = -\kappa(r)c^2dt^2 + \sigma(r)dr^2 + r^2d\Omega^2 \ . \tag{1}$$

The geodesic equations for a test particle motion in equatorial plane under the influence of the space time given by Eq. (1) leads to the following relation

$$\frac{\sigma(r)}{\kappa(r)^2}\left(\frac{dr}{dt}\right)^2 + \frac{\alpha_1}{r^2} - \frac{c^2}{\kappa(r)} = -\alpha_2 c^2, \tag{2}$$

where α_1 ($\equiv \frac{r^4}{\kappa^2}\left(\frac{d\phi}{dt}\right)^2$, and α_2 ($\equiv \left(\kappa\frac{dt}{d\tau}\right)^{-2}$ for massive particle and $\alpha_2 = 0$ for mass less particle) are associated with the constants of motion, α_1 is related to the angular momentum of the particle and α_2 is related to the energy ϵ of the particle. At the distance of closest approach r_o, $\frac{dr}{dt}$ must vanish, which gives

$$\alpha_1 = c^2\left[-\alpha_2 + \frac{1}{\kappa(r_o)}\right]r_o^2, \tag{3}$$

and $\alpha_2 = \frac{m^2c^4}{\epsilon^2}$, m and and ϵ ($\equiv mc^2\kappa\frac{d(t)}{d\tau}$) are the mass and energy of the particle. Hence the time required by a particle to traverse a distance from r_o to r is given by

$$\Delta t\ (r, r_o) = \frac{1}{c}\int_{r_o}^{r}\sqrt{P(r, \alpha_2)}\,dr, \tag{4}$$

where,

$$P(r,\alpha_2)=\frac{\sigma(r)/\kappa(r)}{\left[1-\alpha_2\,\kappa(r)+\frac{{r_o}^2}{r^2}\left(\alpha_2\,\kappa(r)-\frac{\kappa(r)}{\kappa(r_o)}\right)\right]}. \tag{5}$$

Therefore the difference in proper time between transmission and reception in a round trip journey of the signal to be measured by the observer at r_o is

$$\Delta\tau=2\sqrt{\kappa(r_o)}\Delta t\,(r,r_o), \tag{6}$$

Since the expression in Eq. (6) through Eq. (4) involves integration of the function $P(r,\alpha_2)$ which involves the metric coefficients $\sigma(r)$ and $\kappa(r)$, explicit expressions for $\sigma(r)$ and $\kappa(r)$ are required to proceed further. In the following sections we shall evaluate the proper time between transmission and reception for three different physically viable choices of $\sigma(r)$ and $\kappa(r)$.

3 GTA of a particle with non-zero mass in Schwarzschild geometry

In the Schwarzschild geometry i.e. when $\kappa(r)=\sigma(r)^{-1}=1-\frac{2\mu}{r}$ where $\mu=GM/c^2$, G is the gravitational constant and c is the speed of light, the coordinate time delay in round trip journey by a particle of mass m between A and B up to the first order accuracy of μ is given by

$$\begin{aligned}\Delta t_m^{Sch}=\frac{2}{c\sqrt{1-\alpha_2}}\Bigg[&\sqrt{r_A^2-r_o^2}+\sqrt{r_B^2-r_o^2}\\&+\frac{\mu\,(2-3\alpha_2)}{(1-\alpha_2)}\ln\frac{\left(r_A+\sqrt{r_A^2-r_o^2}\right)\left(r_B+\sqrt{r_B^2-r_o^2}\right)}{r_o^2}\\&+\frac{\mu}{(1-\alpha_2)}\left(\sqrt{\frac{r_A-r_o}{r_A+r_o}}+\sqrt{\frac{r_B-r_o}{r_B+r_o}}\right)\Bigg],\end{aligned} \tag{7}$$

The first term in the right hand side of the above expression gives the special relativistic time take for the propagation whereas the rest of the terms are the 'the Shapiro delay 'in Schwarzschild spacetime. For a particle of mass m and energy ϵ, $\alpha_2=\frac{m^2c^4}{\epsilon^2}$. Hence the difference in proper time between transmission and reception of a particle of mass m from A to B and back to be measured by the observer at A reads

$$\begin{aligned}\Delta\tau_m^{Sch}=\sqrt{B(r_A)}\Delta t_m^{Sch}\simeq\frac{2}{c\sqrt{1-\alpha_2}}\Bigg[&\left(\sqrt{r_A^2-r_o^2}+\sqrt{r_B^2-r_o^2}\right)\left(1-\frac{\mu}{r_A}\right)\\&+\frac{\mu\,(2-3\alpha_2)}{(1-\alpha_2)}\ln\frac{\left(r_A+\sqrt{r_A^2-r_o^2}\right)\left(r_B+\sqrt{r_B^2-r_o^2}\right)}{r_o^2}\end{aligned}$$

$$+\frac{\mu}{(1-\alpha_2)}\left(\sqrt{\frac{r_A-r_o}{r_A+r_o}}+\sqrt{\frac{r_B-r_o}{r_B+r_o}}\right)\Bigg]. \tag{8}$$

Since both $\frac{\mu}{r_A}$ and Shapiro delay terms are small compare to special relativistic term, here we have ignored their higher order and cross terms. In the absence of the gravitating object (i.e. in flat space time) the time required by a particle of mass m and energy ϵ to travel between A and B is $\left(\sqrt{r_A^2-r_o^2}+\sqrt{r_B^2-r_o^2}\right)/\left(c\sqrt{1-m^2c^4/\epsilon^2}\right)$. Due to gravitational effect this time is shorten by a factor $(1-\mu/r_A)$ (first term in the right hand side of the above expression) which leads gravitational time advancement. The observed time will be smaller than the special relativistic time of propagation i.e. there will be a net GTA when the distance between A and B exceeds a certain value so that μ/r_A factor overcomes the Shapiro delay. The above expression thus gives the GTA (describes the situation when the gravitational time advancement effect overcompensates the Shapiro delay) for particles with mass m. The net GTA for massless particles such as photon can be readily obtained from the above equation by putting $\alpha_2 = 0$ (corresponding to $m = 0$).

If r_B is much larger than r_A and r_o, the expression for net GTA of particle with mass m can be approximated as

$$\Delta\tau_m^{Sch} \approx \frac{2}{c\sqrt{1-\alpha_2}} r_B\left(1-\frac{\mu}{r_A}\right), \tag{9}$$

For relativistic particles ($\epsilon >> m$) and when $r_o \sim r_A$ the Eq. (9) reduces to

$$\Delta\tau_m^{Sch} \approx \frac{2r_B}{c}\left[\left(1-\frac{\mu}{r_A}\right)\left(1+\frac{m^2c^4}{2\epsilon^2}\right)\right]. \tag{10}$$

Therefore, the difference in arrival times after a round trip journey between particle with mass m and energy ϵ and photon those emitted at the same time reads

$$\Delta\tau_m^{Sch} - \Delta\tau_\gamma^{Sch} \approx \frac{m^2c^3r_B}{\epsilon^2}\left(1-\mu/r_A\right), \tag{11}$$

The first part in the right hand side of the above expression is the special relativistic effect whereas the second part is the GR correction.

Under the same conditions the difference in arrival times between particles with the same mass but different energies ϵ_1 and ϵ_2 with $\epsilon_2 > \epsilon_1$ is given by

$$\Delta\tau_m^{Sch}(\epsilon_2) - \Delta\tau_m^{Sch}(\epsilon_1) \approx m^2c^3r_B\left(\frac{1}{\epsilon_2^2}-\frac{1}{\epsilon_1^2}\right)\left(1-\mu/r_A\right), \tag{12}$$

Here an important point to be noted by examining the Eq. 7 that the sign of the expression of Shapiro time delay does not change for traveling from a stronger field to a weaker one and back again instead of traveling from a weak gravitational field to a stronger one and return back (the Shapiro delay is the same in both the situation).

Rather a new effect, owing to the fact that that clock runs differently in gravitational field depending on the curvature, comes into play that leads to negative time delay or GTA in all the cases. The Shapiro delay mainly varies logarithmically with distance while the GTA varies linearly with distance. For a particle traveling from a weak gravitational field to a stronger one and return back magnitude of the negative time delay effect is much smaller than that of the Shapiro time delay, the resulting delay thus is a positive one. But when a particle travels from a stronger field to a weaker one and back again, the negative delay component starts dominating after a certain (small) distance, leading to a net GTA.

We have not mentioned any particular particle so far, our results are very general, applicable to any particle with non-zero mass and even with zero mass. However, charged particles also suffer electromagnetic interaction and therefore, only stable neutral particles can be exploit to examine the GTA/Shapiro time delay effect in a realistic situation. Neutrons with life time around 15 minutes in its rest frame, can be utilized to test GTA/Shapiro delay in certain astrophysical situations not involving very large distances. Neutrinos are stable but their mass is not definitely known yet. Moreover the upper limit of their mass is too small so that the mass effect on GTA of neutrinos is very small.

We would estimate the magnitude of the GTA effect for a simple situation as follows: Consider that photon and thermal neutron are simultaneously sent from the top of the Earths atmosphere towards the Moon where they (photon and neutron) are reflected back at the originating point. To survive without decay, the kinetic energy of the neutron has to be at least around 1 MeV. The Shapiro delay of photon and 1 MeV neutron in the mentioned case are 0.07 ns and 0.07 μs respectively whereas the GTA of photon and 1 MeV neutron will be $\sim$ 0.9 ns and 1.8 μs respectively. The difference in arrival times between two neutrons, one with kinetic energy 1 MeV and other having kinetic energy 10 MeV will be about 1.6 μs. The magnitude of the net GTA effect in the mentioned situation is thus well within the reach of the modern experiments.

The future astrometric missions Beyond Einstein Advanced Coherent Optical Network (BEACON) [23] or the GRACE Follow-On (GRACE-FO) [19] are expected to detect the GTA effect employing laser beam from space craft. The mission BEACON will put six numbers of small spacecraft in a circular orbit of radius 80,000 km and each spacecraft will be equipped with laser transceivers. Introduction of thermal neutron transceivers along with laser transceivers in such a future mission will lead to detect the GTA effect of particles.

4 Effect of Dark sector on GTA of a relativistic particle

A wide variety astrophysical observations suggest that ordinary baryonic matter composes only 4.9% of the matter in the Universe [1]. The rest is mainly composed of dark energy (68.3%) and dark matter (26.8%) components of unknown nature [1]. In this section we shall examine the effect of dark matter and dark energy on GTA. We shall consider the same physical scenario as depicted in Fig. 1.

The presence of dark energy and dark matter lead to some modification of the Schwarzschild metric as the exterior space-time of a spherically symmetric mass

distribution. Let us consider the following functional form of $\sigma(r)$ and $\kappa(r)$ in Eq. (1)

$$\kappa(r) = 1 - 2\mu/r - \beta_1 r^n \tag{13}$$

and

$$\sigma(r) = 1 + 2\mu/r + \beta_2 r^n \tag{14}$$

where n, β_1 and β_2 are constants. We shall consider the following cases:

Case 1: The choice $n = 1$, and $\beta_1 = \beta_2 = -\beta = -\left(5.42 \times 10^{-39} \frac{M_B}{M_\odot} + 3.06 \times 10^{-28}\right)$ m^{-1} (i.e. a linear potential), where M_B is mass of baryonic matter in galaxy, has been found to describe well the observed flat rotation curves (with maximum extension upto extending around 100 kpc) of a sample of 111 spiral galaxies [15,16]. Since the radial extension of dark matter in a galaxy is not known, maximum radial distance of validity of the model can not be stated with certainty. But in general the model should not be extended to intergalactic scale.

Case 2: When $n = 2$, $\beta_1 = \beta_2 = \Lambda/3$ the above metric represents the Schwarzschild-de Sitter (SDS) or Kotler space-time which is the exterior space time due to a static spherically symmetric mass distribution in presence of the cosmological constant Λ with $\Lambda \sim 10^{-52}$m^{-2} [12].

The coordinate time required by a particle to traverse a round trip distance from r_A, which coincides with the distance of closest approach, to r_B under the influence of space time geometry defined by Eqs. (1), (13) and (14) is given by [20]

$$\begin{aligned}\Delta t_n(r_B, r_A) &\approx \Delta t_m^{Sch}(r_B, r_A) \\ &+ \frac{1}{c\sqrt{1-\alpha_2}} \left\{ \left[\beta_1 + \beta_2 - \frac{\beta_1 \alpha_2}{(1-\alpha_2)} \right] \mathcal{I}_n^1 - \frac{\beta_1}{(1-\alpha_2)} \mathcal{I}_n^2 \right\},\end{aligned} \tag{15}$$

where, $\mathcal{I}_n^1$ and $\mathcal{I}_n^2$ are integrals defined by $\mathcal{I}_n^1 = \int_{r_A}^{r_B} \frac{{r_B}^{n+1}\, dr}{\sqrt{({r_B}^2 - r_A^2)}}$ and $\mathcal{I}_n^2 = r_A^2 \int_{r_A}^{r_B} \frac{r_B({r_B}^n - r_A^n)\, dr}{({r_B}^2 - r_A^2)\sqrt{({r_B}^2 - r_A^2)}}$. In the above equation $\alpha_2 = \frac{m^2}{(1-2\mu/r_o - \beta_1 r^n)\epsilon^2}$ which is also to be used here in Δt_m^{Sch}.

For $n = 1$ and $n = 2$ corresponding to DM and DE model respectively, we have analytical solutions of $\mathcal{I}_1^1, \mathcal{I}_1^2$ and $\mathcal{I}_2^1, \mathcal{I}_2^2$ which are given below

$$\begin{aligned}\mathcal{I}_1^1 &= \frac{r_B}{2}\sqrt{r_B^2 - r_A^2} + \frac{r_A^2}{2} \ln \frac{r_B + \sqrt{r_B^2 - r_A^2}}{r_A}, \\ \mathcal{I}_1^2 &= -r_A^2 \sqrt{\frac{r_B - r_A}{r_B + r_A}} + r_A^2 \ln \frac{r_B + \sqrt{r_B^2 - r_A^2}}{r_A}. \\ \mathcal{I}_2^1 &= \frac{1}{3}\sqrt{r_B^2 - r_A^2}\left(r_B^2 + 2r_A^2\right),\end{aligned} \tag{16}$$

$$\mathcal{I}_2^2 = r_A^2\sqrt{r_B^2 - r_A^2}. \tag{17}$$

Thus for the dark matter model i.e. when $n = 1$, $\beta_1 = \beta_2 = -\beta$ the proper time required for the travel by a particle with mass m and energy ϵ for the round trip travel between A to B as measured by an observer at A is given by

$$\begin{aligned}\Delta\tau_m^{\beta} \simeq \Delta\tau_m^{Sch} - \frac{1}{c\sqrt{1-\alpha_2}}\Bigg[&\left(\beta - \frac{\beta\alpha_2}{2(1-\alpha_2)}\right)\\ &\left(r_B\sqrt{r_B^2 - r_A^2} + r_A^2 \ln\frac{r_B + \sqrt{r_B^2 - r_A^2}}{r_A}\right)\\ &- \frac{\beta r_A^2}{(1-\alpha_2)}\left(\sqrt{\frac{r_B - r_A}{r_B + r_A}} + \ln\frac{r_B + \sqrt{r_B^2 - r_A^2}}{r_A}\right) + \beta r_A\sqrt{r_B^2 - r_A^2}\Bigg]\end{aligned} \tag{18}$$

In the above expression we have ignored the cross terms between M and β and higher order terms in β. It is noted from the above equation that β reduces the net time advancement.

In the presence of the cosmological constant ($n = 2$, $\beta_1 = \beta_2 = \Lambda/3$), the proper time required for the travel by a particle with mass m and energy ϵ for the round trip journey between A to B as measured by an observer at A reads

$$\begin{aligned}\Delta\tau_m^{\Lambda} \simeq \Delta\tau_m^{Sch} + \frac{1}{3\,c\sqrt{1-\alpha_2}}\Bigg[&\left(2\Lambda - \frac{\Lambda\alpha_2}{1-\alpha_2}\right)\left(\frac{1}{3}\sqrt{r_B^2 - r_A^2}\left(r_B^2 + 2r_A^2\right)\right)\\ &- \frac{\Lambda}{1-\alpha_2}\left(r_A^2\sqrt{r_B^2 - r_A^2}\right) - \Lambda r_A^2\sqrt{r_B^2 - r_A^2}\Bigg]\end{aligned} \tag{19}$$

when $r_B >> r_A$, considering only the leading order terms, for relativistic particles the Eqs. (18) and (19) respectively reduce to

$$\Delta\tau_m^{\beta} \approx \frac{2r_B}{c}\left[\left(1 - \frac{\mu}{r_A} - \beta r_B/2\right)\left(1 + \frac{m^2c^4}{2\epsilon^2}(1 - \beta r_A)\right)\right]. \tag{20}$$

and

$$\Delta\tau_m^{\Lambda} \approx \frac{2r_B}{c}\left[\left(1 - \frac{\mu}{r_A} + \Lambda r_B^2/9\right)\left(1 + \frac{m^2c^4}{2\epsilon^2}(1 + \Lambda r_A^2/3)\right)\right]. \tag{21}$$

The GTA of photons/GW can be obtained from the above expressions by putting $m = 0$. Therefore, the difference in arrival times after one way journey (half of the round trip travel time) from B to A between particle with mass m and energy ϵ and photon/GW those emitted at the same time reads

$$\Delta\tau_m^{\beta} - \Delta\tau_{\gamma}^{\beta} \approx \frac{m^2 r_B c^3}{2\epsilon^2}\left(1 - \beta r_B/2\right), \tag{22}$$

$$\Delta\tau_m^{\Lambda} - \Delta\tau_\gamma^{\Lambda} \approx \frac{m^2 r_B c^3}{2\epsilon^2}\left(1 + \Lambda r_B^2/9\right), \tag{23}$$

In the expressions for GTA of particles the first order effects of flat rotation curve and cosmological constant appear separately from the contribution of mass (Schwarzschild term) as revealed from Eqs. (18) to (21). Since the contribution of dark matter and dark energy are visible only at large distance scales, neutrons are not suitable for probing the dark matter/energy through GTA effect of particles. Neutrinos seem the only option in this regards.

Another pertinent issue is that getting reflecting back a particle at the Earth from a large distance away is not a realistic idea. So instead of two way motion, we need to consider just one way motion. Measurement of GTA through one way motion can be performed, at least in principle, by sending light/particle from artificial satellite/space station to the Earth. Since the time of emission from a distant source is not known, measurement of GTA or Shapiro delay from one way travel is not possible in such cases. Instead the measurement of difference of arrival times of two particles (or a particle and a photon or two same kind of particles but with different energies) gives an opportunity to test GR and dark matter/energy models provided the relative time of emission of the particles is known within a small uncertainty.

In the next section we shall see how the GTA effect alters the prevailing result of Shapiro time delay of the neutrinos from SN-1987. We shall also estimate the magnitude of dark matter contribution on the GTA of neutrinos from SN 1987.

5 Discussion and conclusion

In Schwarzschild space time particles with non-zero mass suffers GTA when the observer is at stronger gravitational potential compare to the gravitational field encounter by the particle during its journey. The net GTA of particles with non-zero mass is found smaller than that of photons/GW. Due to lower speed, particles with non-zero mass should arrive later than the photon/GW if both were departed at the same instant from the source and the delay of particles with respect to photons can easily be estimated using special relativity. The gravitational time delay enhances the delay for particles with non-zero mass. The net delay in arrival time of relativistic particles, however, reduces to half of the gravitational time delay when proper time of the observer is taken into account.

The dark matter field under the framework of conformal gravity leads to larger GTA. More importantly the GTA is influenced by the dark matter gravitational field at the source position. Thus if the source is located at large distance away (at the outskirt of the galaxy), the dark matter contribution to GTA can be quite large. Interestingly in the presence of dark matter field the prevailing condition for GTA that the observer has to be in stronger gravitational field is no more required. In the dark matter field the net GTA of particles with non-zero mass is found larger than that of photons/GW.

In contrast to dark matter field effect the cosmological constant (dark energy) is found to reduce the magnitude of GTA which could be due to the repulsive nature of cosmological constant. Similar to dark matter case the contribution of cosmological

constant to time delay can be large because the gravitational field due to cosmological constant at the source position contributes in the net delay.

When the distance of the source is quite large compare to the observer distance from the gravitational object the GTA for particles with non zero mass is proportional to square of particle mass and goes inversely with the square of the energy of the particles. So measurement of GTA can be exploit to evaluate mass or put limit on the mass of particles with unknown mass, at least in principle. Another relevant issue is that how far the dark matter halo extends to? The stability criterion can severely constrain the extent of the H1 gas in a galaxy and thereby leads to some testable upper limit on the size of a galaxy [13]. The GTA effect can in principle be exploit to probe the extension of our galaxy.

To exemplify the points stated above we consider the case of photons and neutrinos from the well known supernovae 1987A in the Large Magellanic Cloud. The neutrinos from SN '1987A arrived about four hours earlier than the appearance of the optical counterpart. Since the observer at the Earth is at higher gravitational field of the galaxy for the propagation of photons and neutrinos from the supernovae 1987A to the Earth, one needs to consider the proper time for evaluating the true time delay.

The SN1987A is located at a distance about 50 Kpc [17] and the travel time of a photon from SN1987a to the Earth is about 1.62×10^5 years. Considering that the total mass of the galaxy inside 60 kpc is about $6 \times 10^{11}\ M_\odot$ and the distance between the Earth and Center of the galaxy is about 12 kpc, the gravitational time delay (without considering proper time) experienced a photon while traveling from SN1987a to the Earth is about 1.2×10^7 s [5,14]. After considering the proper time interval and treating the galactic gravitational field as purely Schwarzschild in nature, the net delay will be nearly 2.85×10^6 s (here r_B is not much larger than r_o and hence the full expression as given in Eq. (9) needs to apply). So there is no time advancement in this case but the net gravitational delay is nearly an order less than that reported earlier [5,14]. If we consider the dark matter model described by case 1 of Eqs. (13) and (14), and assuming baryonic mass of the galaxy is about 16% of the total galactic mass the net delay for a photon will be -6.2×10^6 s i.e. there will be nearly half an year time advancement instead of time delay. At the distance of SN1987a, the effect of cosmological constant is quite small and its contribution ($\sim$ 240 s) to the net gravitational time delay thus can be ignored.

If we turn to SN1987a neutrinos, a major issue is that despite a huge progress in neutrino physics over the last three decades or so, the definite mass of the three neutrinos: electron, muon and tau neutrinos (and antineutrinos) are still unknown though experimental evidence of neutrino oscillations suggest that they are not massless. The cosmological observations give an upper bound on the sum of the active neutrinos $\sum m_\nu^i < 0.23$ eV, [1] here the superscript i denotes the mass eigenstate of neurinos. The Lyman alpha forest power spectrum suggests more stringent limits $\sum m_\nu^i < 0.12$ eV [18]. The energy of the detected neutrinos from SN1987a is of the order of 10 MeV. Therefore, there will be no significant difference in time of arrival between photon and neutrinos emitted at same point of time, the correction term due to mass is less than a nano-second; much less than the intrinsic error .

In the above analysis we assumed that metric parameters are identical for all the particles following the Einstein equivalence principle. To examine a possible violation

of Einstein equivalence principle one usually employ the post-parameterized Newtonian (PPN) metric i.e. $\kappa(r) = 1 - \frac{2\mu}{r}$ and $\sigma(r) = 1 + \frac{2\gamma_i\mu}{r}$, (up to the accuracy of μ) where γ_i is the first PPN parameter that can be different for different particles, the subscript i denotes species of the particle. γ is unity in general relativity, zero in the Newtonian theory. The observations suggests γ is very close to 1 [3]. For the PPN metric the difference in proper time between transmission and reception of a particle of mass m from A to B and back to be measured by the observer at A reads

$$\Delta\tau_m^{PPN} \simeq \frac{2}{c\sqrt{1-\alpha_2}}\left[\left(\sqrt{r_A^2 - r_o^2} + \sqrt{r_B^2 - r_o^2}\right)\left(1 - \frac{\mu}{r_A}\right) + \frac{\mu\,(1+\gamma_i - (2+\gamma_i)\alpha_2)}{(1-\alpha_2)} \ln \frac{\left(r_A + \sqrt{r_A^2 - r_o^2}\right)\left(r_B + \sqrt{r_B^2 - r_o^2}\right)}{r_o^2} + \frac{\mu}{(1-\alpha_2)}\left(\sqrt{\frac{r_A - r_o}{r_A + r_o}} + \sqrt{\frac{r_B - r_o}{r_B + r_o}}\right)\right]. \tag{24}$$

and therefore, when $r_A \simeq r_o$ the difference in arrival times after a round trip journey between a relativistic particle with mass m and energy ϵ and a photon those emitted at the same time reads

$$\Delta\tau_m^{PPN} - \Delta\tau_\gamma^{PPN} \simeq \frac{2}{c}\left[\sqrt{r_B^2 - r_A^2}\left(1 - \frac{\mu}{r_A}\right)\frac{m^2c^4}{2\epsilon^2} + \mu ln\frac{r_B + \sqrt{r_B^2 - r_A^2}}{r_A}\left(\gamma_m - \gamma_\gamma\right) + 3\mu\sqrt{\frac{r_B - r_A}{r_B + r_A}}\frac{m^2c^4}{2\epsilon^2}\right], \tag{25}$$

Since neutrino mass is very small, the middle term of the right hand side of the above equation will dominate and hence effectively one gets the same expression that was used in [14] to examine the Einstein equivalence principle using SN 1987A data considering neutrinos are massless particle.

The recent detection of a few gravitational wave transients from sources at large distances creates better opportunity to examine the gravitational time advancement and its consequences. The gravitational waves and neutrinos are expected to emit within a short period (few seconds at most) of time from such binary black hole/neutron star coalescence or from supernova explosions. The observation of arrival time difference between gravitational wave and neutrinos from such large distance sources may provide an independent way to constrain on the mass of the neutrinos.

In conclusion in the present work we have obtained expressions for GTA of particles in Schwarzschild geometry for the first time by considering proper time interval of propagation of a particle with non-zero mass between two points in a gravitational field. Out findings suggest that the gravitational time advancement may take place when the observer is situated at stronger gravitational field compare to the gravitational field encountered by the particle during its journey. Subsequently we study the effect of dark matter and dark energy on gravitational time advancement. It is found that dark matter

leads to larger gravitational time advancement whereas dark energy always produces time delay. We have demonstrated how the present findings can be tested in a real observational situation. Finally after applying our findings to neutrinos (and photons) from SN 1987, we have shown that the net time delay of a photon/gravitational wave is much smaller than quoted in the prevailing literature due to GTA effect.

Recently ICECUBE experiment and Fermi telescope detected neutrinos and photons within a short time period from BLAZER TXS 0506+056 [10,11]. More such kind of detection from various sources are expected in near feature. The present findings will have direct application to test various underlying physics related issues of GR and particle physics from the measurement of the difference in time of arrivals of photons/gravitational wave and neutrinos from such astrophysical sources.

Acknowledgements The authors would like to thank an anonymous reviewer for insightful comments and very useful suggestions that helped us to improve and correct the manuscript.

References

1. Ade, P.A.R., et al.: (Planck Collaboration), Planck 2013 results. XVI. Cosmological parameters, Astron. Astrophys. **571**, A16 (2014)
2. Asada, H.: Gravitational time delay of light for various models of modified gravity. Phys. Lett. B **661**, 78 (2008)
3. Bertotti, B., Iess, L., Tortora, P.: A test of general relativity using radio links with the Cassini spacecraft. Nature **425**, 374 (2003)
4. Bhadra, A., Nandi, K.K.: Gravitational time advancement and its possible detection. Gen. Relativ. Gravity **42**, 293 (2010)
5. Bose, S.K., McGlinn, W.D.: Effect of finite mass on gravitational transit time. Phys. Rev. D **38**, 2335 (1988)
6. Corongiu, A., Burgay, M., Possenti, A., Camilo, F., D'Amico, N., Lyne, A.G., Manchester, R.N., Sarkissian, J.M., Bailes, M., Johnston, S., et al.: A Shapiro Delay Detection in the Binary System Hosting the Millisecond Pulsar PSR J1910–5959A. Astrophys. J. **760**, 100 (2012). arXiv:1210.1167
7. Demorest, P.B., Pennucci, T., Ransom, S.M., Roberts, M.S.E., Hessels, J.W.T.: A two-solar-mass neutron star measured using Shapiro delay. Nature **467**, 1081 (2010)
8. Deng, Xue-Mei, Xie, Yi: Gravitational time advancement under gravity's rainbow. Phys. Lett. B **772**, 152 (2017)
9. Ghosh, S., Bhadra, A.: Influences of dark energy and dark matter on gravitational time advancement. Eur. Phys. J. C **75**, 494 (2015)
10. Collaboration, IceCube, et al.: Multimessenger observations of a flaring blazar coincident with high-energy neutrino IceCube-170922A. Science **361**, 146 (2018)
11. Collaboration, IceCube: Neutrino emission from the direction of the blazar TXS 0506+056 prior to the IceCube-170922A alert. Science **361**, 147 (2018)
12. Kottler, F.: ber die physikalischen Grundlagen der Einsteinschen Gravitationstheorie. Ann. Phys. (Leipzig) **361**, 401 (1918)
13. Nandi, K.K., Bhadra, A.: Comment on Impact of a Global Quadratic Potential on Galactic Rotation Curves. Phys. Rev. Lett. **109**, 079001 (2012)
14. Longo, M.J.: New precision tests of the Einstein equivalence principle from SN1987A. Phys. Rev. Lett. **60**, 173 (1988)
15. Mannheim, P.D., OBrien, J.G.: Impact of a global quadratic potential on galactic rotation curves. Phys. Rev. Lett. **106**, 121101 (2011)
16. Mannheim, P.D., OBrien, J.G.: Fitting galactic rotation curves with conformal gravity and a global quadratic potential. Phys. Rev. D **85**, 124020 (2012)
17. Panagia, N.: New distance determination to the LMC. Memorie della Societa Astronomia Italiana **69**, 225 (1998)

18. Palanque-Delabrouille, N., et al.: Neutrino masses and cosmology with Lyman-alpha forest power spectrum. J. Cosmol. Astropart. Phys. **11**, 011 (2015)
19. Pierce, R., Leitch, J., Stephens, M., Bender, P., Nerem, R.: Intersatellite range monitoring using optical interferometry. Appl. Opt. **47**, 5007 (2008)
20. Sarkar, T., Ghosh, S., Bhadra, A.: Effects of the dark energy and flat rotation curve on the gravitational time delay of particle with non-zero mass. Eur. Phys. J. C **76**, 405 (2016)
21. Shapiro, I.I.: Fourth test of general relativity. Phys. Rev. Lett. **13**, 789 (1964)
22. Shapiro, I.I., Ash, M.E., Tausner, M.J.: Radar verification of the Doppler formula. Phys. Rev. Lett. **17**, 933 (1966)
23. Turyshev, S.G., Shao, M., Girerd, A., Lane, B.: A search for new physics with the BEACON mission. Int. J. Mod. Phys. D **18**, 1025 (2009)